Indexed
PubMed and
PubMed Central
included
JCR (Journal Citation Reports®)

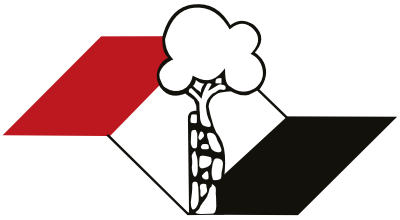

ISSN 1413-7852

Acta Ortopédica Brasileira

Volume 34 – Number 2 – Year 2026

Special

ISSN 1413-7852

Acta Ortopédica Brasileira

Department of Orthopedics and Traumatology, Faculdade de Medicina da Universidade de São Paulo (DOT/FMUSP), São Paulo, SP, Brazil

Affiliated with Associação Brasileira de Editores Científicos

Indexed in PubMed, PubMed Central, Web of Science, JCR, Scopus Elsevier, SciELO, Redalyc (Red de Revistas Cientificas de America Latina y el Caribe,España y Portugal), LILACS (Latin America Health Science Literature) and DOAJ (Directory of open access journals).

EDITORIAL BOARD

Advisory Editor – Arthur Tadeu de Assis
Executive Editor – Ana Carolina de Assis

Administrative Editor – Atha Comunicação Editora
Logo creation – Caio Augusto de Souza Nery

Editorial coordination, creation, desktop publishing and graphic production Atha Comunicação e Editora - e-mail: 1atha@uol.com.br

SUMMARY

VOLUME 34 – Nº 2 – SPECIAL – 2026

Original Article

DOI: http://dx.doi.org/10.1590/1413-785220263402e303941

EWING SARCOMA OF THE CALCANEUS: A RETROSPECTIVE OBSERVATIONAL STUDY

SARCOMA DE EWING DO CALCÂNEO: UM ESTUDO OBSERVACIONAL RETROSPECTIVO

Mariana Vendramin Mateussi[1,2], *Filipe Marques de Oliveira*[1,2], *Jairo Greco Garcia*[1,2], *Marcelo Toledo Petrilli*[1,2], *Dan Carai Viola*[1,2], *Reynaldo Jesus-Garcia Filho*[1,2]

1. Departamento de Ortopedia e Traumatologia (DOT), Hospital Sao Paulo, Universidade Federal de Sao Paulo (UNIFESP), Sao Paulo, SP, Brazil.
2. Hospital do GRAACC (Grupo de Apoio ao Adolescente e a Criança com Cancer), Sao Paulo, SP, Brazil.

ABSTRACT

Objective: To describe the clinical, tumoral, therapeutic characteristics and outcomes of patients with Ewing sarcoma of the calcaneus treated at referral centers for orthopedic oncology. Methods: This was a retrospective observational, descriptive study based on the review of medical records of patients with histopathologically confirmed Ewing sarcoma of the calcaneus, treated between 1996 and 2023 at two quaternary hospitals. Demographic data, tumor characteristics, treatments performed, follow-up duration, and clinical outcomes were analyzed. Results: Six patients were included, with ages at diagnosis ranging from 9 to 33 years, showing a slight male predominance (4/6). All cases involved the calcaneus, with extension to adjacent foot bones in two patients. Pulmonary metastasis was identified in two cases, one at diagnosis and the other as a late, stable finding. All patients underwent multimodal treatment, including systemic chemotherapy combined with surgery and/or radiotherapy. Transtibial amputation was required in two patients. Follow-up ranged from less than 1 year to approximately 14 years. At the last follow-up, all six patients were alive; two were disease-free, one was alive and off treatment, one was alive following transtibial amputation, and two remained under treatment or clinical follow-up. Conclusion: Ewing sarcoma of the calcaneus is a rare presentation associated with diagnostic and therapeutic challenges. In this case series, multimodal treatment in specialized centers allowed adequate local disease control and outcomes consistent with those reported in the literature, highlighting the importance of individualized local control strategies. ***Level of Evidence IV; Case series - retrospective observational study.***

Keywords: Ewing Sarcoma; Calcaneus; Bone Neoplasms; Orthopaedics; Medical Oncology.

RESUMO

Objetivo: Descrever as características clínicas, tumorais, terapêuticas e os desfechos de pacientes com sarcoma de Ewing do calcâneo tratados em centros de referência em oncologia ortopédica. Métodos: Este foi um estudo observacional, descritivo e retrospectivo, baseado na revisão de prontuários de pacientes com sarcoma de Ewing do calcâneo confirmado histopatologicamente, tratados entre 1996 e 2023 em dois hospitais quaternários. Foram analisados dados demográficos, características tumorais, tratamentos realizados, tempo de seguimento e desfechos clínicos. Resultados: Foram incluídos seis pacientes, com idades ao diagnóstico variando de 9 a 33 anos, com discreto predomínio do sexo masculino (4/6). Todos os casos acometeram o calcâneo, com extensão para ossos adjacentes do pé em dois pacientes. Metástase pulmonar foi identificada em dois casos, uma ao diagnóstico e outra como achado tardio e estável. Todos os pacientes foram submetidos a tratamento multimodal, incluindo quimioterapia sistêmica combinada com cirurgia e/ou radioterapia. Amputação transtibial foi necessária em dois pacientes. O seguimento variou de menos de 1 ano a aproximadamente 14 anos. No último seguimento, todos os seis pacientes estavam vivos; dois estavam livres de doença, um estava vivo e fora de tratamento, um estava vivo após amputação transtibial, e dois permaneciam em tratamento ou seguimento clínico. Conclusão: O sarcoma de Ewing do calcâneo é uma apresentação rara associada a desafios diagnósticos e terapêuticos. Nesta série de casos, o tratamento multimodal em centros especializados permitiu controle local adequado da doença e desfechos compatíveis com os relatados na literatura, destacando a importância de estratégias individualizadas de controle local. ***Nível de evidência IV; Série de casos - estudo observacional retrospectivo.***

Descritores: *Sarcoma de Ewing; Calcâneo; Neoplasias Ósseas; Ortopedia; Oncologia Médica.*

Citation: Mateussi MV, Oliveira FM, Garcia JG, Petrilli MT, Viola DC, Jesus-Garcia Filho R. Ewing sarcoma of the calcaneus: a retrospective observational study. Acta Ortop Bras. [online]. 2026;34(Spe.2): Page 1 of 4. Available from URL: http://www.scielo.br/aob.

All authors declare no potential conflict of interest related to this article.

The study was conducted at Departamento de Ortopedia e Traumatologia (DOT), Hospital Sao Paulo – UNIFESP e Hospital do GRAACC (Grupo de Apoio ao Adolescente e a Crianca com Cancer), Sao Paulo, SP, Brazil.
Correspondence: Mariana Vendramin Mateussi. 740, Rua Botucatu, 1º andar, Vila Clementino, Sao Paulo, SP, Brazil. 04023-900. marianavendramin@hotmail.com

Article received on 12/19/2025 approved on 05/07/2026.
Handling Editor: Rodrigo Souza Macedo

<< SUMÁRIO

INTRODUCTION

Malignant tumors of the foot pose a significant diagnostic challenge, as their initial manifestations are often nonspecific and may be mistaken for benign or infectious conditions. In this context, Ewing sarcoma of the calcaneus represents a particularly rare presentation, whose clinical and radiological similarities to conditions such as osteomyelitis, bone cysts, and benign tumors may hinder early recognition, as widely reported in the literature.[1-3]

Ewing sarcoma is the second most common malignant bone tumor in children and adolescents and is histologically characterized by small round cells and, in most cases, by the presence of the EWSR1–FLI1 gene fusion.[4] Although it predominantly affects long bones, only 3% to 6% of cases involve the bones of the foot, with the calcaneus being one of the least frequently affected sites.[5-7] The rarity of this location contributes to additional challenges in the interpretation of clinical and imaging findings, which are often described as atypical or poorly specific, potentially influencing the diagnostic and therapeutic course.[1,2,3,8]

Despite advances in the multimodal treatment of Ewing sarcoma over recent decades, reflected in improved overall survival rates observed in population-based studies such as those derived from the Surveillance, Epidemiology, and End Results (SEER) database of the National Cancer Institute,[9] these benefits are not uniformly distributed across different anatomical locations. Rare tumors of the foot, particularly those of the calcaneus, pose specific challenges to local disease control, especially due to the difficulty in achieving wide surgical margins. Historically, amputation has frequently been employed as an oncological control strategy; however, more conservative approaches, including partial or total calcanectomy, with or without reconstruction, have demonstrated promising results in selected cases.[5,6,10,11]

Given the rarity of this presentation and the scarcity of national case series, a systematic description of the clinical, tumoral, therapeutic characteristics and outcomes associated with Ewing sarcoma of the calcaneus is warranted. Therefore, the objective of this study is to describe a case series treated at quaternary referral centers, contextualizing the observed findings considering the specialized literature.

PATIENTS AND METHODS

Study Design

This was a retrospective observational, descriptive study that analyzed patients with histopathologically confirmed Ewing sarcoma of the calcaneus, treated between 1996 and 2023 at two quaternary referral hospitals specializing in orthopaedic oncology.

Ethics Committee

The study was approved by the Research Ethics Committee of the Federal University of São Paulo (CEP/UNIFESP) under approval number 7,869,939 (CAAE 86294224.6.0000.5505), in accordance with Brazilian National Health Council Resolution No. 510/2016 and Law No. 14,874/2024. As this was a retrospective study based on secondary data, the requirement for written informed consent was waived.

Inclusion and Exclusion Criteria

All patients with histopathologically confirmed Ewing sarcoma localized to the calcaneus were included, regardless of the presence of local extension or metastatic disease. Patients with Ewing sarcoma involving other locations of the foot or the axial or appendicular skeleton, as well as those without diagnostic confirmation or without minimum clinical identification data, were excluded.

Data Collection

Data were collected through a review of physical and electronic medical records, previously anonymized by the participating institutions. The variables analyzed included demographic data (sex and age at diagnosis); tumor characteristics, such as laterality, extension to adjacent foot bones, and presence of metastatic disease at diagnosis or during follow-up; treatments performed, including chemotherapy, surgical procedures, and radiotherapy; clinical course, follow-up duration, and outcome at the last follow-up. Missing or undocumented information in the medical records was categorized as "not reported."

Statistical Analysis

Given the small number of cases, data were analyzed using descriptive statistics. Continuous variables were presented as medians with minimum and maximum values, while categorical variables were described as absolute frequencies. No inferential statistical tests were performed.

RESULTS

Six patients with a diagnosis of Ewing sarcoma of the calcaneus were identified, and their initial clinical characteristics are summarized in Table 1. Age at diagnosis ranged from 9 to 33 years, encompassing childhood, adolescence, and adulthood. A slight male predominance was observed (4/6 patients). Due to incomplete age recording in one case, a precise overall median age could not be reliably calculated.

Regarding tumor characteristics (Table 2), all cases involved the calcaneus, and two patients presented extension to adjacent foot bones, including the talus, cuboid, navicular, and metatarsals. Pulmonary metastasis at diagnosis was identified in one patient, while another developed late pulmonary metastasis, which remained stable during the follow-up period.

The treatment approach was multimodal in all cases, as detailed in Table 3, involving systemic chemotherapy combined with surgical

Table 1. Initial clinical characteristics of patients with Ewing sarcoma of the calcaneus.

Case	Sex	Age at diagnosis (years)	Metastasis at diagnosis
1	F	9	No
2	M	12	Yes, pulmonary.
3	F	33	No
4	M	Adolescence*	Not reported
5	F	26	No
6	M	9	No

Legend: Distribution of patients according to age at diagnosis, sex, and presence of metastasis at the time of diagnosis. *In Case 4, age was recorded only as "adolescence."

Table 2. Anatomical characteristics and tumor extent.

Case	Side	Topography / extent within the foot	Metastatic disease
1	Right	Calcaneus	Late local recurrence (no metastasis reported)
2	Left	Calcaneus	Initial pulmonary metastasis
3	Left	Calcaneus + cuboid + metatarsals	No
4	Left	Calcaneus	Not reported
5	Not reported	Calcaneus + talus + cuboid + navicular	No documented metastases
6	Right	Calcaneus	Late stable pulmonary metastasis

Legend: Location of Ewing sarcoma in the calcaneus, laterality, involvement of adjacent foot bones, and presence of metastatic disease at diagnosis or during follow-up.

resection and/or radiotherapy, according to the extent of the disease. Transtibial amputation was required in two patients, primarily due to local recurrence and oncological considerations. The remaining patients were managed with limb-salvage procedures or systemic therapy, depending on disease extent and response to treatment. Follow-up duration ranged from less than 1 year to approximately 14 years (Table 3). At the last follow-up, all six patients were alive. Two patients were disease-free, one was alive and off treatment, one was alive following transtibial amputation, and two patients remained under treatment or clinical follow-up. No disease-related deaths were recorded in this series.

Table 3. Treatment, follow-up, and clinical outcomes.

Case	Treatment (summary)	Follow-up (years)	Clinical course	Outcome
1	CT + RT; transtibial amputation due to recurrence	8	Initial response; late recurrence	Alive, disease-free
2	Systemic CT (VDC/IE)	< 1	Local and pulmonary tumor reduction	Under follow-up
3	Surgical resections + CT	2	No local or systemic recurrence	Alive, disease-free
4	CT + RT; transtibial amputation	~14	Late recurrence treated surgically	Alive, post-amputation
5	Systemic CT (ICE-VAC)	< 1	Locally extensive disease	Under treatment
6	Calcaneal resection + CT + RT	10	Stable pulmonary metastasis; no local recurrence	Alive, off treatment

Legend: Therapeutic modalities employed, follow-up duration, clinical course, and patient status at the last follow-up. CT: chemotherapy; RT: radiotherapy; VDC/IE: vincristine, doxorubicin, and cyclophosphamide alternating with ifosfamide and etoposide; TT: transtibial; ICE-VAC: ifosfamide, carboplatin, and etoposide alternating with vincristine, actinomycin, and cyclophosphamide.

DISCUSSION

Ewing sarcoma of the calcaneus is an extremely rare entity, frequently associated with diagnostic difficulties, due both to its low prevalence and to the nonspecific clinical presentation described in the literature. In the present series, the occurrence of metastatic disease in two of the six cases and the need for transtibial amputation in two patients reflect this therapeutic complexity.[1-3]

Epidemiological studies indicate that only 3% to 6% of Ewing sarcomas involve the bones of the hands and feet, with the calcaneus being one of the most rarely affected sites.[5-7] This anatomical rarity adds further challenges to the interpretation of imaging findings, as classical radiological patterns may be absent or atypical. Recent reviews report that initial radiographs may be normal or show lesions with a benign appearance, while magnetic resonance imaging may reveal cystic features or diffuse bone marrow edema, making differentiation from inflammatory or infectious processes difficult.[2,3] In such situations, adequate biopsy, combined with immunohistochemical analysis, remains essential for establishing a definitive diagnosis, particularly given the risk of inconclusive results from superficial samples.[8]

Regarding treatment, multimodal management, combining systemic chemotherapy with local control strategies through surgery and/or radiotherapy, remains the cornerstone of Ewing sarcoma therapy. Although therapeutic advances have improved overall survival over recent decades, population-based data suggest that these benefits are not uniformly distributed across anatomical sites.[9] In large institutional series, prognostic factors such as metastatic status at diagnosis, tumor volume, and response to chemotherapy have been shown to significantly influence survival outcomes in patients with Ewing sarcoma, reinforcing the prognostic relevance of disease extent at presentation.[12] Distal tumors, such as those of the calcaneus, tend to be diagnosed at more advanced stages and may present greater challenges in achieving effective local control, potentially negatively affecting oncological outcomes.[1,3] In the present series, the occurrence of metastatic disease in two patients and the need for transtibial amputation in another two reflect this therapeutic complexity. Notably, no disease-related deaths were observed in this series, although follow-up duration varied among patients.

Historically, transtibial amputation has been widely employed as a local control strategy for hindfoot tumors, due to the difficulty in achieving adequate surgical margins.[5,6] However, recent advances have expanded the possibilities for limb-salvage procedures in selected cases. Studies have reported satisfactory functional outcomes following partial or total calcanectomy, particularly when there is a good response to neoadjuvant chemotherapy and no extensive soft-tissue involvement.[10] Other reconstructive strategies, including calcaneal allografts in young patients, have also been described with promising long-term outcomes.[11] The heterogeneity of approaches observed in this series underscores the need for individualized decision-making, considering tumor extent and oncological safety.

This study should be interpreted considering its limitations, inherent to the retrospective design and the small number of cases, an expected feature given the extreme rarity of Ewing sarcoma of the calcaneus. Variability in therapeutic strategies and follow-up duration limits direct comparisons between patients and precludes inferential analyses. Nevertheless, the data presented contribute to the limited national evidence base, reinforcing the importance of maintaining a high index of clinical suspicion for persistent hindfoot lesions and of managing such cases in specialized centers with integrated multidisciplinary care.

Future perspectives include the development of multicenter registries and interinstitutional collaborations capable of increasing the number of analyzed cases, standardizing therapeutic strategies, and deepening the understanding of prognosis, postoperative function, and limb-salvage possibilities in Ewing sarcoma of the calcaneus.

CONCLUSION

Ewing sarcoma of the calcaneus is a rare condition with a frequently nonspecific clinical presentation, which contributes to the diagnostic challenges described in the literature. In this case series, the adoption of an appropriate diagnostic workup, including advanced imaging and histological confirmation, combined with multimodal treatment in specialized centers, allowed effective local disease control and clinical outcomes consistent with those previously reported.

Local control strategies should be individualized, considering tumor extent, response to chemotherapy, and oncological safety, with the possibility of either limb salvage or amputation, depending on the characteristics of each case.

Despite the limitations inherent to the retrospective design and the small sample size, the findings contribute to the scarce national evidence base and reinforce the importance of maintaining a high index of diagnostic suspicion for persistent hindfoot lesions, as well as the role of specialized multidisciplinary management in this uncommon presentation of Ewing sarcoma.

CONTRIBUTIONS OF THE AUTHORS

Each author contributed individually and significantly to the development of this article. MVM: Conceptualization; Methodology; Investigation; Data Curation; Writing: Original Draft; Writing: Review & Editing. FMO: Investigation; Data Curation; Writing: Review & Editing. JGG: Investigation; Resources; Writing: Review & Editing. MTP: Supervision; Conceptualization; Writing: Review & Editing. DCV: Supervision; Conceptualization; Writing: Review & Editing. RJ-GF: Supervision; Methodology; Formal Analysis; Writing: Review & Editing.

DATA AVAILABILITY DECLARATION

The data that support the findings of this study are not publicly available.

REFERENCES

1. Sherif P, Santa A. Ewing□s sarcoma of the calcaneum. Indian J Med Paediatr Oncol. 2017;38(4):542-4. doi: 10.4103/ijmpo.ijmpo_50_16.
2. Mohanty P, Hota A, Govardhan T, Mohapatra SS. "Ewing□s Sarcoma of Calcaneum" an Uncommon Tumor in an Unusual Site with Skip Metastasis. J Med Sci. 2022;42(4):180-2. doi: 10.4103/jmedsci.jmedsci_51_21.
3. Tos SM, Al-Karaja L, Giacaman N, Ibdah MG, Hussein A, Ass'ad OM, et al. Ewing sarcoma in calcenous presented as chronic osteomyelitis: a case report and literature review. Ann Med Surg. 2023;85(1):28-31. doi: 10.1097/ms9.0000000000000044.
4. Kennedy JG, Frelinghuysen P, Hoang BH. Ewing sarcoma: current concepts in diagnosis and treatment. Curr Opin Pediatr. 2003;15(1):53-7. doi: 10.1097/00008480-200302000-00009.
5. Adkins CD, Kitaoka HB, Seidl RK, Pritchard DJ. Ewing□s Sarcoma of the Foot. Clin Orthop Relat Res. 1997;(343):173-82.
6. Parida L, Fernandez-Pineda I, Uffman J, Navid F, Davidoff AM, Neel M, et al. Clinical management of Ewing sarcoma of the bones of the hands and feet: a retrospective single-institution review. J Pediatr Surg. 2012;47(10):1806-10. doi: 10.1016/j.jpedsurg.2012.05.022.
7. Froeb D, Ranft A, Boelling T, Paulussen M, Klco-Brosius S, Jürgens H, et al. Ewing Sarcoma of the Hand or Foot. Klin Padiatr. 2012;224(6):348-52. doi: 10.1055/s-0032-1327607.
8. Zöllner SK, Amatruda JF, Bauer S, Collaud S, de Álava E, DuBois SG, et al. Ewing Sarcoma—Diagnosis, Treatment, Clinical Challenges and Future Perspectives. J Clin Med. 2021;10(8):1685. doi: 10.3390/jcm10081685.
9. Esiashvili N, Goodman M, Marcus RB. Changes in incidence and survival of Ewing sarcoma patients over the past 3 decades: Surveillance Epidemiology and End Results data. J Pediatr Hematol Oncol. 2008;30(6):425-30. doi: 10.1097/mph.0b013e31816e22f3.
10. Khan IU, Shaheen M, Board A, Pant R. Calcanectomy in primary high-grade sarcomas: Foot salvage without the need for any reconstruction. J Musculoskelet Surg Res. 2022;7:52-61. doi: 10.25259/jmsr_130_2022.
11. Torner F, Nuñez JH, Inarejos Clemente EJ, Garraus M, Suñol M, Martínez AD, et al. Total calcaneal allograft reconstruction of an Ewing□s sarcoma in a child: Outcome and review of the literature. Cancer Rep (Hoboken). 2022;5(9):e1626. doi: 10.1002/cnr2.1626.
12. Bacci G, Longhi A, Ferrari S, Mercuri M, Versari M, Bertoni F. Prognostic factors in non-metastatic Ewing's sarcoma tumor of bone: An analysis of 579 patients treated at a single institution with adjuvant or neoadjuvant chemotherapy between 1972 and 1998. Acta Oncol. 2006;45(4):469-75. doi: 10.1080/02841860500519760.

DOI: http://dx.doi.org/10.1590/1413-785220263402e300733

ULTRASOUND-GUIDED ILIOHYPOGASTRIC NERVE BLOCK FOR DIAGNOSIS AND TREATMENT OF HIP PAIN

BLOQUEIO DO NERVO ÍLIO-HIPOGÁSTRICO GUIADO POR ULTRASSONOGRAFIA PARA DIAGNÓSTICO E TRATAMENTO DE DOR DO QUADRIL

Kevin Kenzo Oishi[1], *Erica Blenda da Silva*[1], *Lucas Riolo Salles*[1], *Victor Fantin Amaral*[1], *Rodrigo Goncalves Pagnano*[1], *Francisco Fontes Cintra*[1]

1. Departamento de Ortopedia, Reumatologia e Traumatologia, Faculdade de Ciencias Medicas da Universidade Estadual de Campinas, Campinas, SP, Brazil.

ABSTRACT

Periarticular hip pain is a common complaint in clinical practice. Among the underdiagnosed neuropathic etiologies, iliohypogastric nerve neuralgia—particularly of the lateral cutaneous branch—has emerged as a relevant source of persistent pain, especially when conventional treatments fail. This case series study evaluated the clinical outcomes of ultrasound-guided iliohypogastric nerve blocks in 11 patients with refractory periarticular hip pain. All patients underwent physical examination, exclusion of inguinal hernias via ultrasound, and a minimum follow-up of six months. The nerve block was performed through ultrasound-guided anatomical localization of the nerve, followed by precise injection of a local anesthetic at the target site. Pain intensity was assessed using the Numerical Rating Scale (NRS), with outcomes classified as excellent (≥70% reduction), significant (50–69%), or partial (<50%). The procedure demonstrated high efficacy, with excellent outcomes in 100% of patients presenting isolated inguinal pain and a global success rate above 80%. The findings support the use of ultrasound-guided iliohypogastric nerve block as a safe, low-cost, and effective diagnostic and therapeutic option for neuropathic periarticular hip pain, with potential for broader application in public health settings. ***Level of evidence IV, case series.***

Keywords: Neuralgia; Musculoskeletal Pain; Nerve Block; Ultrasonography, Interventional; Pain Management.

RESUMO

A dor periarticular do quadril é uma queixa comum na prática clínica. Entre as etiologias neuropáticas subdiagnosticadas, a neuralgia do nervo ilio-hipogástrico, especialmente do ramo cutâneo lateral, tem se destacado como uma fonte relevante de dor persistente. Este estudo de série de casos avaliou o desfecho clínico de bloqueios do nervo ilio-hipogástrico guiados por ultrassom em 11 pacientes com dor periarticular do quadril refratária. Eles foram submetidos a exame físico, exclusão de hérnias inguinais por ultrassonografia e tiveram um acompanhamento mínimo de seis meses. A técnica de bloqueio consistiu na identificação anatômica guiada por ultrassonografia, seguida de aplicação precisa do anestésico no ponto-alvo. A intensidade da dor foi avaliada por meio da Escala Numérica de Dor (END), com os desfechos classificados como excelente (redução ≥70%), significativo (50–69%) ou parcial (<50%). O procedimento demonstrou alta eficácia, com desfechos excelentes em 100% dos pacientes com dor inguinal isolada e uma taxa de sucesso global superior a 80%. Os achados sustentam o uso do bloqueio do nervo ilio-hipogástrico guiado por ultrassom como uma opção diagnóstica e terapêutica segura, de baixo custo e eficaz para dor periarticular do quadril de origem neuropática, com potencial de aplicação mais ampla no contexto da saúde pública. ***Nível de evidência IV, série de casos.***

Descritores: *Neuralgia; Dor Musculoesquelética; Bloqueio Nervoso; Ultrassonografia de Intervenção; Manejo da Dor.*

Citation: Oishi KK, Silva EB, Salles LR, Amaral VF, Pagnano RG, Cintra FF. Ultrasound-guided iliohypogastric nerve block for diagnosis and treatment of hip pain. Acta Ortop Bras. [online]. 2026;34(Spe.2): Page 1 of 4. Available from URL: http://www.scielo.br/aob.

INTRODUCTION

Periarticular hip pain is a prevalent condition in clinical practice, often attributed to tendinous, bursal, or neuropathic disorders. This pain typically manifests in three specific regions: lateral pain is frequently associated with trochanteric bursitis or abductor muscle tendinopathy; posterior pain is commonly related to sacroiliitis; and anterior pain may result from psoas tendinopathy or inguinal hernia. However, a significant number of patients do not respond satisfactorily to conservative treatments, suggesting the presence of underlying differential diagnoses that require further investigation [1,2]. Among potential neuropathic etiologies, iliohypogastric nerve neuralgia—particularly of its lateral cutaneous branch—stands out. Originating from the ventral rami of L1 and partially T12, this nerve follows an anatomical path that makes it susceptible to

All authors declare no potential conflict of interest related to this article.

The study was conducted at Universidade Estadual de Campinas, Campinas, SP, Brazil.
Correspondence: Kevin Kenzo Oishi. Codigo de Endereco Postal: 13083-970. kenzo@unicamp.br

Article received on 09/10/2025 approved on 09/16/2025.
Handling Editor: Helder de Souza Miyahara

compression or injury, potentially leading to pain symptoms in the lateral, posterior and anterior hip regions (Figure 1)[2,3].
Techniques such as ultrasound-guided iliohypogastric nerve block have shown efficacy in managing these cases. In addition to providing pain relief, this procedure allows confirmation of neuropathic involvement, given the lack of effective diagnostic methods via imaging or electromyography. It assists in differentiating other causes of periarticular pain. Recent studies highlight the high accuracy and safety of this technique in clinical settings[1,4,5]. Ultrasound guidance for nerve localization and anesthetic block is widely validated, with reports of significant pain score improvements and low incidence of adverse effects. These findings underscore the technique's potential as a versatile diagnostic and therapeutic tool in physical rehabilitation and pain management contexts[3,4].
In this context, by enabling more accurate diagnosis and targeted intervention, ultrasound-guided iliohypogastric nerve block may contribute to improved clinical outcomes and patients' quality of life.

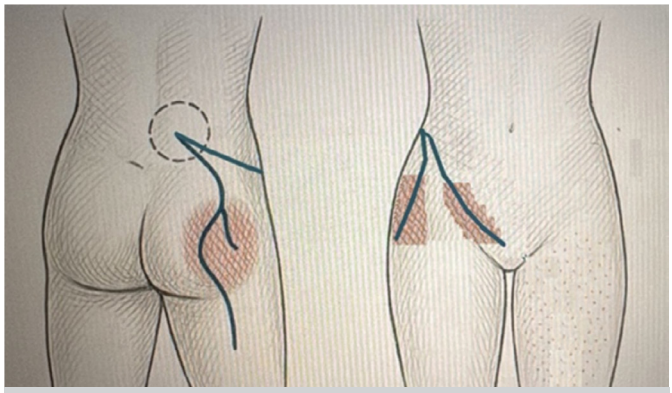

Figure 1. Anatomical pain regions potentially associated with iliohypogastric nerve neuralgia.

METHODOLOGY

This study included patients with persistent periarticular hip pain who did not experience satisfactory relief from prior conservative treatments, including physical therapy and analgesic medication. All had inguinal ultrasound with no evidence of inguinal hernias and were followed for at least six months after treatment. Exclusion criteria included patients with previous abdominal surgery, due to the risk of intraoperative injury to the iliohypogastric nerve, and those diagnosed with meralgia paresthetica confirmed by electromyography.
The iliohypogastric nerve block technique was performed using a convex transducer set at 7.5 MHz to identify the L1 vertebra and 12th rib, with the probe held at a 15-degree caudal inclination, as shown in Figure 2. The needle was inserted lateral to the probe, 1 to 2 cm lateral to the transverse process of the L1 vertebra. The injection site and anatomical landmarks are shown in Figure 3. The blocks were performed using a standardized injectate composed of 2 mL of dexamethasone 0.4% (4 mg/mL), 2 mL of 0.5% bupivacaine with vasoconstrictor, and 6 mL of normal saline, totaling 10 mL per procedure.
Pain intensity was assessed using the verbally reported Numerical Rating Scale (NRS). Due to the consistently severe and treatment-refractory nature of symptoms at baseline, a standardized score of 10 was adopted for all patients to ensure uniformity in calculating percentage pain reduction. Follow-up NRS scores were obtained three months after the last nerve block. Pain improvement was calculated using the formula:

$$\text{Pain Reduction} = (\text{Initial NRS} - \text{Final NRS}) / \text{Initial NRS} \times 100$$

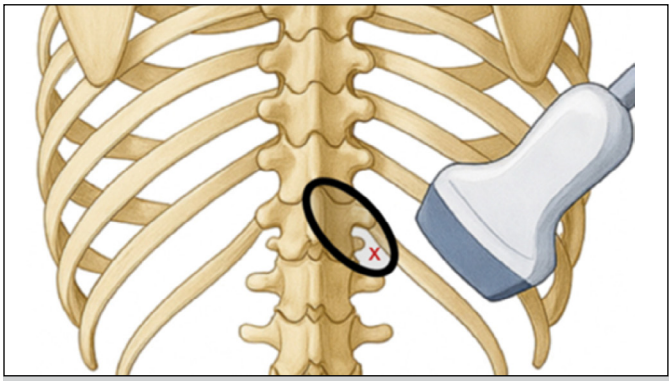

Figure 2. Probe positioning for iliohypogastric nerve block, with the probe held at a 15-degree caudal inclination at the L1 level.

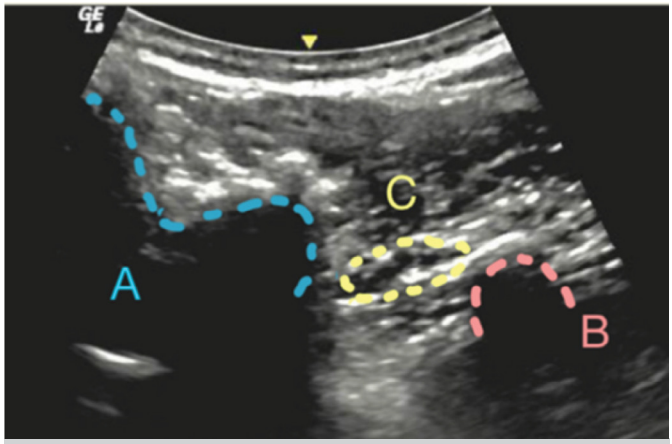

Figure 3. Ultrasound image illustrating key anatomical landmarks for the iliohypogastric nerve block. The L1 vertebra is identified (A), with visualization of both the spinous and transverse processes highlighted by the blue trace. The 12th rib is labeled as (B), serving as an additional reference point. The needle entry site for local anesthetic injection is marked as (C), positioned lateral to the transverse process of L1.

Patients with ≥70% reduction were classified as having "excellent improvement," those with 50-69% reduction as "significant improvement," and <50% as "partial improvement." These cut-off points align with international standards for evaluating pain management interventions, such as those proposed by the International Association for the Study of Pain (IASP), and evidence from relevant clinical studies[6,7].
This study was conducted in accordance with the ethical standards of the institutional research committee and was approved by the Ethics Committee, under registration number 86768325.0.0000.5404.

RESULTS

Eleven patients aged 42 to 70 years (mean: 56.3 years) were included, with 7 females (63.6%) and 4 males (36.4%), all presenting with clinically diagnosed periarticular hip pain refractory to conventional therapy. Right-side pain predominated (72.7%). Analysis of pain patterns showed that 4 patients (36.4%) had isolated inguinal pain, while 7 (63.6%) had mixed pain with associated trochanteric and/or cluneal components (Table 1).
Imaging exams showed variable findings in 5 cases (45.5%). Musculoskeletal ultrasound identified gluteal tendinopathy in two patients and trochanteric bursitis in another two. One patient had radiographic signs of mild coxarthrosis. Other imaging findings were unremarkable.
The therapeutic protocol included one or two ultrasound-guided anesthetic blocks based on the initial clinical response. In cases

of insufficient improvement, additional procedures were indicated based on complementary clinical and anatomical assessment. Three patients with persistent cluneal pain received lumbar facet blocks (L1–L3). Two patients with refractory inguinal pain underwent hydrodissection of the external oblique fascia. One patient underwent Alcock canal block for persistent pubic pain. Another patient with trochanteric pain, who did not respond to initial blocks, received a steroid injection in the trochanteric bursa. Lastly, one patient experienced initial significant improvement, but symptoms recurred within 48 hours, suggesting a multifactorial or mechanical etiology. Adjuvant pharmacotherapy included pregabalin in 60% of cases and gabapentin in 40%, based on clinical profile and drug tolerability. Therapeutic response was evaluated based on NRS score reduction three months after the procedure. Patients with isolated inguinal pain had an excellent response rate (≥70% reduction) in 100% of cases. In contrast, those with trochanteric or cluneal-associated pain showed more heterogeneous outcomes, including isolated cases of partial response (<50% reduction). Detailed clinical response data are presented in Table 2.

Table 1. Demographic and clinical characteristics of patients (n = 11).

Variable	Total (n = 11)
Sex	
Female	7 (63.6%)
Male	4 (36.4%)
Mean age (range)	56 years (42–70)
Affected side	
Right	8 (72.7%)
Left	3 (27.3%)
Reported pain pattern	
Isolated inguinal pain	4 (36.4%)
Trochanteric-associated pain	5 (45.5%)
Cluneal-associated pain	3 (27.3%)
Imaging abnormalities	5 cases (45.5%)
Gluteal tendinopathy	2
Trochanteric bursitis	2
Mild coxarthrosis	1

Table 2. Pain improvement at 3-month follow-up, categorized by pain type.

Pain Type	≥70% improvement	50–69% improvement	<50% improvement
Trochanteric pain	3	6	1
Inguinal pain	9	2	1
Cluneal pain	9	1	1

DISCUSSION

Ultrasound-guided iliohypogastric nerve block proved highly effective in managing periarticular hip pain in patients unresponsive to conventional therapy. Most patients experienced significant or excellent pain relief after one or two procedures, with a success rate over 80%, reinforcing the technique's diagnostic and therapeutic value in neuropathic etiologies.

The methodological choice of standardizing initial pain as NRS 10 was consistent with the sample profile, patients with intense and persistent pain, and enabled more objective comparison of therapeutic outcomes. The Numerical Rating Scale (NRS) is a widely accepted and validated tool for quantifying subjective pain intensity in clinical and research settings. It offers a simple, reproducible, and reliable method, allowing patients to express their pain on a scale from 0 (no pain) to 10 (worst imaginable pain). Its ease of application and strong correlation with functional outcomes make it particularly useful in monitoring responses to interventional pain management strategies. [8].

The accuracy of ultrasound-guided lateral cutaneous branch block of the iliohypogastric nerve is well established in the literature. Pruidze et al. reported 91.7% accuracy in a cadaveric study validated by anatomical dissection[1,9]. Ultrasound guidance, now a gold standard for nerve localization in anesthesia and peripheral blocks, increases the likelihood of success while reducing the required volume of local anesthetic [10].

In addition to therapeutic efficacy, the iliohypogastric nerve block also stands out as a valuable diagnostic method. Immediate pain relief following local anesthetic injection confirms neurogenic pain origin—an important differential in cases where imaging and electromyography are inconclusive [4,11]. This diagnostic capacity is crucial for guiding targeted treatment and avoiding unnecessary therapies for alternative etiologies. The complexity of diagnosing chronic hip pain, often radiating to the spine or knee and potentially arising from non-orthopedic causes, underscores the need for precise diagnostic approaches [4]. Practically, this is a minimally invasive, low-risk, low-cost procedure, estimated at less than R$40 in supplies. This affordability makes the block applicable even in resource-constrained settings like the Brazilian public health system.

The findings of this study provide additional evidence supporting the use of ultrasound-guided iliohypogastric nerve block as a safe, effective, and accessible diagnostic and therapeutic tool for neuropathic periarticular hip pain. Although the sample size is limited, results align with existing literature and highlight ultrasound's role as a precise and safe guide for this intervention. Identifying varying response patterns, such as higher success rates in patients with isolated inguinal pain, suggests future research is warranted to better stratify patients and refine indications—potentially exploring anatomical variations of the nerve[12].

CONCLUSION

Ultrasound-guided iliohypogastric nerve block has proven to be an effective and safe technique for managing periarticular hip pain, especially in patients unresponsive to conventional therapies. The results of this study suggest a relevant clinical benefit, reinforcing this approach's role in both diagnosing and treating neuropathic and musculoskeletal pain. This procedure represents a valuable and accessible option that may significantly contribute to improved clinical outcomes and patient quality of life.

CONTRIBUTIONS OF THE AUTHORS

Each author made a personal and significant contribution to the development of this article. OKO: Literature review and preparation of figures and tables. SEB: Literature review, manuscript drafting, and methodological designa. SLR: Literature review, manuscript drafting, and critical revision of the manuscript. AVF: Methodology, statistical analysis, and interpretation of the results. PRG: Methodology and critical revision of the manuscript for important intellectual content. CFF: Data collection, ultrasonographic procedures, clinical assessment, and final approval of the version to be published.

DATA AVAILABILITY DECLARATION

The contents will be available upon publication of the article.

REFERENCES

1. Pruidze P, Rossmann T, Schwendt KM, Liederer A, Rauschka H, Weninger WJ, et al. Ultrasound-Guided Blockade of the Lateral Cutaneous Branch of the Iliohypogastric Nerve to Differentiate Neuropathy From Greater Trochanteric Pain Syndrome: Cadaver Study and Initial Case Series. Ultrasound Med Biol. 2024;50(11):1745-51. doi: 10.1016/j.ultrasmedbio.2024.08.007.
2. Traycoff RB. "Pseudotrochanteric bursitis": the differential diagnosis of lateral hip pain. J Rheumatol. 1991;18(12):1810-2.
3. Kumar A, Zaidi M. Ilioinguinal, Iliohypogastric, and Genitofemoral Nerve Pain Syndromes. In: Musculoskeletal Sports and Spine Disorders. Cham: Springer International Publishing; 2017. p. 179-83.
4. Ahuja V, Thapa D, Patial S, Chander A, Ahuja A. Chronic hip pain in adults: Current knowledge and future prospective. J Anaesthesiol Clin Pharmacol. 2020;36(4):450-7. doi: 10.4103/joacp.JOACP_170_19.
5. Elahwal L, Elrahwan S, Elbadry AA. Ilioinguinal and Iliohypogastric Nerve Block for Acute and Chronic Pain Relief After Caesarean Section: A Randomized Controlled Trial. Anesth Pain Med. 2022;12(2):e121837. doi: 10.5812/aapm.121837.
6. Orr PM, Shank BC, Black AC. The Role of Pain Classification Systems in Pain Management. Crit Care Nurs Clin North Am. 2017;29(4):407-18. doi: 10.1016/j.cnc.2017.08.002.
7. INTERNATIONAL ASSOCIATION FOR THE STUDY OF PAIN. Classification of chronic pain: descriptions of chronic pain syndromes and definitions of pain terms. 2. ed. Revised. IASP Press; 2019.
8. Karcioglu O, Topacoglu H, Dikme O, Dikme O. A systematic review of the pain scales in adults: Which to use?. Am J Emerg Med. 2018;36(4):707-14. doi: 10.1016/j.ajem.2018.01.008.
9. Tavoletti D, Nanka O, Rosano E, Cerchiara P, Cerutti E, Pecora L. A novel technique of ultrasound-guided lateral cutaneous branch of the iliohypogastric nerve block: A cadaveric study. Acta Anaesthesiol Scand. 2022;66(8):1003-8. doi: 10.1111/aas.14110.
10. Merz-Herrala J, Leu N, Anderson E, Lambeck A, Jefferson J, Sobrero M, et al. Safety and Pain Reduction in Emergency Practitioner Ultrasound-Guided Nerve Blocks: A One-Year Retrospective Study. Ann Emerg Med. 2024;83(1):14-21. doi: 10.1016/j.annemergmed.2023.08.482.
11. Linares Gago M, Cano Plasencia G, Díaz-Cano Carmona I, Rodríguez García J, Alarcón Mora LE. Iliohypogastric Nerve Block for Chronic Pelvic Pain Treatment: Ultrasound-Guide Technique Description and Cases Series. Int Arch Med. 2015. doi: 10.3823/1814
12. Manolakos K, Zygogiannis K, Manolakos O, Mousa C, Papadimitriou G, Fotoniatas I. Anatomical variations of ilioinguinal nerve: A systematic review of the literature. Surg Neurol Int. 2024;15:225. doi: 10.25259/SNI_232_2024.

DOI: http://dx.doi.org/10.1590/1413-785220263402e297565

INTRAOPERATIVE ASSESSMENT OF COMPONENTS IN NAVIGATED KNEE ARTHROPLASTY IN THE ELDERLY

AVALIAÇÃO INTRAOPERATÓRIA DOS COMPONENTES NA ATJ NAVEGADA EM IDOSOS

MARCOS VINICIUS AMORIM SILVA[1], *ADRIANO FERRO ROTONDANO FILHO*[1], *REBECCA GOMES MOURA BASTOS*[1], *EDIMAR GOMES CUSTODIO JUNIOR*[1]

1. Instituto Ortopedico de Goiania (IOG), Departamento de Ortopedia e Traumatologia, Goiania, Goias, Brazil.

ABSTRACT

Objective: This study aims to evaluate the sizing and positioning of femoral and tibial components in Primary Total Knee Arthroplasty (TKA) procedures conducted at the Instituto Ortopédico de Goiânia (IOG), Goiânia, Goiás Brazil. Methodology: Elderly patients undergoing primary TKA with the use of SCORE® prostheses and the Amplivision Navigation System were included in the study. The size and positioning of the femoral and tibial components were analyzed. Data collection was performed using the Amplivision system and statistical analysis was conducted using Minitab21 software. The study was approved by the Ethics Committee and is in accordance with the Brazilian General Data Protection Law (LGPD). Results: All patients received the SCORE® prosthesis, with a higher prevalence of procedures on the right knee (60%). No statistically significant differences were observed in the positioning of femoral and tibial components. Conclusion: Surgical navigation proved to be effective in optimizing the sizing and positioning of implants, contributing to the technical quality of the procedure and the durability of prosthetic components. ***Level of Evidence: III, Cross-Sectional Observational Study.***

Keywords: Arthroplasty, Replacement, Knee; Aged; Surgery, Computer-Assisted; Knee Prosthesis.

RESUMO

Objetivo: Este estudo tem como objetivo avaliar o dimensionamento e o posicionamento dos componentes femoral e tibial em procedimentos de Artroplastia Total Primária de Joelho (ATJ) realizados no Instituto Ortopédico de Goiânia (IOG), Goiânia, Goiás, Brasil. Metodologia: Foram incluídos no estudo pacientes idosos submetidos à ATJ primária com uso de próteses SCORE® e do Sistema de Navegação Amplivision. Foram analisados o tamanho e o posicionamento dos componentes femoral e tibial. A coleta de dados foi realizada por meio do sistema Amplivision e a análise estatística foi conduzida utilizando o software Minitab21. O estudo foi aprovado pelo Comitê de Ética e está em conformidade com a Lei Geral de Proteção de Dados (LGPD). Resultados: Todos os pacientes receberam a prótese SCORE®, com maior prevalência de procedimentos no joelho direito (60%). Não foram observadas diferenças estatisticamente significativas no posicionamento dos componentes femoral e tibial. Conclusão: A navegação cirúrgica mostrou-se eficaz na otimização do dimensionamento e posicionamento dos implantes, contribuindo para a qualidade técnica do procedimento e para a durabilidade dos componentes protéticos. ***Nível de Evidência: III, Estudo Observacional Transversal.***

Descritores: *Artroplastia do Joelho; Idoso; Cirurgia Assistida por Computador; Prótese do Joelho.*

Citation: Silva MVA, Rotondano Filho AF, Bastos RGM, Custodio Junior EG. Intraoperative assessment of components in navigated knee arthroplasty in the elderly. Acta Ortop Bras. [online]. 2026;34(Spe.2): Page 1 of 6. Available from URL: http://www.scielo.br/aob.

INTRODUCTION

Total knee arthroplasty (TKA) is one of the most frequently performed orthopedic procedures worldwide, primarily indicated for the management of end-stage knee osteoarthritis. With the progressive aging of the population and increasing life expectancy, the demand for TKA continues to rise. Despite its high success rates, the procedure's long-term outcomes are closely dependent on the accurate restoration of limb alignment, joint line positioning, and soft tissue balance. Failures in achieving these parameters have been associated with accelerated wear, aseptic loosening, instability, persistent pain, and early revision surgery.[1,2]

Traditional mechanical alignment techniques in TKA aim to place components perpendicular to the mechanical axis of the lower limb. While this approach has been the gold standard for decades, recent evidence suggests that a one-size-fits-all alignment philosophy may neglect patient-specific variations in joint anatomy and kinematics, potentially compromising postoperative satisfaction and functionality[3,4]. This has led to the emergence of personalized alignment strategies, such as kinematic and functional alignment, which attempt to restore the native pre-arthritic alignment of the knee[5]. The advent of computer-assisted surgery (CAS), and more specifically, navigation systems, has revolutionized the technical execution

All authors declare no potential conflict of interest related to this article.

The study was conducted at Instituto Ortopedico de Goiania (IOG), Goias, Brazil.
Correspondence: Marcos Vinicius Amorim Silva. Goiania, Goias, Brazil. marcos_pbs14@hotmail.com

Article received on 06/05/2025 approved on 09/19/2025.
Handling Editor: Fabio Janson Angelini

of TKA. Navigation technologies employ infrared tracking, 3D mapping, and real-time visual feedback to guide bone cuts and component placement with sub-millimetric precision. These systems register anatomical landmarks and construct a virtual model of the joint, allowing surgeons to assess and modify surgical parameters intraoperatively without reliance on intramedullary guides[6,7].

Among the many benefits of navigation-assisted TKA are the increased accuracy of component alignment, reduction in outliers, elimination of intramedullary instrumentation (which may reduce embolic complications), and adaptability to different alignment philosophies. Studies have demonstrated that navigation can lead to improved load distribution, better joint mechanics, and more natural gait patterns when compared to conventional techniques[8–10]. Moreover, by providing objective intraoperative data, navigation systems contribute to standardizing the surgical procedure and may serve as valuable tools for training and quality control.

Despite these advantages, the incorporation of navigation systems into routine clinical practice remains uneven globally, particularly in developing countries. Barriers such as cost, learning curve, lack of training infrastructure, and limited high-quality local data have restricted its widespread adoption. In Brazil, few institutions systematically apply navigation in primary TKA, and even fewer have documented their clinical experiences using implant-specific protocols.

To address this gap, the present study was conducted at the Instituto Ortopédico de Goiânia (IOG), a high-complexity orthopedic center. The main objective is to evaluate the sizing and positioning of femoral and tibial components in primary TKA procedures performed using the Amplivision® navigation system in conjunction with the SCORE® prosthesis. These data are essential to determine the reliability and reproducibility of navigated TKA in the Brazilian clinical setting, with direct implications for surgical training, patient safety, and implant durability.

The justification for this study rests on the growing body of international evidence supporting navigated TKA as a superior alternative in terms of technical precision and patient-specific customization[11–14]. However, the extrapolation of these findings to the Brazilian population and local health systems requires regionally validated data. By documenting objective metrics of implant positioning, this research seeks to inform best practices, contribute to clinical guidelines, and encourage evidence-based integration of navigation technologies in orthopedic centers across the country.

Expected outcomes include confirmation of high levels of accuracy in component placement using navigation, with minimal variation in sizing and alignment parameters. The study also aims to reinforce the feasibility of navigation as a viable strategy for improving long-term outcomes and reducing the rate of technical complications in TKA.

METHODOLOGY

Study Design and Participants

This study employed a quantitative, observational, and descriptive research design, conducted at the Instituto Ortopédico de Goiânia (IOG), a high-complexity orthopedic referral center located in Goiânia, Brazil. The institution is recognized for its expertise in joint reconstruction procedures and the implementation of advanced surgical technologies. The investigation specifically targeted elderly patients undergoing primary total knee arthroplasty (TKA), with all procedures performed using computer-assisted navigation systems to ensure precision in component sizing and positioning.

The sample included 83 elderly individuals (mean age: 70.10 years), composed of 62 females (75.29%) and 21 males (24.71%). With respect to laterality, 51 procedures (60%) were performed on the right knee and 34 procedures (40%) on the left.

Ethical Considerations

This study was approved by the Research Ethics Committee UFG under protocol number 3.845.175 and conducted in full accordance with the ethical principles established by the Declaration of Helsinki (2013 revision), which governs research involving human subjects. In addition, the study complied with Brazilian national ethical regulations, particularly Resolution No. 466/2012 of the National Health Council, which outlines guidelines for research involving human beings, and Law No. 13.709/2018 – the General Data Protection Law (Lei Geral de Proteção de Dados – LGPD), ensuring the confidentiality, privacy, and protection of personal data. All participants were informed about the objectives, procedures, potential risks, and benefits of the study, and voluntarily signed a written informed consent form prior to their inclusion in the research. The confidentiality of all collected data was guaranteed throughout the study, with secure storage and restricted access in accordance with data protection protocols.

Inclusion and Exclusion Criteria

The inclusion criteria established for this study encompassed patients aged 60 years or older, with a confirmed clinical and radiographic diagnosis of primary knee osteoarthritis, and a clear indication for primary total knee arthroplasty (TKA). Eligible participants were those who underwent the procedure using the SCORE® prosthesis in combination with the AMPLIVISION® computer-assisted navigation system, and who had voluntarily signed a written informed consent form, authorizing their participation and the use of their data for research purposes.

Conversely, individuals were excluded from the study if they had undergone revision TKA procedures or if they received implants other than the SCORE® system. Patients diagnosed with inflammatory joint diseases (e.g., rheumatoid arthritis) or secondary osteoarthritis (due to trauma or metabolic conditions) were also excluded, as were those presenting with significant extra-articular deformities that could interfere with the reliability of navigation-based alignment assessments. Additional exclusion criteria included the presence of cognitive or neurological impairments that might compromise the ability to provide informed consent or adhere to postoperative evaluations, as well as cases with incomplete or invalid intraoperative data generated by the navigation system.

Surgical System and Prosthesis

All surgical procedures included in this study were performed using the SCORE® total knee arthroplasty system, manufactured by Amplitude Surgical (Valence, France). This prosthesis features a high congruity rotating platform design, which promotes greater articular stability, reduces polyethylene wear, and accommodates the anatomical variability commonly observed in elderly patients. Its biomechanical characteristics aim to optimize joint function and increase implant longevity.

Intraoperative guidance was provided by the AMPLIVISION® navigation system, an advanced, wireless, real-time 3D optical tracking platform that enhances surgical precision. The system uses infrared technology and reflective markers to register key anatomical landmarks and track the spatial positioning of instruments and bone structures throughout the procedure. This allows for accurate measurement of implant size and component positioning, without requiring the use of intramedullary alignment guides.

Data generated by the system are digitally processed and stored, enabling standardized, objective documentation of the surgical procedure. The integration of the SCORE® prosthesis with the AMPLIVISION® system provides a reliable platform for performing total knee arthroplasty with high technical accuracy and reproducibility.

Data Collection Protocol

The intraoperative data were systematically obtained using the AMPLIVISION® navigation system, a wireless optical tracking platform that provides high-resolution, real-time 3D modeling of anatomical structures during total knee arthroplasty (TKA). This system enables precise spatial orientation of the surgical instruments and prosthetic components throughout the procedure, eliminating the need for traditional intramedullary guides and enhancing both the safety and accuracy of the intervention.

The data collection process commenced with the digital registration of anatomical landmarks, including the medial and lateral femoral condyles, the proximal tibial plateaus, the Whiteside line, and the centers of the hip, knee, and ankle. These reference points were captured through reflective markers and processed by the system to construct a patient-specific three-dimensional virtual model of the knee. This step also enabled the definition of mechanical axes for both the femur and tibia, which served as intraoperative references for alignment and measurement.

Following this, the navigation system performed real-time calibration of the limb's anatomical orientation. The spatial relationships among bones and surgical tools were updated continuously, ensuring accurate visualization and execution of bone resections. With these calibrations in place, the surgeon proceeded with navigation-assisted bone cuts, where the system provided dynamic feedback for each resection plane, minimizing variability and increasing precision.

Based on the registered anatomical data, the system generated automatic implant size suggestions, estimating the optimal dimensions for the femoral and tibial components to ensure proper cortical coverage and joint congruence. After the prosthetic trial and final component placement, the AMPLIVISION® system recorded the definitive values regarding the size and position of each component.

The collected variables included the numerical size (in mm) of both the femoral and tibial components, selected from the standardized options available in the SCORE® prosthesis system. In addition to dimensional sizing, several parameters related to component positioning were analyzed in angular measurements (degrees).

For the femoral component, coronal alignment was recorded as the angle of deviation from the mechanical axis, indicating varus ($< 0°$) or valgus ($> 0°$) positioning, while sagittal alignment referred to the flexion ($> 0°$) or extension ($< 0°$) inclination of the component in relation to the femoral shaft.

For the tibial component, the variables included coronal alignment (varus or valgus) in degrees (°), axial rotation (internal or external), measured relative to the tibial tuberosity and the second metatarsal line, also expressed in degrees, and posterior slope, which was quantified as the angle (°) between the horizontal plane and the inclination of the tibial tray in the sagittal plane. These values were captured directly and automatically by the navigation system, minimizing subjectivity in the assessment process.

All collected data were digitally stored in the AMPLIVISION® database and subsequently exported in tabular format for statistical processing. The precision and standardization ensured by this method provided a robust and objective foundation for the analysis of implant configuration and surgical reproducibility.

Statistical Analysis

All intraoperative data collected through the AMPLIVISION® navigation system were exported to a dedicated database and subsequently analyzed using the Minitab21® statistical software (Minitab Inc., State College, PA, USA). Prior to statistical testing, data integrity and consistency were verified, and all variables were assessed for completeness and validity. The dataset included both continuous and categorical variables related to patient demographics, component sizing, and implant positioning.

A descriptive statistical analysis was conducted to characterize the study sample and summarize the distribution of the surgical variables. Measures of central tendency, such as the mean, and measures of dispersion, including the standard deviation (SD), were calculated for continuous variables (e.g., age, angles of alignment, and posterior slope in degrees). Categorical variables, such as operated side (right or left knee) and prosthetic component size classifications, were expressed in terms of absolute frequencies and percentages.

To assess potential differences between subgroups, particularly between right and left knee procedures, inferential statistical tests were applied. The Student's t-test for independent samples was used to compare the means of continuous variables between these groups, under the assumption of normal distribution and homogeneity of variance. The test evaluated whether statistically significant differences existed in component alignment angles or prosthetic sizes based on surgical laterality or other stratifying factors.

The level of statistical significance was set at $p < 0.05$, meaning that any p-value below this threshold was interpreted as indicative of a significant difference between groups. All statistical tests were two-tailed. The analysis aimed to identify not only the central tendencies of the variables studied, but also to verify the consistency and reproducibility of implant sizing and positioning in surgeries performed with the aid of computer-assisted navigation. This statistical approach provided a robust foundation for interpreting the precision and uniformity of navigated total knee arthroplasty in the sample studied, supporting evidence-based conclusions regarding surgical standardization.

RESULTS

All participants in this study underwent primary total knee arthroplasty (TKA) with the implantation of the SCORE® cemented prosthesis, developed by Amplitude Surgical (Valence, France). Surgical laterality revealed a predominance of procedures on the right knee, corresponding to 60% of cases, while 40% were performed on the left knee.

Regarding the dimensional distribution of prosthetic components, Size 3 was the most frequently selected for both femoral and tibial components, representing 31.32% of the implants used. Component size selection followed the intraoperative recommendations of the AMPLIVISION® system, which proposed optimal sizing based on anatomical calibration. Figure 1 illustrates the distribution of component sizes used in the study population.

Analysis of the femoral component positioning revealed no statistically significant differences for most angular measurements. The mean values were 4.90° (±2.35) for flexion ($p = 0.003$), 1.92° (±1.62) for rotation, 0.62° (±0.90) for varus alignment, and 0.61° (±1.61) for valgus alignment ($p = 0.70$ for all except flexion).

For the tibial component, the mean values were 2.10° (±0.14) for posterior slope, 6.32° (±0.62) for rotation ($p = 0.001$), 0.36° (±0.06) for varus alignment, and 0.31° (±0.06) for valgus alignment ($p = 0.81$ for all except rotation). These results are summarized in Table 1.

The analysis of component sizing and alignment demonstrated a high degree of consistency in surgical execution when using the AMPLIVISION® navigation system in conjunction with the SCORE® prosthesis. The predominance of intermediate sizes—particularly size 3—suggests a common anatomical profile among the elderly population studied, while the balanced distribution of other sizes confirms the system's adaptability to interindividual anatomical variability. The ability to tailor component selection intraoperatively based on real-time 3D mapping reinforces the accuracy and reproducibility of navigation-assisted total knee arthroplasty.

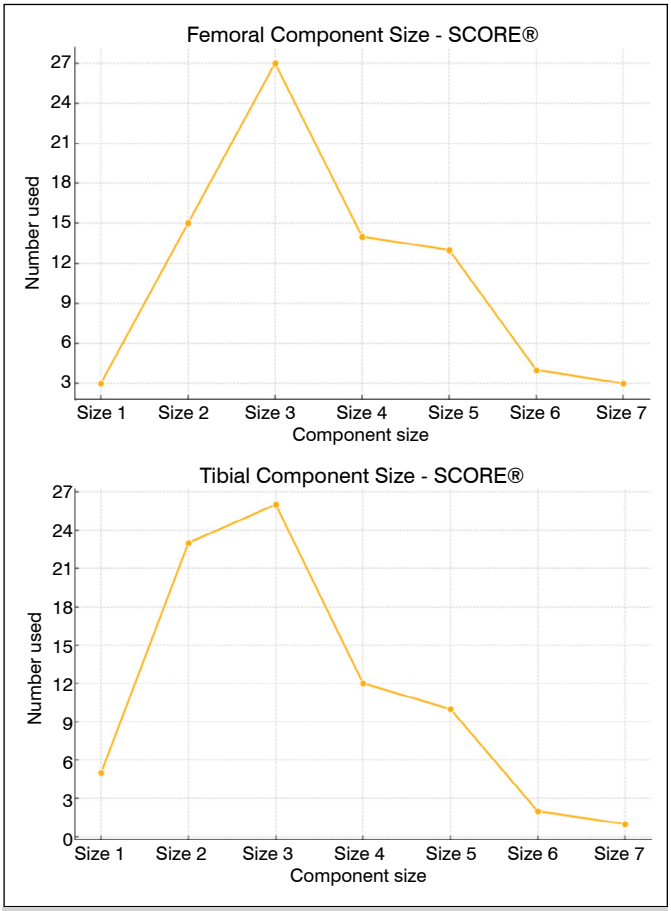

Figure 1. Distribution of Femoral and Tibial Component Sizes Used (SCORE® Prosthesis).

Table 1. Angular Positioning of Femoral and Tibial Components.

Component	Movement	Mean (°) SD	p-value
Femoral	Flexion	4.90 ± 2.35	0.003*
	Rotation	1.92 ± 1.62	0.70
	Varus	0.62 ± 0.90	0.70
	Valgus	0.61 ± 1.61	0.70
Tibial	Posterior Slope	2.10 ± 0.14	0.81
	Rotation	6.32 ± 0.62	0.001*
	Varus	0.36 ± 0.06	0.81
	Valgus	0.31 ± 0.06	0.81

*Statistically significant according to Student's t-test ($p \leq 0.05$). Values are expressed in degrees (°) as mean ± standard deviation.

Furthermore, the absence of statistically significant deviations in most alignment parameters—except for femoral flexion and tibial rotation—indicates that the navigation protocol contributed to maintaining neutral and physiologically appropriate implant positioning across the sample. These findings suggest that computer-assisted navigation can support surgical standardization and improve component placement without excessive variability, thereby contributing to optimized joint biomechanics and potentially enhancing long-term clinical outcomes.

DISCUSSION

The findings of this study provide robust evidence supporting the importance of accurate implant sizing and positioning in total knee arthroplasty (TKA), particularly when using computer-assisted navigation systems such as AMPLIVISION® and high-performance implants like the SCORE® rotating platform prosthesis. In the context of an aging population, where biomechanical integrity and early postoperative recovery are essential for preserving autonomy and functional independence, surgical precision plays a decisive role. The predominance of size 3 for both femoral and tibial components (31.32%) reflect the anatomical consistency of the sample, as well as the system's ability to suggest prosthetic dimensions based on patient-specific 3D mapping. This feature reduces the risk of intraoperative estimation errors and reinforces what Morcos et al.[1] and Yamamoto et al.[2] describe as a pivotal benefit of real-time digital planning in elderly patients, who often present morphological changes associated with degenerative disease. Avoiding oversizing helps minimize soft tissue over-tensioning, while undersizing prevention avoids instability and early loosening.

Notably, femoral component flexion averaged 4.90°, a value within clinically favorable thresholds. As discussed by Almaawi et al.[3] and Gao et al.[5], this slight anterior tilt of the component contributes to maintaining the posterior femoral offset, supporting a natural flexion pattern that benefits quadriceps efficiency and reduces anterior impingement during daily activities. For elderly patients, who often demonstrate reduced muscle mass and proprioceptive capacity, maintaining biomechanical synergy between the implant and the extensor mechanism is fundamental for pain-free ambulation and functional range.

The external rotation of the tibial component (mean: 6.32°) found in this study is equally relevant. This alignment improves patellar tracking, reducing lateral retinacular tension, and has been correlated with reduced anterior knee pain — a persistent challenge in TKA recovery[7,8]. Navigation appears essential for achieving such precision, particularly in osteoarthritic knees where bony landmarks may be obscured. Patellar maltracking, a common source of functional dissatisfaction, can thus be mitigated with accurate rotational alignment, enhancing patient comfort and mobility.

Additionally, the lack of statistically significant deviations in varus/valgus alignment for both components reinforces the mechanical consistency afforded by the navigation system. As Schiraldi et al.[6] and Srivastava et al.[9] highlight, deviations beyond ±3° from the neutral axis are associated with asymmetric distribution, increased polyethylene wear, and long-term implant failure. The ability to maintain alignment within this safety window contributes not only to prosthetic survival but also to more stable gait and reduced fatigue during weight-bearing tasks.

The posterior tibial slope, averaging 2.10°, was consistent across the cohort and remained within recommended values. This parameter is essential in posterior-stabilized or rotating platform implants like SCORE®, as excessive inclination may increase posterior translation and compromise implant congruence. On the other hand, insufficient slope may impede flexion and lead to abnormal loading. Giurazza et al.[4] and Gao et al.[5] emphasize that controlled slope contributes to flexion mechanics and supports a functional range of motion without overstressing ligaments or posterior structures.

Functionally, this degree of precision in implant positioning is strongly associated with improved patient-reported outcomes. Studies by Hadi et al.[10], Nisar et al.[11], and Gousopoulos et al.[15] demonstrate that when alignment and sizing are accurately controlled, patients report reduced pain, better function, and greater satisfaction. These outcomes are especially significant in elderly populations, where prolonged recovery is associated with increased risks of deconditioning, falls, and dependence.

Patients in this study benefited from a streamlined intraoperative protocol that avoided the use of intramedullary guides, thereby reducing surgical invasiveness — a key consideration in geriatric orthopedic care. As Schnurr et al.[16] and Li et al.[17] point out, the avoidance of medullary canal instrumentation reduces intraoperative

bleeding, lowers embolic risk, and supports safer anesthesia management, which collectively translate to fewer complications and faster postoperative mobilization.

These findings align with large-scale evidence. de Steiger et al.[18] and Lei et al.[19] found that computer-assisted navigation in TKA leads to fewer malpositioned implants and lower revision rates. In a broader context, where health systems face increasing demands from aging populations, technologies that enhance procedural consistency while reducing failure rates contribute not only to better outcomes but also to cost-effectiveness and surgical sustainability. Moreover, the SCORE® prosthesis used in this study integrates high-congruity surfaces and a rotating platform that allows for controlled axial rotation. This mechanical behavior accommodates minor physiological variances and provides a "self-aligning" capacity, especially useful in elderly patients with asymmetric loading or soft tissue imbalances. Winnock de Grave et al.[13], Bigoni et al.[20], and Elbuluk et al.[21] note that such implants reduce anterior knee discomfort and promote greater confidence in movement, contributing to improved performance in mobility tests such as the Timed Up and Go (TUG) and six-minute walk test (6MWT).

In the context of the current study, the integration of a navigation system and a biomechanically adaptive implant design resulted in highly reproducible and physiologically favorable component positioning, which likely underpins improved functional trajectories for the sample. Although this analysis did not directly measure clinical outcomes such as range of motion, gait parameters, or patient satisfaction, the literature consistently supports the conclusion that precision in intraoperative execution — as demonstrated here — is closely linked to functional recovery, reduced complication rates, and greater prosthesis longevity[18,19,22].

The results of this investigation reinforce the understanding that accurate positioning and sizing of components, enabled by surgical navigation, are critical to achieving optimal functional outcomes in TKA. Particularly for elderly patients, who may be more vulnerable to biomechanical deviations, technological adjuncts such as AMPLIVISION® allow surgeons to deliver highly standardized care, supporting early mobilization, autonomy preservation, and ultimately, an improved quality of life.

CONCLUSION

This study aimed to evaluate the precision of component sizing and positioning in primary total knee arthroplasty (TKA) procedures performed with the aid of the AMPLIVISION® navigation system and the SCORE® cemented rotating platform prosthesis. The results demonstrated a high level of intraoperative accuracy in implant alignment and dimensioning, with minimal variability in key parameters such as femoral flexion, tibial rotation, coronal alignment, and posterior slope.

The consistent selection of prosthetic sizes, particularly the predominance of size 3, reflects anatomical compatibility within the studied elderly population and reinforces the reliability of the navigation system in facilitating patient-specific surgical planning. Furthermore, the precise placement of femoral and tibial components within biomechanically favorable ranges supports the notion that real-time, computer-assisted techniques contribute directly to improved joint function and enhanced postoperative recovery.

In conclusion, the integration of the AMPLIVISION® system with the SCORE® prosthesis proved to be an effective strategy for optimizing the surgical execution of TKA. By ensuring accurate implant positioning without the use of intramedullary guides, this approach not only improves procedural safety but also lays a foundation for better long-term functional outcomes in elderly patients undergoing knee arthroplasty.

CONTRIBUTIONS OF THE AUTHORS

Each author made a personal and significant contribution to the development of this article. MVAS: Conceptualization, Methodology, Investigation, Data curation, Writing – original draft. AFRF: Formal analysis, Writing – review & editing. RGMB: Investigation, Formal analysis, Writing – original draft. EGCJ: Data curation, Formal analysis, Writing – review & editing.

DATA AVAILABILITY DECLARATION

The authors confirm that the data supporting the findings of this study are available within the article.

REFERENCES

1. Morcos MW, Beckers G, Salvi AG, Bennani M, Massé V, Vendittoli PA. Excellent results of restricted kinematic alignment total knee arthroplasty at a minimum of 10 years of follow-up. Knee Surg Sports Traumatol Arthrosc. 2025;33(2):654-65. doi: 10.1002/ksa.12452.
2. Yamamoto T, Fukushima S, Toyono S, Miyaji T, Nakajima T, Wanezaki Y, et al. Kinematic alignment in Japanese patients shows significant improvement 2 years after total knee replacement surgery. J Exp Orthop. 2025;12(2):e70264. doi: 10.1002/jeo2.70264.
3. Almaawi AM, Hutt JRB, Masse V, Lavigne M, Vendittoli PA. The impact of mechanical and restricted kinematic alignment on knee anatomy in total knee arthroplasty. J Arthroplasty. 2017;32(7):2133-40. doi: 10.1016/j.arth.2017.02.028.
4. Giurazza G, Campi S, Hirschmann MT, Franceschetti E, Tanzilli A, Gregori P, et al. Cartilage thickness can be accurately measured intraoperatively in total knee arthroplasty: a step further in calipered kinematic alignment. J Exp Orthop. 2025;12(1):e70155. doi: 10.1002/jeo2.70155.
5. Gao ZX, Long NJ, Zhang SY, Yu W, Dai YX, Xiao C. Comparison of kinematic alignment and mechanical alignment in total knee arthroplasty: a meta-analysis of randomized controlled clinical trials. Orthop Surg. 2020;12(6):1567-78. doi: 10.1111/os.12826.
6. Schiraldi M, Bonzanini G, Chirillo D, de Tullio V. Mechanical and kinematic alignment in total knee arthroplasty. Ann Transl Med. 2016;4(7):130. doi: 10.21037/atm.2016.03.31.
7. Calliess T, Bauer K, Stukenborg-Colsman C, Windhagen H, Budde S, Ettinger M. PSI kinematic versus non-PSI mechanical alignment in total knee arthroplasty: a prospective, randomized study. Knee Surg Sports Traumatol Arthrosc. 2017;25(6):1743-8. doi: 10.1007/s00167-016-4136-8.
8. Howell SM, Papadopoulos S, Kuznik KT, Hull ML. Accurate alignment and high function after kinematically aligned TKA performed with generic instruments. Knee Surg Sports Traumatol Arthrosc. 2013;21(10):2271-80. doi: 10.1007/s00167-013-2621-x.
9. Srivastava A, Lee GY, Steklov N, Colwell CW Jr, Ezzet KA, D'Lima DD. Effect of tibial component varus on wear in total knee arthroplasty. Knee. 2012;19(5):560-3. doi: 10.1016/j.knee.2011.11.003.
10. Hadi M, Barlow T, Ahmed I, Dunbar M, McCulloch P, Griffin D. Does malalignment affect patient reported outcomes following total knee arthroplasty: a systematic review of the literature. Springerplus. 2016;5(1):1201. doi: 10.1186/s40064-016-2790-4.
11. Sappey-Marinier E, Pauvert A, Batailler C, Swan J, Cheze L, Servien E, et al. Kinematic versus mechanical alignment for primary total knee arthroplasty with minimum 2 years follow-up: a systematic review. SICOT J. 2020;6:18. doi: 10.1051/sicotj/2020014.
12. Hetaimish BM, Khan MM, Simunovic N, Al-Harbi HH, Bhandari M, Zalzal PK. Meta-analysis of navigation vs conventional total knee arthroplasty. J Arthroplasty. 2012;27(6):1177-82. doi: 10.1016/j.arth.2011.12.028.
13. Winnock de Grave P, Luyckx T, Claeys K, Tampere T, Kellens J, Müller J, et al. Higher satisfaction after total knee arthroplasty using restricted inverse kinematic alignment compared to adjusted mechanical alignment. Knee Surg Sports Traumatol Arthrosc. 2022;30(2):488-99. doi: 10.1007/s00167-020-06165-4.

14. Moskal JT, Capps SG, Mann JW, Scanelli JA. Navigated versus conventional total knee arthroplasty. J Knee Surg. 2014;27(3):235-48. doi: 10.1055/s-0033-1360659.
15. Gousopoulos L, Dobbelaere A, Ratano S, Bondoux L, Tibesku CO, Aït-Si-Selmi T, et al. Custom total knee arthroplasty combined with personalised alignment grants 94% patient satisfaction at minimum follow-up of 2 years. Knee Surg Sports Traumatol Arthrosc. 2023;31(4):1276-83. doi: 10.1007/s00167-023-07318-x.
16. Schnurr C, Csécsei G, Eysel P, König DP. The effect of computer navigation on blood loss and transfusion rate in TKA. Orthopedics. 2010;33(7):474. doi: 10.3928/01477447-20100526-08.
17. Li M, Li J, Hu S, Jia B. Comparison of intramedullary versus extramedullary alignment technique in total knee arthroplasty: A PRISMA-compliant meta-analysis. Medicine (Baltimore). 2023;102(5):e32277. doi: 10.1097/MD.0000000000032277.
18. de Steiger RN, Liu YL, Graves SE. Computer navigation for total knee arthroplasty reduces revision rate for patients less than sixty-five years of age. J Bone Joint Surg Am. 2015;97(8):635-42. doi: 10.2106/JBJS.M.01496.
19. Lei K, Liu L, Chen X, Feng Q, Yang L, Guo L. Navigation and robotics improved alignment compared with PSI and conventional instrument, while clinical outcomes were similar in TKA: a network meta-analysis. Knee Surg Sports Traumatol Arthrosc. 2022;30(2):721-33. doi: 10.1007/s00167-021-06436-8.
20. Bigoni M, Zanchi N, Turati M, Pirovano G, Zatti G, Munegato D. Short-term differences in anterior knee pain and clinical outcomes between rotating and fixed platform posterior stabilized total knee arthroplasty with a new femoral component design. World J Orthop. 2019;10(3):128-36. doi: 10.5312/wjo.v10.i3.128.
21. Elbuluk AM, Jerabek SA, Suhardi VJ, Sculco PK, Ast MP, Vigdorchik JM. Head-to-head comparison of kinematic alignment versus mechanical alignment for total knee arthroplasty. J Arthroplasty. 2022;37(8S):S849-51. doi: 10.1016/j.arth.2022.01.052.
22. Kim YH, Park JW, Kim JS, Park SD. The relationship between the survival of total knee arthroplasty and postoperative coronal, sagittal and rotational alignment of knee prosthesis. Int Orthop. 2014;38(2):379-85. doi: 10.1007/s00264-013-2097-9.

DOI: http://dx.doi.org/10.1590/1413-785220263402e290496

TOURNIQUET USE DOES NOT AFFECT BLEEDING AND SURGICAL TIME IN ROBOTIC-ASSISTED KNEE ARTHROPLASTY

TORNIQUETE NÃO ALTERA O SANGRAMENTO E NEM O TEMPO CIRÚRGICO NA ARTROPLASTIA DE JOELHO COM ASSISTÊNCIA ROBÓTICA

João Paulo F. Guerreiro[1,2,3], *João Vitor Dias Balan*[1], *Marsal M. H. de Vilhena*[2], *Sergio Guimarães M. V. Filho*[2], *Paulo Roberto Bignardi*[1], *Marcus Vinicius Danieli*[1,2,3]

1. Pontifícia Universidade Catolica do Parana, Londrina, Parana, Brazil.
2. Hospital Evangelico de Londrina, Londrina, Parana, Brazil.
3. Hospital de Ortopedia UNIORTE, Londrina, Parana, Brazil.

ABSTRACT

Objective: To compare bleeding and surgical time in patients undergoing Total Knee Arthroplasty (TKA) with robotic assistance with and without the use of a tourniquet. Methods: Retrospective study with analysis of medical records. Patients were divided into two groups: one group in which robotic-assisted TKA was performed using a tourniquet and the other without. The values of hemoglobin (Hb) and hematocrit (Ht) preoperative and 24 hours after surgery, the estimated blood loss, number of transfusions and surgical time were compared between the groups. Results: 108 patients were included, with 59 in the group using a tourniquet and 49 without. There was no difference between the mean Hb and Ht values between the groups preoperatively ($p = 0.287$ and $p = 0.508$) and 24 hours ($p = 0.252$) after surgery. There was also no difference between the estimated blood loss in each group ($p = 0.265$). Surgical time was not different between groups ($p = 0.179$). There was no need for transfusions in any patient. Conclusion: Robotic-assisted TKA surgeries, whether performed with or without a tourniquet, showed no significant differences in the drop in Hb and Ht levels 24 hours after surgery, estimated blood loss, transfusions, and surgical time. ***Level of Evidence III; Retrospective cohort study.***

Keywords: Robotic surgical procedures; Arthroplasty; Bleeding; Knee; Tourniquet.

RESUMO

Objetivo: Comparar o sangramento e o tempo cirúrgico em pacientes submetidos à Artroplastia Total do Joelho (ATJ) com assistência robótica com e sem uso de torniquete. Métodos: Estudo retrospectivo com análise de prontuários. Os pacientes foram divididos de forma aleatória por sorteio em dois grupos: um grupo em que a ATJ assistida por robótica foi realizada com torniquete e outro sem. Os valores de hemoglobina (Hb) e hematócrito (Ht) pré-operatórios e 24 horas após a cirurgia, a perda sanguínea estimada, o número de transfusões e o tempo cirúrgico foram comparados entre os grupos. Resultados: foram incluídos 108 pacientes, sendo 59 no grupo que utilizou torniquete e 49 sem. Não houve diferença entre os valores médios de Hb e Ht entre os grupos no pré-operatório ($p = 0,287$ e $p = 0,508$) e 24 horas ($p = 0,252$) após a cirurgia. Também não houve diferença entre a perda sanguínea estimada em cada grupo ($p = 0,265$). O tempo cirúrgico não foi diferente entre os grupos ($p = 0,179$). Não houve necessidade de transfusões em nenhum paciente. Conclusão: As cirurgias de ATJ assistidas por robô, realizadas com ou sem torniquete, não mostraram diferenças significativas na queda dos níveis de Hb e Ht 24 horas após a cirurgia, perda sanguínea estimada, transfusões e tempo cirúrgico. ***Nível de Evidência III; Estudo de coorte retrospectiva.***

Descritores: *Procedimentos cirúrgicos robóticos; Artroplastia; Sangramento; Joelho; Torniquete.*

Citation: Guerreiro JPF, Balan JVD, Vilhena MMH, V. Filho SGM, Bignardi PR, Danieli MV. Tourniquet use does not affect bleeding and surgical time in robotic-assisted knee arthroplasty. Acta Ortop Bras. [online]. 2026;34(Spe.2): Page 1 of 4. Available from URL: http://www.scielo.br/aob.

INTRODUCTION

The use of robotic technology in surgery has proven effective in improving precision during soft tissue dissection, as well as contributing to enhancing the postoperative rehabilitation process in different medical fields.[1] Robotic-Assisted Total Knee Arthroplasty (TKA) allows for better precision in bone cuts, leading to improved implant positioning and less soft tissue damage[2], factors that may be related to higher patient satisfaction and increased implant longevity.[3] Additionally, it could be associated to reduced blood loss[4] and decrease postoperative pain in patients[5].

All authors declare no potential conflict of interest related to this article.

The study was conducted at Hospital de Ortopedia UNIORT.E, Londrina, Parana, Brazil.
Correspondence: João Paulo F. Guerreiro. Londrina, Paraná, Brazil. drjoaopauloguerreiro@gmail.com

Article received on 01/19/2025 approved on 09/23/2025.
Handling Editor: Camilo Partezani Helito

The use of a tourniquet in TKA procedures has become a topic of debate in the literature in recent years.[6] In conventional TKA, some studies have shown an increase in hidden intraoperative blood loss[7], a higher incidence of infections[8], and postoperative pain, in patients operated with a tourniquet compared to those where it was not used.[6] In robotic-assisted TKA, this divergence regarding the use of the tourniquet persists, and there are few comparative studies. Lai et al.[9]demonstrated greater hidden bleeding, more postoperative pain, and muscle injury in patients operated with a tourniquet during robotic-assisted arthroplasty and justified these findings by the longer intraoperative time related to the robotic assistance. However, a recent meta-analysis showed no significant difference in surgical time between conventional and robotic surgery[10].
Given the ongoing controversy, this study aimed to compare patients undergoing robotic-assisted TKA with and without the use of a tourniquet. The focus was on analyzing whether there was a difference in blood loss 24 hour after surgery and in surgical time.

METHODS

The present study was conducted after approval by the Research Ethics Committee in accordance with resolution No. 466/2012 of the National Health Council and the Declaration of Helsinki with number CAAE: 71836523.2.0000.5696. A retrospective study was performed with the analysis of medical records of patients who underwent robotic-assisted TKA between October 2022 and June 2023. Patients with a diagnosis of rheumatoid arthritis, patients with coagulation disorders, or the useof anticoagulants up to 7 days before surgery were not included. Patients were divided into two groups (one in which the surgery was performed using a tourniquet and another without) randomly by draw and operated by four surgeons with more than 10 years of experience in knee arthroplasties from the same team and following the same protocol. Preoperative Hb and Ht values, as well as those 24 hours after surgical procedure, the estimated blood loss calculation, and the time required to perform the procedure, were recorded and compared between the groups.
All patients operated on during the period were included and had blood samples collected via peripheral puncture preoperatively and 24 hours after surgery. Additionally, the surgical time for each procedure was recorded by the nursing and anesthesia team. All patients underwent spinal anesthesia, were operated on via a medial parapatellar approach, maintaining ischemia from the beginning of the skin incision until the final dressing in the cases of tourniquet use. The implants used were always cemented, without patellar replacement, and using the same instrumentation with robotic arm assistance during surgery (ROSA® Knee System, Zimmer, Warsaw, IN, USA). No suction drains were used in any case. All patients received 1g of intravenous tranexamic acid at anesthetic induction. Mechanical thromboembolic prophylaxis was implementedusingelastic stockings and an intermittent pneumatic compression pump for the first 24 hours after the procedure. Pharmacological prophylaxis consisted of 10mg of oral rivaroxaban administered 6 hours after the procedure, followed by a dose every 24 hours during hospitalization and continuing until the tenth postoperative day for all patients.
The obtained results were statistically analyzed by comparing the two groups. The following parameters underwent statistical analysis: Hb and Ht values before and 24 hours after surgery, decrease in Hb and Ht values 24 hours after the procedure, calculation of estimated blood loss by Body Mass Index (BMI) (using estimates from Nadler et al.[11] and equations described by Lisander et al.[12]), surgery time, sex, age, BMI, and number of transfusions. The criterion for indicating transfusion was Hb less than 7g/dl associated with clinical symptoms such as hemodynamic instability, oliguria, decreased level of consciousness, or poor general condition.
The categorical variable was presented by frequency and percentage. Quantitative variables were analyzed for normality using the Shapiro-Wilk test. The values are described as mean ± standard deviation (SD). Pearson's chi-square test was used to assess the statistical significance of qualitative variables, and the t-test was used for numerical data according to normality. The results were analyzed using the Statistical Package for the Social Sciences (SPSS) - 23.0 (IBM Corp., Armonk, NY, USA), with a confidence level of 5% established for all tests applied.

RESULTS

One hundred and eight patients were included in the study. The tourniquet group consisted of 59 patients, whilethe non-tourniquet group had 49 patients (Figure 1). The mean age inthe tourniquet group was 68.1 years, with a standard deviation of 7.6 years, while in the non-tourniquet group it was 67.4 years, with a standard deviation of 9.5 years. There was no statistically significant difference in age between the groups. There was also no statistically significant difference related to gender distribution, BMI, preoperative Hb and Ht between groups (Table 1).
A shorter mean operative time was observed in the tourniquet group (108.7 ± 20.4 min) compared to the non-tourniquet group (114.4 ± 23.2 min), but without a significant statistical difference (Table 2). Regarding bleeding evaluation, the mean reduction in Hb was slightly lower in the tourniquet group (2.28 ± 0.92 g/dL) compared to the non-tourniquet group (2.54 ± 1.36 g/dL), but it was also not statistically significant (Table 2). Estimated blood loss was lower in the tourniquet group (765.4 ± 290.6 mL) compared to the non-tourniquet group (842.4 ± 421.4 mL), however, this difference was also not statistically significant (p=0.265). No patient required a blood transfusion (Table 2).

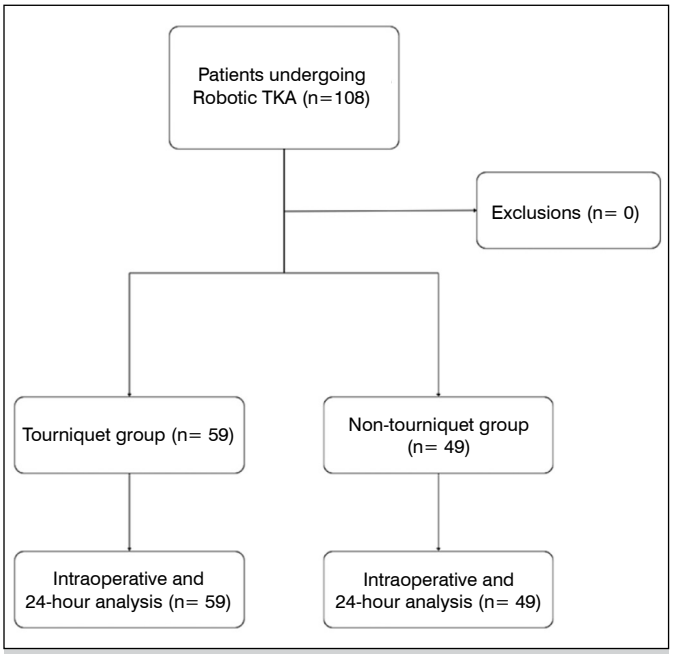

Total Knee Arthroplasty (TKA).

Figure 1. Flowchart of patients evaluated after robotic TKA.

DICUSSION

This study suggests that the use of a tourniquet in robotic assisted TKA does not lead to reduce bleeding 24 hours after surgery (p=0.265), nor does it reduce operative time. Lai et al.[9] conducted a randomized, controlled, double-blind trial comparing similar

<< SUMÁRIO

Table 1. Demographic characteristics of the study population.

Variable	Tourniquet group (n=59)	Non-tourniquet group (n=49)	P*
Age (years) (mean±SD)	68.1 ± 7.6	67.4 ± 9.5	0.648
Male, n (%)	24 (40.7)	29 (59.2)	0.056
BMI (mean±SD)	30.1 ± 4.4	30.4 ± 4.9	0.712
Hemoglobin, g/dl (mean±SD)	13.97 ± 1.30	14.25 ± 1.48	0.287
Hematocrit, % (mean±SD)	41.60 ± 3.86	42.12 ± 4.41	0.508

Standard deviation (SD); Body mass index (BMI).

Table 2. Comparison between the groups regarding surgical time and bleeding.

Variable	Tourniquet group (n=59)	Non-tourniquet group(n=49)	P*
Surgical time, min (mean±SD)	108.7 ± 20.4	114.4 ± 23.2	0.179
Hemoglobin reduction (g/dL)	2.28 ± 0.92	2.54 ± 1.36	0.252
Estimated blood loss (ml)	765.4 ± 290.6	842.4 ± 421.4	0.265
Transfusion (n)	0	0	N/A

Standard deviation (SD).

outcomes, including bleeding and operative time, in patients undergoing robotic-assisted TKA, but with only 14 patients in each group. Many studies compare robotic TKA to conventional techniques but do not compare the use or not of the tourniquet[13,14,15]. We have shown that the use of a tourniquet in robotic-assisted TKA resulted in a slightly lower mean blood loss but not significantly different in volume compared to the non-ischemic technique (765.4 ml vs. 842.4 ml). Similarly, the study conducted by Lai et al.[9] showed that although the tourniquet appeared to reduce intraoperative blood loss, it did not reduce hidden blood loss. Another study evaluating conventional TKA also found similar results regarding bleeding with tourniquet use.[16] Robotic-assisted surgery already indicates better outcomes in terms of blood loss compared to conventional techniques when both are performed with a tourniquet.[17]

Another data point that did not show a significant difference between the groups was surgical time. This finding differs from recent meta-analyses conducted with data from surgeries without robotic assistance, which indicate the tourniquet as a factor reducing surgical time.[6,7] We understand that including a larger number of patients in the study might possibly show some difference in this variable.The surgeons experience in operating without a tourniquet couldalready narrowed the surgical time even using robotic arm assistance.

This study has limitations. First, because it is a retrospective study. A prospective randomized study with the same number of patients might yield different results. Second, it uses data from a single center, which may limit the number of patients studied, although it reduces the bias of comparing different surgeons with different practices. Third, we did not have evaluations beyond 24 hours post-surgery because many patients were discharged before 48 hours after surgery, making it difficult to collect new bloodtests. At the end of the study, it was observed that robotic-assisted surgery can be performed without the use of a tourniquet without compromising surgical time and without causing significant bleeding. This may help avoid the complications already described related to tourniquet use.[6,18]

CONCLUSION

Robotic-assisted TKA surgeries performed with and without the use of a tourniquet showed no significant difference in the decrease in Hb and Ht levels 24 hours after surgery, estimated blood loss, transfusions, and surgical time.

ACKNOWLEDGEMENTS

All authors declare thanks to everyone involved in some way in the project directly and indirectly.

CONTRIBUTIONS OF THE AUTHORS

Each author contributed individually and significantly to the development of the article. JPFG: wrote and reviewed the article, analyzed the results and developed the statistical analysis, participated in the intellectual conception of the study and coordinated the entire project; JVDB: collected data, wrote and revised the article; MMHV: collected data, wrote and revised the article; SGMVF: collected data, wrote and revised the article; VT: collected data, wrote and revised the article PRB: analyzed the results and developed the statistical analysis; MVD: reviewed the article, participated in the intellectual conception of the study.

DATA AVAILABILITY DECLARATION

The contents underlying the research are available in the manuscript.

REFERENCES

1. Haddad FS. Evolving techniques: the need for better technology. Bone Joint J. 2017;99-B(2):145-6. doi: 10.1302/0301-620X.99B2.38085.
2. Pailhé R. Total knee arthroplasty: Latest robotics implantation techniques. Orthop Traumatol Surg Res. 2021;107(1S):102780. doi: 10.1016/j.otsr.2020.102780.
3. Rivière C, Iranpour F, Auvinet E, Howell S, Vendittoli PA, Cobb J, Parratte S. Alignment options for total knee arthroplasty: A systematic review. Orthop Traumatol Surg Res. 2017;103(7):1047-56. doi: 10.1016/j.otsr.2017.07.010.
4. Onggo JR, Onggo JD, De Steiger R, Hau R. Robotic-assisted total knee arthroplasty is comparable to conventional total knee arthroplasty: a meta-analysis and systematic review. Arch Orthop Trauma Surg. 2020;140(10):1533-49. doi: 10.1007/s00402-020-03512-5.
5. Kayani B, Konan S, Huq SS, Tahmassebi J, Haddad FS. Robotic-arm assisted total knee arthroplasty has a learning curve of seven cases for integration into the surgical workflow but no learning curve effect for accuracy of implant positioning. Knee Surg Sports Traumatol Arthrosc. 2019;27(4):1132-41. doi: 10.1007/s00167-018-5138-5.
6. Ahmed I, Chawla A, Underwood M, Price AJ, Metcalfe A, Hutchinson CE, et al. Time to reconsider the routine use of tourniquets in total knee arthroplasty surgery. Bone Joint J. 2021;103-B(5):830-9. doi: 10.1302/0301-620X.103B.BJJ-2020-1926.R1.
7. Sun C, Zhang X, Ma Q, Tu Y, Cai X, Zhou Y. Impact of tourniquet during total knee arthroplasty when tranexamic acid was used: a meta-analysis of randomized controlled trials. J Orthop Surg Res. 2022;17(1):18. doi: 10.1186/s13018-021-02898-1.
8. Magan AA, Dunseath O, Armonis P, Fontalis A, Kayani B, Haddad FS. Tourniquet use in total knee arthroplasty and the risk of infection: a meta-analysis of randomised controlled trials. J Exp Orthop. 2022;9(1):62. doi: 10.1186/s40634-022-00485-9.
9. Lai YH, Xu H, Su Q, Wan XF, Yuan MC, Zhou ZK. Effect of tourniquet use on blood loss, pain, functional recovery, and complications in robot-assisted total knee arthroplasty: a prospective, double-blinded, randomized controlled trial. J Orthop Surg Res. 2022;17(1):118. doi: 10.1186/s13018-022-02992-y.
10. Ren Y, Cao S, Wu J, Weng X, Feng B. Efficacy and reliability of active robotic-assisted total knee arthroplasty compared with conventional total knee arthroplasty:

a systematic review and meta-analysis. Postgrad Med J. 2019;95(1121):125-33. doi: 10.1136/postgradmedj-2018-136190.
11. Nadler SB, Hidalgo JH, Bloch T. Prediction of blood volume in normal human adults. Surgery. 1962;51(2):224-32.
12. Lisander B, Ivarsson I, Jacobsson SA. Intraoperative autotransfusion is associated with modest reduction of allogeneic transfusion in prosthetic hip surgery. Acta Anaesthesiol Scand. 1998;42(6):707-12. doi: 10.1111/j.1399-6576.1998.tb05305.x.
13. Kim YH, Yoon SH, Park JW. Does Robotic-assisted TKA Result in Better Outcome Scores or Long-Term Survivorship Than Conventional TKA? A Randomized, Controlled Trial. Clin Orthop Relat Res. 2020;478(2):266-75. doi: 10.1097/CORR.0000000000000916. Erratum in: Clin Orthop Relat Res. 2021;479(6):1407.
14. Song EK, Seon JK, Park SJ, Jung WB, Park HW, Lee GW. Simultaneous bilateral total knee arthroplasty with robotic and conventional techniques: a prospective, randomized study. Knee Surg Sports Traumatol Arthrosc. 2011;19(7):1069-76. doi: 10.1007/s00167-011-1400-9.
15. Bensa A, Sangiorgio A, Deabate L, Illuminati A, Pompa B, Filardo G. Robotic-assisted mechanically aligned total knee arthroplasty does not lead to better clinical and radiological outcomes when compared to conventional TKA: a systematic review and meta-analysis of randomized controlled trials. Knee Surg Sports Traumatol Arthrosc. 2023;31(11):4680-91. doi: 10.1007/s00167-023-07458-0.
16. Liu D, Graham D, Gillies K, Gillies RM. Effects of tourniquet use on quadriceps function and pain in total knee arthroplasty. Knee Surg Relat Res. 2014;26(4):207-13. doi: 10.5792/ksrr.2014.26.4.207.
17. Xu JZ, Li LL, Fu J, Xu C, Zhang GQ, Chai W, et al. Comparison of serum inflammatory indicators and radiographic results in MAKO robotic-assisted versus conventional total knee arthroplasty for knee osteoarthritis: a retrospective study of Chinese patients. BMC Musculoskelet Disord. 2022;23(1):418. doi: 10.1186/s12891-022-05373-y.
18. Pavão DM, Pires eAlbuquerque RS, de Faria JLR, Sampaio YD, de Sousa EB, Fogagnolo F. Optimized Tourniquet Use in Primary Total Knee Arthroplasty: A Comparative, Prospective, and Randomized Study. J Arthroplasty. 2023;38(4):685-90. doi: 10.1016/j.arth.2022.10.026.

DOI: http://dx.doi.org/10.1590/1413-785220263402e301177

PEDIATRIC GIANT CELL TUMOR: A NATIONAL MULTICENTER STUDY

TUMOR DE CÉLULAS GIGANTES PEDIÁTRICO: ESTUDO NACIONAL MULTICÊNTRICO

Pedro Egon Gewehr[1], Julie Cerutti[1], Gabriella Sitya Moojen da Silveira[2], Bruno Pereira Antunes[1], Olavo Pires de Camargo[3], Marcelo Barbosa Ribeiro[4], Eduardo Areas Toller[5], Sylvio Cesar Sargentini[5], Alexandre David[6], Glauco Jose Pauka Mello[7], Alex Guedes[8], Edgard Eduard Engel[9], Michelle Ghert[10], Ricardo Gehrke Becker[1]

1. Hospital de Clinicas de Porto Alegre (HCPA), Departamento de Oncologia Ortopedica, Porto Alegre, RS, Brazil.
2. Pontificia Universidade Catolica do Rio Grande do Sul, Faculdade de Medicina, Porto Alegre, RS, Brazil.
3. Universidade de Sao Paulo, Faculdade de Medicina, Hospital das Clinicas, (HC-FMUSP), Departamento de Ortopedia e Trauma, Sao Paulo, SP, Brazil.
4. Universidade Federal do Piaui, Teresina, PI, Brazil.
5. Hospital do Cancer de Barretos, Departamento de Oncologia Ortopedica, Sao Paulo, SP, Brazil.
6. Santa Casa de Porto Alegre, Servico de Ortopedia e Trauma, Porto Alegre, RS, Brazil.
7. Hospital Erasto Gaertner, Servico de Ortopedia e Trauma, Curitiba, PR, Brazil.
8. Hospital Santa Izabel, Salvador, BA, Brazil.
9. Hospital das Clinicas de Ribeirao Preto, Ribeirao Preto, SP, Brazil.
10. University of Maryland, Baltimore, USA.

ABSTRACT

Objective: To describe the clinical and epidemiological profile and local recurrence rate of pediatric giant cell tumor of bone (GCTB) in patients under 14 years, based on a Brazilian multicenter cohort. Methods: Retrospective analysis of 18 patients (≤14 years) with histologically confirmed GCTB treated at 7 oncology centers. Some of the collected variables included demographics, tumor location, and Campanacci radiographic grade. Data were centrally consolidated following validation. Results: The median age was 13 years (range, 7–14 years), and 67% of the patients were female. Long bones were affected in 67% of the cases. Five tumors involved the hand/wrist and were mostly Campanacci's grade 3. Treatments included curettage (44%) and resection (50%), with local adjuvants used in 50% of cases. Local recurrence occurred in 11% of patients. Denosumab was used in 39%, with no subsequent recurrences. No pulmonary metastasis was observed. Conclusions: Most patients were adolescent girls with tumors arising in long bones, especially around the knee, or in the hand and wrist, where lesions were more aggressive and frequently grade 3. The demographic and clinical profile was similar to that of adults, but with a lower risk of recurrence in long bones. ***Level of evidence III; Retrospective cohort study.***

Keywords: Giant Cell Tumor of Bone; Bone Neoplasms; Local Neoplasm Recurrence; Medical Oncology; Epiphyses; Therapeutics.

RESUMO

Objetivo: Descrever perfil clínico e epidemiológico e taxa de recidiva local do tumor de células gigantes do osso (TCG) em crianças com menos de 14 anos, com base em uma coorte multicêntrica brasileira. Métodos: Análise retrospectiva de 18 pacientes (≤14 anos) com diagnóstico histológico confirmado de TCG tratados em 7 centros de oncologia. Algumas das variáveis coletadas incluíram dados demográficos, localização tumoral e classificação de Campanacci. Os dados foram consolidados centralmente. Resultados: A mediana de idade foi 13 anos (intervalo 7–14); 67% eram do sexo feminino. Ossos longos foram acometidos em 67%. Cinco tumores envolveram mão/punho. Os tratamentos incluíram curetagem (44%) e ressecção (50%), com uso de adjuvantes locais em 50%. Recorrência local ocorreu em 11%. Denosumabe foi utilizado em 39% dos casos, sem recorrências subsequentes. Não foram observadas metástases pulmonares. Conclusões: A maioria dos pacientes eram adolescentes do sexo feminino com tumores localizados em ossos longos, especialmente ao redor do joelho, ou na mão e no punho, onde as lesões se mostraram mais agressivas e frequentemente classificadas como grau 3. O perfil demográfico e clínico foi semelhante ao de adultos, mas com menor risco de recidiva nos ossos longos. ***Nível de evidência III; Estudo de coorte retrospectivo.***

Descritores: *Tumor de Células Gigantes do Osso; Neoplasias Ósseas; Recidiva Local de Neoplasia; Oncologia; Epífises; Terapêutica.*

Citation: Gewehr PE, Cerutti J, Silveira GSM, Antunes BP, Camargo OP, Ribeiro MB, Toller EA, Sargentini SC, David A, Mello GJP, Guedes A, Engel EE, Ghert M, Becker RG. Pediatric giant cell tumor: a national multicenter study. Acta Ortop Bras. [online]. 2026;34(Spe.2): Page 1 of 5. Available from URL: http://www.scielo.br/aob.

All authors declare no potential conflict of interest related to this article.

The study was conducted at Hospital de Clinicas de Porto Alegre (HCPA) as the coordinating center with the participation of Hospital Sao Marcos, Hospital de Amor, Santa Casa de Misericordia de Porto Alegre, Hospital de Clinicas de Ribeirao Preto, Institute of Orthopedics and Trauma of HC-FMUSP, Hospital Santa Izabel, and Hospital Erasto Gaertner.
Correspondence: Ricardo Gehrke Becker. 339/701, Rua Antonio Parreiras, Porto Alegre, RS, Brazil. 90450050. rbecker@hcpa.edu.br

Article received on 11/03/2025 approved on 04/15/2026.
Handling Editor: Andre Ferrari de Camargo

INTRODUCTION

Giant cell tumor of the bone (GCTB) is a rare neoplasm, representing approximately 5% of all primary bone tumors.[1] In youth, GCTB is even less common but tends to behave more aggressively than in adults. Most pediatric cases occur in adolescents, with a slightly higher prevalence in females than in males. The mean age at diagnosis ranges between 12 and 16 years, and the tumor most frequently affects the long bones, particularly the distal femur, distal radius, and proximal tibia.[2-5] Pulmonary metastases are rare and indicate more aggressive behavior and a worse prognosis.[6]

While epiphyseal or metaepiphyseal involvement is typical due to active bone growth in skeletally immature patients with open physis, GCTB may arise exclusively in the metaphysis. This atypical presentation challenges the classical concept of a predominantly epiphyseal lesion and broadens the differential diagnosis of primary metaphyseal bone tumors in younger patients.[3]

Pediatric GCTB also demonstrates distinct biological behavior, with significantly higher rates of local recurrence than in adults, especially in the presence of open physes and pathological fractures.[2,3,7] Despite these clinical differences, the histological spectrum remains similar to that observed in adults, characterized by multinucleated giant cells distributed within a fibrohistiocytic stroma. At the molecular level, pediatric tumors harbor Histone H3.3 family A (H3F3A) mutations and show increased Receptor Activator of Nuclear Factor Kappa-B Ligand (RANKL) expression and elevated Matrix Metallopeptidase 9 (MMP-9) levels, findings that have been associated with a greater risk of recurrence and fracture in this population.[8,9]

The management of GCTB in children follows principles similar to that in adults; however, treatment decisions must carefully balance local control with the preservation of joint function and growth potential.[7] Surgery remains the mainstay of therapy, while systemic agents such as denosumab are considered for cytoreduction or inoperable cases, and bisphosphonates may be used as adjuvants in recurrent or vertebral lesions.[4,9-15]

To better understand the epidemiology, treatment strategies, and local recurrence rates of pediatric GCTB in Brazil, we analyzed a multicenter cohort of patients aged ≤ 14 years. This study aimed to provide a descriptive analysis of the clinical and epidemiological profiles of these patients, as well as to identify the rate of local recurrence based on data from the participating centers.

PATIENTS AND METHODS

This retrospective cohort study was conducted using the database of a national multicenter project on orthopedic tumors, coordinated by the Brazilian Association of Orthopedic Oncology. A total of 18 patients diagnosed with GCTB up to the age of 14 years were included. A cutoff of 14 years was established to ensure that only skeletally immature patients with open physes were analyzed, since these biological characteristics influence both tumor presentation and the risk of local recurrence.

Data were obtained from seven orthopedic oncology centers in Brazil. Only patients with histopathological confirmation of GCTB and complete medical records available at the treating institution were included in this study. Patients were excluded if their diagnosis was uncertain or if their primary treatment was performed outside the referral center.

The study protocol was approved by the Research Ethics Committee of the Hospital de Clínicas de Porto Alegre, as well as by all participating institutions (CAAE 94280918.0.0000.5327). All procedures complied with the Declaration of Helsinki, the Brazilian General Data Protection Law, and the ethical guidelines established by the current resolutions of the Brazilian National Health Council.

Patient confidentiality was preserved by assigning a numerical code to each case. Data were extracted from electronic and paper medical records, reviewed locally, and subsequently forwarded to the coordinating center using a secure system. Inconsistencies or missing information were returned to the respective institutions for clarification before final consolidation of the data. After validation, the dataset was compiled and analyzed using Microsoft Excel and SPSS (version 28.0).

The variables assessed included demographic information (age and sex), tumor location, presence of pathological fracture, treatment modality (curettage, resection, or amputation), use of local adjuvants, type of cavity filling (bone graft or polymethylmethacrylate), systemic therapy (denosumab or bisphosphonates), and presence of pulmonary metastases at diagnosis. Tumor aggressiveness was classified using the Campanacci system.[16] Local recurrence was defined as radiological or histological evidence of tumor regrowth after the initial treatment. Continuous variables were summarized using the mean, median, standard deviation, or interquartile range, while categorical variables were expressed as absolute numbers and proportions.

RESULTS

Demographics and tumor characteristics

The mean duration of follow-up was 50.8 months (from diagnosis to last follow-up visit). The median age at diagnosis was 13 years (range, 7–14 years), with a predominance of female patients (12, 66.7%). The majority of cases originated in the long bones (12, 66.7%), particularly around the knee, including the distal femur (four), proximal tibia (three), and distal radius (three). Involvement of the hand and wrist was noted in five patients (27.8%), often exhibiting aggressive radiographic features. According to the Campanacci's classification, most lesions were grade 3 (nine), followed by grade 2 (seven) and grade 1 (two). Tumors located in the hand and wrist (five) were predominantly classified as grade 3 (four) (Table 1).

Treatment and local recurrence

Seventeen patients underwent surgical treatment: intralesional curettage in eight (44.4%) (Figure 1) and resection in nine (50.0%). A patient with a periacetabular tumor (Figure 2) was treated exclusively with denosumab, remaining in remission until the last evaluation (24 months). The use of surgical adjuvants such as high-speed burr, phenol, or alcohol was documented in nine cases, typically combined with cavity filling using polymethylmethacrylate (Figure 3) or bone grafting. In two cases, reconstruction with autologous fibula grafting and osteosynthesis was required following resection. Local recurrence was observed in two patients (11.1%), both females with Campanacci's grade 3 tumors (Table 2). In these cases involving the sacrum, one patient initially underwent curettage without adjuvant therapy, resulting in recurrence after approximately 16 months, which was subsequently managed with a second curettage. The other patient was treated with resection, experienced recurrence after 4 months, and commenced treatment with denosumab. Both patients achieved local disease control until the last follow-up. Notably, none of the patients who received adjuvant therapy experienced recurrence. Systemic therapy with denosumab was administered to seven patients (38.9%), most commonly as a neoadjuvant approach for cytoreduction prior to surgery, and in one case for recurrent disease. No pulmonary metastases were identified in this cohort of patients.

DISCUSSION

The age distribution in our series, characterized by a median age of 13 years, aligns with the observation that giant cell tumor of bone

Table 1. Clinical and demographic characteristics of the patients.

Characteristics	n (%)
Sex	
Female	12 (66.67%)
Age (years)	
< 12 years	4 (22.22%)
≥ 12 and < 14 years	14 (77.78%)
Campanacci's classification	
Grade 1	2 (11.11%)
Grade 2	7 (38.89%)
Grade 3	9 (50.00%)
Surgery	
No	1 (5.56%)
Yes	17 (94.44%)
Type of surgery	
None	1 (5.56%)
Curettage	8 (44.44%)
Resection	9 (50.00%)
Filling type	
None	9 (50.00%)
Cement	5 (27.78%)
Bone graft	4 (22.22%)
Adjuvants	
Drilling	4 (22.22%)
Fulguration	5 (27.78%)
Alcohol	2 (11.11%)
None	7 (38.89%)
Site	
Pelvic girdle	3 (16.67%)
Foot and ankle	4 (22.22%)
Elbow	1 (5.56%)
Hand and wrist	5 (27.78%)
Knee	3 (16.67%)
Others	2 (11.11%)
Pulmonary metastases	
No	18 (100.00%)
Local recurrence	
No	16 (88.89%)
Yes	2 (11.11%)
Denosumab	
No	11 (61.11%)
Yes	7 (38.89%)
Indication of denosumab	
Recurrence	1 (5.56%)
Cytoreduction	6 (33.33%)

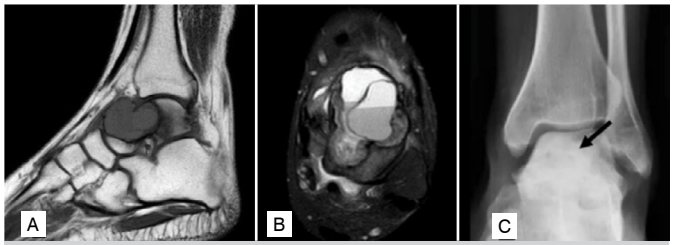

Figure 1. Case 12. (A) T1-weighted MRI of the left ankle showing a giant cell tumor of bone (GCTB) in the talus with cortical rupture (Campanacci grade 3); (B) axial T2 SPIR sequence demonstrating fluid–fluid levels consistent with a secondary aneurysmal bone cyst; (C) late postoperative frontal radiograph after curettage and cavity filling (black arrow).

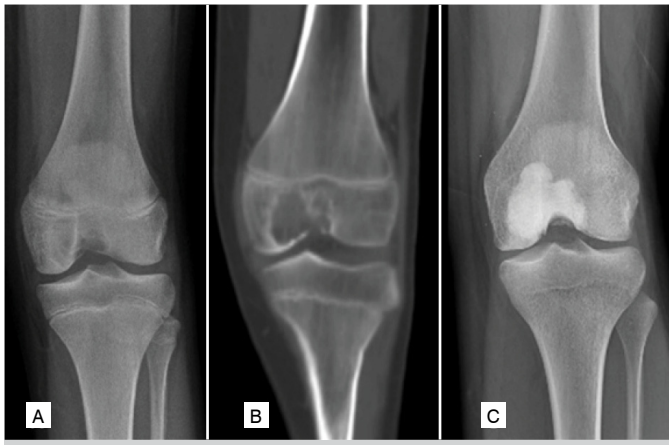

Figure 2. Case 8. (A) Anteroposterior radiograph and (B) coronal computed tomography of the left knee demonstrating a giant cell tumor of bone (GCTB) in the distal femoral epiphysis. (C) Anteroposterior radiograph at 24 months postoperatively showing PMMA filling without evidence of local recurrence.

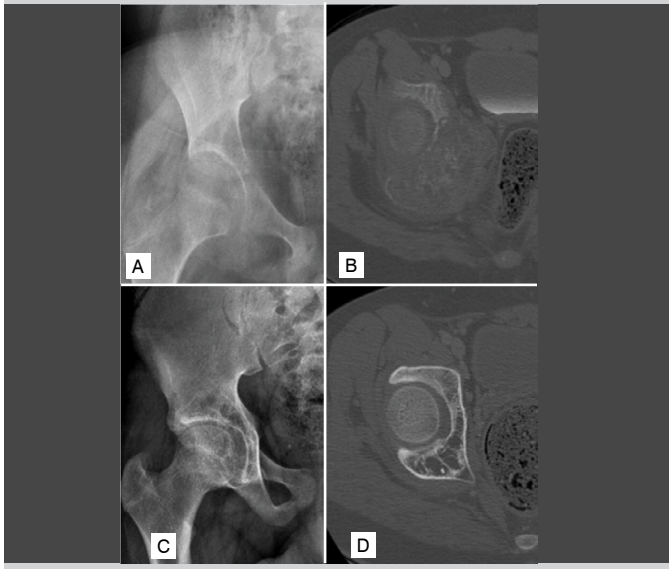

Figure 3. Case 4. (A) Anteroposterior radiograph and (B) axial computed tomography showing a large right periacetabular giant cell tumor of bone (GCTB). (C) Anteroposterior radiograph and (D) axial computed tomography demonstrating tumor volume reduction and ossification after denosumab therapy.

(GCTB) in pediatric patients is predominantly diagnosed in older children and adolescents. This pattern has been corroborated by other studies, such as those conducted in Korea and India, which have reported that the majority of cases occur during the second decade of life, particularly around puberty, when skeletal growth is most active.[3,17] The predominance of female patients in our cohort is also consistent with previous reports, suggesting that earlier physeal closure in females may contribute to a relatively higher incidence in this subgroup compared to males.[3,5,9] However, it is important to acknowledge that our findings may be subject to selection bias, as boys generally maintain open physes until later in adolescence; thus, if patients up to 17 years of age had been included, a higher proportion of males might have been represented in the cohort. Regarding anatomical distribution, most tumors arose in the long bones, with the knee region being the most frequently affected site, mirroring the classic adult predilection for the distal femur and proximal tibia reported in the literature.[7] The presence of five cases in the hand and wrist, most of which were classified as Campanacci's grade 3, suggests a more aggressive biological

Table 2. Case series and treatment.

No.	Age (y)	Sex	Site of lesion	Campanacci	Type of surgery	Filling type	Adjuvant	Type of adjuvant	Local recurrence	Denosumab and indication
1	7	F	Distal radius	3	Resection	None	None	-	No	No
2	8	M	Sacrum	3	Resection	None	No	-	Yes (4 mo postop.)	Yes. Recurrence
3	9	M	Phalanx/metacarpal	3	Curettage	None	None	-	No	No
4	10	M	Pelvis	1	None	-	None	-	No	Yes. Cytoreduction
5	12	F	Distal tibia	2	Curettage	Cement	Combined	Extensive curettage + fulguration	No	No
6	12	M	Distal tibia	2	Curettage	Cement	Combined	Extensive curettage + fulguration	No	Yes. Cytoreduction
7	13	F	Proximal fibula	2	Resection	Bone graft	Simple	Phenol/alcohol	No	No
8	13	F	Distal femur	1	Curettage	Cement	Simple	Fulguration	No	No
9	13	M	Mandible	3	Resection	None	None	-	No	Yes. Cytoreduction
10	13	F	Maxilla	3	Resection	None	None	-	No	Yes. Cytoreduction
11	13	F	Metatarsal	2	Resection	Bone graft + osteosynthesis	None	-	No	No
12	13	F	Talus	2	Curettage	Bone graft	Simple	Extensive curettage	No	No
13	13	F	Distal ulna	3	Resection	None	None	-	No	No
14	14	M	Proximal ulna	3	Curettage	Cement	Combined	Extensive curettage + fulguration	No	Yes. Cytoreduction
15	14	F	Phalanx/metacarpal	2	Resection	None	None	-	No	Yes. Cytoreduction
16	14	F	Phalanx/metacarpal	3	Resection	Bone graft	None	-	No	No
17	14	F	Proximal tibia	2	Curettage	Cement	Combined	Phenol/alcohol + fulguration	No	No
18	14	F	Sacrum	3	Curettage	None	None	-	Yes (16 mo postop.)	No

F = female; M = male; postop. = postoperative.

behavior at these sites.[4] This finding has also been highlighted in the adult population, where tumors in small bones often present at advanced radiographic stages due to the limited capacity of these structures to accommodate tumor growth.

Surgical treatments for pediatric GCTB include curettage and *en bloc* resection. Curettage, when combined with a high-speed burr, chemical or thermal adjuvants, and cavity filling, helps preserve the physis and nearby joints, facilitates quicker recovery, and—in our study—curettage with adjuvants did not lead to recurrence, reinforcing its status as the preferred local approach.[18] It is important to note that the sacrum recurrence managed with curettage did not involve adjuvants.[15,19] Nonetheless, it carries a higher risk of pathological fractures and recurrence compared to resection, especially in skeletally immature patients.[2,3] *En bloc* resection achieves lower recurrence rates but at the cost of greater functional morbidity, including joint sacrifice, limb length discrepancy, or deformity. Our two recurrences arose in grade 3 sacral tumors, a site where surgical access is limited and wide margins are constrained by the risk of neurological deficit, reflecting the inherent challenge of axial resections.[14,15]

Less common local modalities include radiotherapy and selective arterial embolization. Radiotherapy can achieve control in unresectable sacral or skull-base tumors, with stabilization and preservation of neurological function reported in adults, particularly when combined with denosumab or embolization. However, its use in children is limited by the risk of growth disturbance and secondary malignancy.[11] Embolization is valuable in hypervascular pelvic or sacral lesions, decreasing intraoperative blood loss, the need for transfusion, and operative time, while offering temporary pain relief or enabling staged resections. The effects are transient, requiring repeated sessions, and complications such as ischemia or neuropathy may occur. Both remain secondary to surgery.[15]

Denosumab has emerged as the most extensively studied systemic treatment for GCTB, particularly in patients with unresectable disease or when cytoreduction is required prior to surgery.[13,14] In our cohort, seven patients received denosumab, primarily as neoadjuvant therapy, and none experienced local recurrence during follow-up, thereby supporting its efficacy in carefully selected cases. In adults, denosumab provides reliable tumor control and can downstage lesions to facilitate joint preservation.[13,14] However, concerns persist regarding its use in skeletally immature patients, as the drug is FDA-approved only for skeletally mature adolescents.[10] Its off-label pediatric use is constrained by risks of growth disturbance, hypocalcemia, osteonecrosis of the jaw, and the potential for increased recurrence when curettage follows preoperative therapy. In our study, no short-term or mid-term complications were observed up to the final follow-up visit.[7,10-14,16,20]

Bisphosphonates, particularly zoledronic acid, have also been evaluated in pediatric and adult GCTB, with reports of symptomatic relief and local control, especially in spinal or pelvic disease where surgical morbidity is considerable. Their advantages include low cost and potential antitumor activity; however, their role remains less defined than that of denosumab. Adverse events include flu-like symptoms, hypocalcemia, and the rare but serious complication of osteonecrosis of the jaw. In children, the additional concern of altered bone metabolism and potential effects on growth plates limits their routine use, reserving them for selected cases of recurrence or axial involvement.[18]

A significant strength of this study is its status as the largest multicenter Brazilian series dedicated exclusively to patients under 14 years of age with giant cell tumor of bone, a rare and underreported demographic. By incorporating cases from multiple referral centers, the findings possess enhanced external validity. This study also provides comprehensive information on clinical presentation and treatment, emphasizing the use of local adjuvants and systemic therapy. Notably, our results highlight the aggressive nature of tumors in small bones, particularly in the hand and wrist, and affirm the efficacy of intralesional techniques with adjuvants in reducing recurrence.

However, this study has certain limitations. The rarity of pediatric GCTB results in a relatively small sample size, which diminishes the statistical power and limits the generalizability of the conclusions. The retrospective design is inherently prone to information bias, and variations in surgical techniques and adjuvant protocols across centers may have influenced the outcomes. Additionally, the follow-up duration was limited for some patients, potentially underestimating late recurrences or long-term complications. Functional outcomes, quality-of-life measures, and growth disturbances were not systematically assessed, restricting conclusions regarding the impact of the different treatment strategies. Finally, the off-label use of denosumab in skeletally immature patients constrains the ability to draw definitive conclusions regarding its long-term safety and efficacy in this population.

CONCLUSION

In pediatric GCTB cases in Brazil, most patients were adolescent girls with tumors arising in long bones, especially around the knee, or in the hand and wrist, where lesions were more aggressive and frequently grade 3. The demographic and clinical profile was broadly similar to that reported in adults, but with a lower risk of recurrence in long bones. Surgical management with curettage and resection yielded comparable outcomes, with local recurrence observed only in the sacrum. Importantly, the use of denosumab did not appear to increase recurrence in this cohort. These findings reinforce the need for individualized strategies that balance oncologic control with preservation of skeletal growth and function in the pediatric population.

CONTRIBUTIONS OF THE AUTHORS

Each author made a personal and significant contribution to the development of this article. GPE: writing of the article and data analysis. CJ: project administration and data analysis. SGSM: data analysis and literature review. ABP: data collection. COP: review of the article. RMB: data collection and review of the article. TEA: data collection and review of the article. SSC: data collection. DA: data collection and review of the article. MGJP: data collection and review of the article. GA: data collection and review of the article. EEE: data collection and review of the article. GM: review of the article. BRG: project administration, writing and review of the article.

DATA AVAILABILITY DECLARATION

The data will be available to reviewers on demand/upon request.

REFERENCES

1. WHO Classification of Tumours Editorial Board. Soft Tissue and Bone Tumors. 5th ed. Lyon: IARC Press; 2020.
2. Klenke FM, Wenger DE, Inwards CY, Rose PS, Sim FH. Giant cell tumor of bone: Risk factors for recurrence. Clin Orthop Relat Res. 2011;469(2):591-9. doi: 10.1007/s11999-010-1501-7.
3. Puri A, Agarwal MG, Shah M, Jambhekar NA, Anchan C, Behle S. Giant cell tumor of bone in children and adolescents. J Pediatr Orthop. 2007;27(6):635-9. doi: 10.1097/bpo.0b013e3181425629.
4. Rabuske WBS, Ghert M, Antunes BP, Galia CR, Pestilho JFCS, da Silveira GSM, et al. Giant Cell Tumor of The Distal Radius: Factors associated with local recurrence. Acta Ortop Bras. 2025;33(1):e289573. doi: 10.1590/1413-785220253301e289573.
5. Picci P, Manfrini M, Zucchi V, Gherlinzoni F, Rock M, Bertoni F, et al. Giant-cell tumor of bone in skeletally immature patients. J Bone Joint Surg Am. 1983;65(4):486-90. doi: 10.2106/00004623-198365040-00009.
6. Bertoni F, Present D, Enneking WF. Giant-cell tumor of bone with pulmonary metastases. J Bone Joint Surg Am. 1985;67(6):890-900. doi: 10.2106/00004623-198567060-00011.
7. Becker RG, Galia CR, Pestilho JFCS, Antunes BP, Baptista AM, Guedes A. Giant cell tumor of bone: A multicenter epidemiological study in Brazil. Acta Ortop Bras. 2024;32(1):e273066. doi: 10.1590/1413-785220243201e273066.
8. Al-Ibraheemi A, Inwards CY, Zreik RT, Wenger DE, Jenkins SM, Carter JM, et al. Histologic Spectrum of Giant Cell Tumor (GCT) of Bone in Patients 18 Years of Age and Below: A Study of 63 Patients. Am J Surg Pathol. 2016;40(12):1702-12. doi: 10.1097/pas.0000000000000715.
9. Pang YR, Zhou J, Chen CY, Zhao QQ, Sun KY, Liu ZY. [Pediatric giant cell tumor of bone: a clinicopathological analysis of 35 cases]. Zhonghua Bing Li Xue Za Zhi. 2024;53(11):1122-6. doi: 10.3760/cma.j.cn112151-20240430-00290.
10. Chawla S, Henshaw R, Seeger L, Choy E, Blay JY, Ferrari S, et al. Safety and efficacy of denosumab for adults and skeletally mature adolescents with giant cell tumor of bone: interim analysis of an open-label phase 2 study. Lancet Oncol. 2013;14(9):901-8. doi: 10.1016/S1470-2045(13)70277-8.
11. Palmerini E, Picci P, Reichardt P, Downey G. Malignancy in Giant Cell Tumor of Bone: A Review of the Literature. Technol Cancer Res Treat. 2019;18:1533033819840000. doi: 10.1177/1533033819840000.
12. Chawla S, Blay JY, Rutkowski P, Le Cesne A, Reichardt P, Gelderblom H, et al. Denosumab in patients with giant-cell tumour of bone: A multicentre, open-label, phase 2 study. Lancet Oncol. 2019;20(12):1719-29. doi: 10.1016/s1470-2045(19)30663-1.
13. Barreto BG, Santili C, Guedes A, Moreira FD, Paz CLD. Denosumab regimens in the treatment of giant cell tumor of bone: A systematic review with meta-analysis. World J Orthop. 2025;16(3):102520. doi: 10.5312/wjo.v16.i3.102520.
14. Barreto BG, Santili C, Guedes A, Paz CLD, Moreira FD, Mattos ESR. Therapeutic schemes of denosumab in the treatment of giant cell tumor of bone - Protocol for a systematic review with meta-analysis. Res Soc Dev. 2022;11(6):e26011629110. doi: 10.33448/rsd-v11i6.29110.
15. Martin C, McCarthy EF. Giant cell tumor of the sacrum and spine: series of 23 cases and a review of the literature. Iowa Orthop J. 2010;30:69-75.
16. Campanacci, M, Baldini N, Boriani S, Sudanese A. Giant-cell tumor of bone. J Bone Joint Surg Am. 1987;69(1):106-14. doi: 10.2106/00004623-198769010-00018.
17. Kim WJ, Kim S, Choi DW, Lim GH, Jung ST. Characteristics of Giant Cell Tumor of the Bone in Pediatric Patients: Our 18-Year, Single-Center Experience. Children (Basel). 2021;8(12):1157. doi: 10.3390/children8121157.
18. Arbeitsgemeinschaft Knochentumoren; Becker WT, Dohle J, Bernd L, Braun A, Cserhati M, et al. Local recurrence of giant cell tumor of bone after intralesional treatment with and without adjuvant therapy. J Bone Joint Surg Am. 2008;90(5):1060-7. doi: 10.2106/jbjs.d.02771.
19. Balke M, Ahrens H, Streitbuerger A, Koehler G, Winkelmann W, Gosheger G, et al. Treatment options for recurrent giant cell tumors of bone. J Cancer Res Clin Oncol. 2008;134(4):401-8. doi: 10.1007/s00432-008-0427-x.
20. Errani C, Tsukamoto S, Leone G, Righi A, Akahane M, Tanaka Y. Denosumab May Increase the Risk of Local Recurrence in Patients with Giant-Cell Tumor of Bone Treated with Curettage. J Bone Joint Surg Am. 2018;100(6):496-504. doi: 10.2106/jbjs.17.00057.

DOI: http://dx.doi.org/10.1590/1413-785220263402e297279

WHICH FACTORS CAN DEFINE THE PROGNOSIS OF ARTICULAR FRACTURES OF THE CAPITELLUM AND TROCHLEA?

QUAIS FATORES PODEM DEFINIR O PROGNÓSTICO DAS FRATURAS ARTICULARES DO CAPÍTULO E DA TRÓCLEA?

Ligia Gianfaldoni Gattás[1], Pedro Henrique Avi[1], Marcelo Fregoneze[2], José Octávio Soares Hungria[2], Rodrigo Peixoto Vargas[1], Caio Zamboni[1]

1. Irmandade da Santa Casa de Misericordia de Sao Paulo, Departamento de Ortopedia e Traumatologia, Sao Paulo, SP, Brazil.
2. Irmandade da Santa Casa de Misericordia de Sao Paulo, Departamento de Ortopedia e Traumatologia, Grupo de Cirurgia, Sao Paulo, SP, Brazil.

ABSTRACT

Introduction: Articular fractures of the distal humerus involving the capitellum and trochlea (AO 13B3) are complex and challenging to manage without consensus in the literature on the most appropriate management. Objective: Evaluate radiographic features and treatment-related factors that may be positively or negatively correlated with the outcome of these fractures. Methods: Sixteen adult patients who underwent surgery between 2007 and 2024 with at least one year of follow-up were analyzed retrospectively. Radiographic characteristics, postoperative range of motion, and complications were evaluated. Statistical analysis used Odds Ratio (OR) and Fisher's Exact Test. Results: Elbow stiffness occurred in 56% of patients, 83% of which were in cases with posterior wall involvement (OR=7.5; p=0.08). Preoperative immobilization for more than seven days was associated with range of motion impairment (60%, OR=3; p=0.58) and ulnar nerve neuropathy (30%, OR=6; p=0.09). All cases of ulnar neuropathy occurred in women with prolonged immobilization (OR=8.08; p=0.09). Conclusion: Posterior wall integrity is a relevant prognostic factor for the final range of motion. The propensity for ulnar neuropathy in women and those with prolonged immobilization, although without statistical significance, suggests the need for larger samples. ***Level of Evidence II; Retrospective study.***

Keywords: Capitellum Humerus Fractures; Trochlear Fractures, Humerus; Orthopedic Surgery; Prognosis; Postoperative Complications; Retrospective Studies.

RESUMO

Introdução: Fraturas articulares do úmero distal envolvendo capítulo e tróclea (AO 13B3) são complexas e de manejo desafiador, sem consenso na literatura com relação ao tratamento mais adequado. Objetivo: Avaliar fatores radiográficos e associados ao tratamento que possam correlacionar-se positiva ou negativamente ao desfecho dessas fraturas. Métodos: Dezesseis pacientes adultos submetidos a cirurgia entre 2007 e 2024, com pelo menos um ano de seguimento, foram analisados retrospectivamente. Foram avaliadas características radiográficas, arco de movimento pós-operatório e complicações. A análise estatística utilizou Odds Ratio (OR) e Teste Exato de Fisher. Resultados: Restrição do arco de movimento ocorreu em 56% dos pacientes, sendo 83% nos casos com acometimento da parede posterior (OR=7,5; p=0,08). Imobilização pré-operatória superior a sete dias associou-se ao comprometimento do arco de movimento (60%, OR=3; p=0,58) e neuropatia do nervo ulnar (30%, OR=6; p=0,09). Todos os casos de neuropatia ulnar ocorreram em mulheres com imobilização prolongada (OR=8,08; p=0,09). Conclusão: A integridade da parede posterior é um fator prognóstico relevante para o arco de movimento final. A propensão para neuropatia ulnar em mulheres e pacientes com imobilização prolongada, embora sem significância estatística, sugere a necessidade de amostras maiores. ***Nível de Evidência II; Estudo retrospectivo.***

Descritores: *Fraturas do Capítulo Umeral; Fraturas Trocleares do Úmero; Cirurgia Ortopédica; Prognóstico; Complicações Pós-Operatórias; Estudos Retrospectivos.*

Citation: Gattás LG, Avi PH, Fregoneze M, Hungria JOS, Vargas RP, Zamboni C. Which factors can define the prognosis of articular fractures of the capitellum and trochlea? Acta Ortop Bras. [online]. 2026;34(Spe.2): Page 1 of 4. Available from URL: http://www.scielo.br/aob.

INTRODUCTION

The distal humerus is divided into two columns, medial and lateral, which are extra-articular and articular, respectively. In its articular segment, it is formed by a "tie arch" connecting the distal end of the lateral column, composed by the capitellum; and in the most medial part, between the medial epicondyle and the capitellum, the trochlea (Figure 1). [1-3]

The capitellum and trochlea are irrigated by perforating condylar vessels that are branches of the recurrent radial, radial collateral, and recurrent interosseous arteries (Figure 2), which maintain an

All authors declare no potential conflict of interest related to this article.

The study was conducted at Irmandade da Santa Casa de Misericordia de Sao Paulo, Sao Paulo, SP, Brazil.
Correspondence: Ligia Gianfaldoni Gattas. 112, Dr. Cesario Mota Junior, Sao Paulo, SP, Brazil, 01221-010. ligia240788@gmail.com

Article received on 01/06/2025 approved on 11/09/2025.
Handling Editor: Kodi Edson

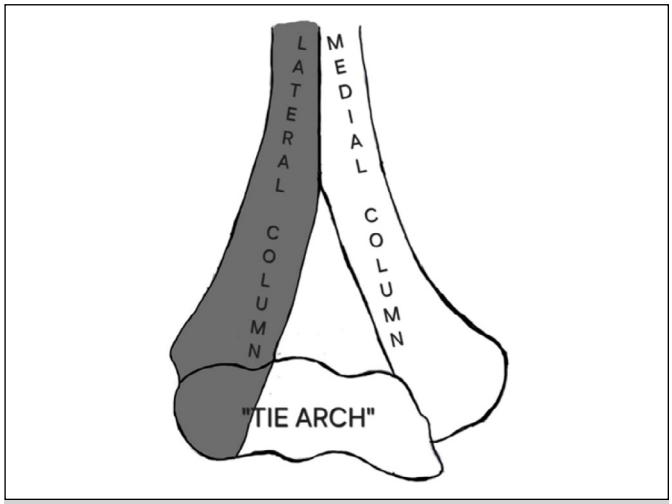

Source: Author's own work.

Figure 1. Column structure of the distal humerus – anterior view.

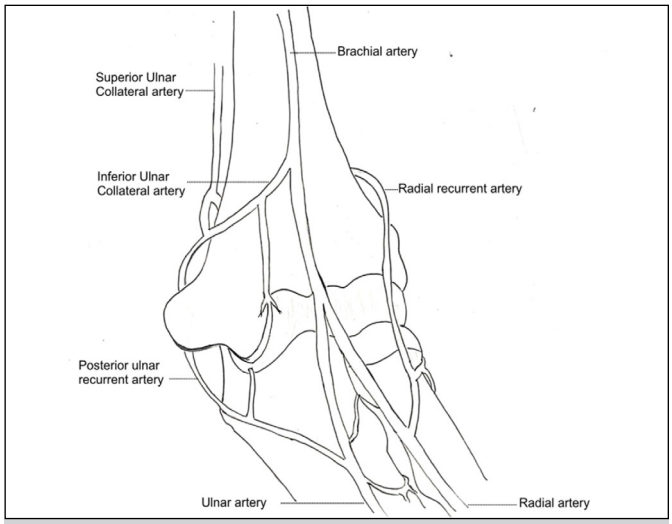

Source: Author's own work.

Figure 2. Extraosseous vascular anatomy – anterior view.

intimate relationship with the posterior wall of the distal end of the humerus, that may potentially suffer devascularization in fractures involving this region. [4-7]

Fractures of the distal humerus, involving the capitellum and trochlea, may occur isolated or combined. Isolated capitellum fractures represent 1% of elbow fractures and 3% to 6% of distal humerus fractures. Isolated trochlea fractures are rare.

Females are the most affected by this type of fracture, and this greater predisposition might be related to osteoporosis, *cubitus valgus* and elbow *recurvatum*.[5,10,11]

Several classifications for this type of fracture can be used. Anatomically, the AO classification divides them into extra-articular (13A), partially articular (13B), and complete articular (13C). In the present study, we will only use partially articular fractures in the coronal plane (13B3) and their respective subdivisions: capitellum fracture (13B3.1), trochlea fracture (13B3.2), and fracture of both (13B3.3).[12] In addition, we also have the Dubberley et al. classification, which is divided into: fracture of the capitellum with or without involvement the lateral trochlear ridge (type I); fracture of the capitellum and trochlea as a single piece (type II); fractures of both the capitellum and trochlea as separate fragments (type III). In this classification, they are subdivided according to posterior wall comminution: no posterior comminution (subtype A) and posterior comminution (subtype B).

There are several possibilities for surgical treatment, including open reduction and internal fixation, closed reduction, fragment excision, and arthroscopic reduction. However, there is no consensus regarding the most appropriate treatment, since distal intra-articular elbow fractures are difficult to manage both clinically and surgically with unpredictable outcomes.

We will retrospectively evaluate possible radiographic factors that correlate better and worse outcomes in operated patients. Among these factors analyzed, the integrity of the posterior wall and both isolated or combined involvement of the capitellum and trochlea. We also evaluated the time to procedure and preoperative immobilization time.

METHODOLOGY

Our work was approved by the ethics and research committee under code CAAE 78440024.2.0000.5479.

Our study consists of a retrospective and descriptive analysis based on the review of medical records of consecutive patients who suffered articular fractures of the distal humerus and underwent procedure by the Trauma Surgery Group of the Department of Orthopedics and Traumatology of Santa Casa de São Paulo from January 2007 to January 2024 with at least one year of follow-up.

The Inclusion criteria were adult patients of both genders with elbow fractures classified as AO 13B3. Patients with pathological bone fractures, incomplete radiographic data, or incomplete medical records were excluded from the study, as were those who did not agree to participate in the study.

Radiographic characteristics of the fracture were analyzed, such as posterior wall involvement, presence of isolated or combined fractures of the capitellum and trochlea, as well as other associated fractures. In addition, patient follow-up included evaluation of postoperative range of motion and complications presented by the patients.

For statistical analysis, the Odds Ratio (OR) was calculated, and Fisher's Exact Test was used to calculate the 95% significance level ($p<0.05$).

RESULTS

From 2007 to 2024, 16 patients with fractures classified as AO 13B3 were operated. Regarding the Dubberley et al. classification, eight patients were classified as type I (two of whom were subtype IB), four patients as type II (two were subtype IIB), and four as type III (two were subtype IIIB).

The average age of the patients was 44 years (26 to 75 years), with nine female patients. In all cases, a capitellum fracture was found, and in eight of these, a trochlea fracture was associated. Other associated fractures included: radial head (three patients), coronoid process (one patient), and medial and lateral condyle of the elbow (one patient), as shown in Table 1.

At the end of follow-up, patients presented an average range of motion of flexion 123° ± 20°, extension -25° ± 16°, pronation 80° ±11°, supination 75° ± 20°. We noted that 56% of operated patients developed elbow stiffness, and evaluating only cases where the posterior wall was compromised, this number rose to 83% (OR= 7.5; p = 0.08).

Among patients who had a preoperative immobilization of more than seven days, 60% developed a restricted range of motion (OR= 3; p = 0.58) and 30% suffered from ulnar nerve neuropathy (OR 6; p = 0.09) (Figure 3).

During follow-up, five patients (31%) presented major complications requiring reoperation: one patient needed synthesis material

Table 1. epidemiological data of patients with AO 13B3 fracture.

Gender	Age at trauma (years)	Posterior Wall Integrity	Dubberley	Associated Fractures	Fl.	Ext.	Pr.	Sup.	Complications
F	39	yes	IA	N	110º	-40º	80º	80º	N
M	26	yes	IA	N	110º	-5º	90º	90º	N
M	28	yes	IA	N	140º	0º	80º	90º	N
F	52	no	IIIB	N	140º	-20º	90º	70º	SMR
M	31	no	IIB	radial head	120º	-30º	80º	90º	N
F	58	no	IIIB	N	130º	-45º	80º	70º	Ulnar n. paresthesia
F	33	yes	IIA	N	90º	-20º	50º	20º	Ulnar n. paresthesia
F	55	yes	IIA	N	130º	-30º	70º	70º	N
M	27	no	IB	N	80º	-10º	90º	90º	SMR and infection
M	36	yes	IA	coronoid process and radial head	130º	-10º	90º	80º	N
M	31	yes	IA	radial head	125º	0º	90º	90º	N
M	75	no	IB	lateral and medial condyle	100º	-20º	90º	90º	N
F	53	no	IIIB	N	130º	-40º	80º	70º	Ulnar n. paresthesia
F	62	yes	IA	N	130º	-40º	70º	40º	N
F	38	yes	IIIA	N	140º	-25º	80º	80º	N
F	66	yes	IIA	N	130º	-20º	70º	80º	N

Source: SAME Medical Records Data - Santa Casa de São Paulo. Legend: M=male, F=female, N=none, SMR = synthesis material removal, ulnar n.=ulnar nerve, Fl.=flexion, Ext.=extension, Pr.=pronation, Sup.=supination.

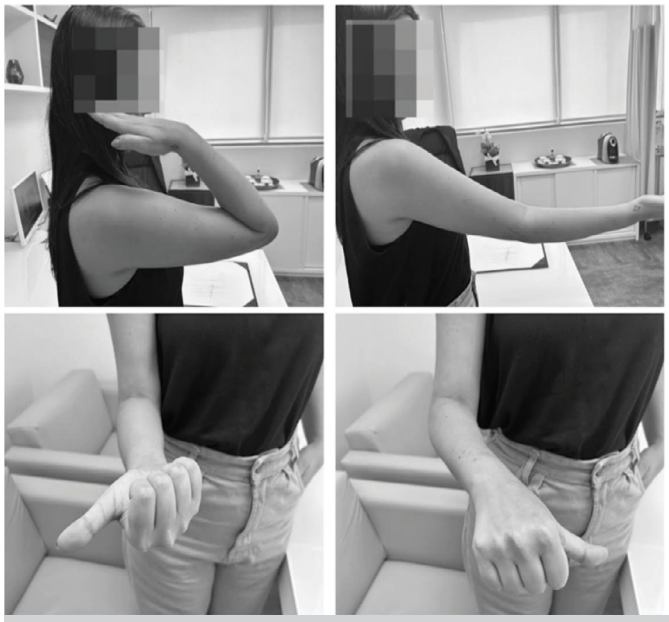

Source: Authors' image file.

Figure 3. Patient No.15 with seven months of postoperative follow-up.

removal (SMR) to gain range of motion, one patient needed SMR due to infection, and three patients had postoperative ulnar nerve paresthesia (Figure 4).

DISCUSSION

Patients with combined capitellum and trochlea fractures (Dubberley type II and III) did not show a worse functional prognosis when compared to those with isolated capitellum fractures (Dubberley type I). This fact surprised us, given that the articular surface was compromised in both the medial and lateral columns, and including the trochlea, which truly serves as a guide for flexion and extension. This highlights a greater importance of the ulnohumeral joint in this movement, and not only in pronation and supination (Figure 5). Hildebrand et al. [13] proposed that due to hypertrophy of the anterior portion of the joint related to a greater distribution of myofibroblasts in this region, extension, when compared to flexion, would be the most compromised movement. However, in our study, flexion was

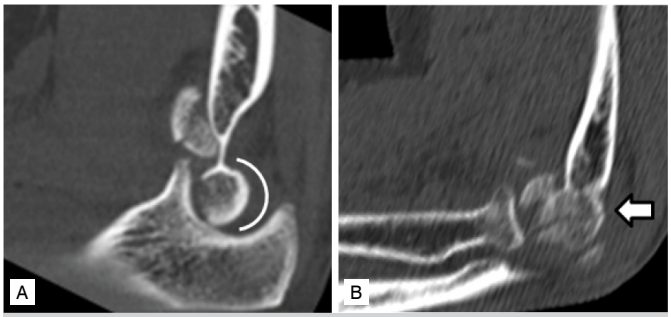

Source: SAME – Santa Casa de São Paulo tomographic archives.

Figure 4. Computed tomography images demonstrating a fracture with preservation of the posterior wall integrity (A) and with posterior wall involvement (B), respectively.

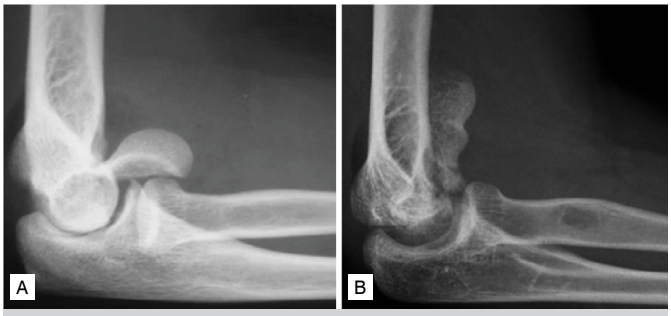

Source: SAME – Santa Casa de São Paulo radiographic archives.

Figure 5. Radiographic images showing isolated capitellum fracture (A) and associated capitellum and trochlea fracture (B), respectively.

the most significant alteration in the range of motion. Among the evaluated patients, 67% demonstrated restriction to flexion, whereas none of the evaluated patients developed restriction to pronation. The relationship between preoperative posterior wall integrity and a worse final range of motion in patients exists and may be related to the blood supply of the capitellum and trochlea, which arises from perforating vessels of the posterior condyle, potentially associated with partial devascularization and non-union.[4] We also considered the importance of fixation in at least two planes was necessary in these situations, as a smaller anterior-to-posterior fixation as well as the other way around would not stabilize this fracture sufficiently (Figure 6).

During follow-up, the most frequent complication was elbow stiffness, followed by ulnar nerve neuropathy.

An association of ulnar nerve neuropathy with males has been described in the literature due to the presence of anatomical changes, such as a larger coronoid process, thicker cubital tunnel *retinaculum*, and lack of adipose tissue around the cubital tunnel, making them more susceptible to nerve compression.[14] Despite this, all patients in our study who developed this complication were females (OR= 8.08; p = 0.09). Immobilization time until the procedure with the elbow flexed at 90° was a risk factor for developing this type of complication, corroborating the relationship previously described in the literature, and all patients who developed ulnar neuropathy had prolonged immobilization time.[14]

Prolonged preoperative immobilization also showed a significant correlation with the recovery of range of motion during the postoperative period, demonstrating and proving the importance of early mobilization, including immediate postoperative passive movement, aiding in the drainage of articular and periarticular fluids.

We cite here the absence of data regarding postoperative immobilization time in some patients as a limiting factor of the study, as it was not possible to establish any relationship with this fact.

Among the patients who underwent olecranon osteotomy during surgical approach, 60% of them developed elbow stiffness (OR= 1.25; p = 1).

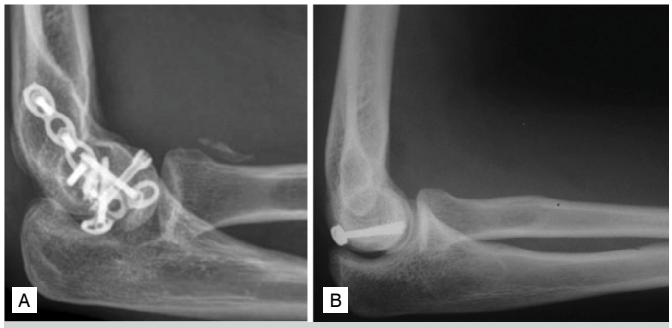

Source: SAME – Santa Casa de São Paulo radiographic archives.

Figure 6. Radiographic images showing fracture fixed in two planes (A) and fracture fixed in only one plane (B), respectively.

CONCLUSION

Our study demonstrated that, although combined capitellum and trochlea fractures did not present a worse functional prognosis when compared to isolated capitellum fractures, posterior wall integrity proved to be a significant factor in the final range of motion. It was also possible to observe, despite the absence of statistical significance, a greater tendency for the occurrence of ulnar nerve neuropathy in women. Likewise, a propensity for ulnar nerve neuropathy in patients with prolonged immobilization time, despite the absence of statistical significance. However, both could be confirmed with larger samples.

CONTRIBUTIONS OF THE AUTHORS

Each author made significant individual contributions to the development of this manuscript. GLG, APH and ZC: manuscript writing, statistical data analysis, intellectual conception of the manuscript, and development of the research project; GLG and APH: collection of clinical data; FM, VRP, and HJOS: review of the article and intellectual concept of the article. All authors have read and approved the final version submitted and take public responsibility for all aspects of the work.

DATA AVAILABILITY DECLARATION

The data underlying this study are contained within the manuscript.

REFERENCES

1. Aquilina AL, Grazette AJ. Clinical anatomy and assessment of the elbow. Open Orthop J. 2017;11(1):1347-52. doi: 10.2174/1874325001711011347.
2. Bryce CD, Armstrong AD. Anatomy and biomechanics of the elbow. Orthop Clin North Am. 2008;39(2):141-54. doi: 10.1016/j.ocl.2007.12.001.
3. Morrey BF, An KN. Stability of the elbow: osseous constraints. J Shoulder Elbow Surg. 2005;14(1 Suppl S):174S-178S. doi: 10.1016/j.jse.2004.09.031.
4. Yamaguchi K, Sweet FA, Bindra B, Morrey BF, Gelberman RH. The extraosseous and intraosseous arterial anatomy of the adult elbow. J Bone Joint Surg Am. 1997;79(11):1653-62. doi: 10.2106/00004623-199711000-00007.
5. Dubberley JH, Faber KJ, MacDermid JC, Patterson SD, King GJW. Outcome after open reduction and internal fixation of capitellar and trochlear fractures. J Bone Joint Surg Am. 2006;88(1):46-54. doi: 10.2106/jbjs.d.02954.
6. Imatani J, Morito Y, Hashizume H, Inoue H. Internal fixation for coronal shear fracture of the distal end of the humerus by the anterolateral approach. J Shoulder Elbow Surg. 2001;10(6):554-6. doi: 10.1067/mse.2001.118005.
7. Lee JJ, Lawton JN. Coronal shear fractures of the distal humerus. J Hand Surg Am. 2012;37(11):2412-7. doi: 10.1016/j.jhsa.2012.09.001.
8. Jo S, Morrey BF. Distal humerus fractures. In: Morrey's the elbow and its disorders. Elsevier; 2018. p. 458-65.
9. He SK, Xu L, Guo JH, Liao JP, Qin TW, Huang FG. The impact of associated injuries and fracture classifications on the treatment of capitellum and trochlea fractures: a systematic review and meta-analysis. Int J Surg. 2018;54(Pt A):37-47. doi: 10.1016/j.ijsu.2018.04.028.
10. Spiegel PG, Mast JW. Fracture and dislocation compendium. Orthopaedic Trauma Association Committee for Coding and Classification. 1996;10(Suppl 1):v-154.
11. Stamatis E, Paxinos O. The treatment and functional outcome of type IV coronal shear fractures of the distal humerus: a retrospective review of five cases. J Orthop Trauma. 2003;17(4):279-84. doi: 10.1097/00005131-200304000-00006.
12. Rüedi TP, Murphy WM. AO principles of fracture management. Vol. 1: principles; vol. 2: specific fractures. Stuttgart: Thieme; 2017.
13. Masci G, Cazzato G, Milano G, Ciolli G, Malerba G, Perisano C, et al. The stiff elbow: current concepts. Orthop Rev (Pavia). 2020;12(Suppl 1):8661. doi: 10.4081/or.2020.8661.
14. Hewson DW, Kurien T, Hardman JG. Postoperative ulnar neuropathy: a systematic review of evidence with narrative synthesis. Br J Anaesth. 2023;131(1):135-49. doi: 10.1016/j.bja.2023.04.010.

DOI: http://dx.doi.org/10.1590/1413-785220263402e305689

ANTERIOR DELTOID THICKNESS AND MUSCLE QUALITY DO NOT PREDICT FUNCTIONAL OUTCOMES AFTER ORIF FOR PROXIMAL HUMERAL FRACTURES

A ESPESSURA DO DELTOIDE ANTERIOR E A QUALIDADE MUSCULAR NÃO PREDIZEM DESFECHOS FUNCIONAIS APÓS ORIF DE FRATURAS PROXIMAIS DO ÚMERO

Leonardo Zanesco[1], *Lucas Mena*[1], *Ana Fabricia Feitosa Dias*[1], *Gabriel Veneziani Zulietti*[1], *Fernando Brandao de Andrade e Silva*[1], *Mauro Emilio Conforto Gracitelli*[1], *Eduardo Angeli Malavolta*[1,2]

1. Hospital das Clínicas HCFMUSP, Faculdade de Medicina, Universidade de Sao Paulo, Sao Paulo, SP, Brazil.
2. Hcor, Sao Paulo, Brazil.

ABSTRACT

Objective: To evaluate whether anterior deltoid thickness and deltoid fatty degeneration measured on postoperative MRI are associated with functional recovery and complications after locking-plate ORIF for proximal humeral fractures. Methods: Exploratory secondary analysis of data from a single-center institutional randomized clinical trial. Patients aged ≥60 years treated with ORIF were eligible; deltoid analyses were restricted to those with a 6-month postoperative shoulder MRI. Anterior deltoid thickness (mm) was measured on axial MRI using a standardized technique, and deltoid muscle quality was graded semi quantitatively as no fatty degeneration, <50%, or ≥50% fatty degeneration. The primary outcome was ASES score at 3, 6, 12, and 24 months, analyzed using linear mixed-effects models with a participant-level random intercept and categorical time. Complications through 24 months and full-thickness rotator cuff tear on the 6-month MRI were assessed using logistic regression and exact tests for categorical comparisons. Results: In the MRI subset (n=25), anterior deltoid thickness was not significantly associated with longitudinal ASES scores (β=1.93 per mm; 95%CI −2.21 to 6.07; p=0.360). ASES scores improved progressively over follow-up. Deltoid fatty degeneration and rotator cuff tear showed directional trends toward higher odds of complications. Conclusions: In older patients undergoing ORIF for proximal humeral fractures, mid-term postoperative deltoid morphology did not predict functional recovery through 24 months and was not consistently associated with complications. ***Level of Evidence II; Prognostic study (secondary analysis; observational cohort).***

Keywords: Shoulder Fractures; Fracture Fixation, Internal; Deltoid Muscle; Magnetic Resonance Imaging; Rotator Cuff; Treatment Outcome.

RESUMO

Objetivo: Avaliar se a espessura do deltoide anterior e a degeneração gordurosa do deltoide, mensuradas na ressonância magnética (RM) pós-operatória, se associam à recuperação funcional e às complicações após osteossíntese com placa bloqueada (ORIF) em fraturas proximais do úmero. Métodos: Análise secundária exploratória de um ensaio clínico randomizado institucional. Foram incluídos pacientes ≥60 anos tratados com ORIF e com RM do ombro aos 6 meses (subconjunto para análise de morfologia do deltoide). A espessura do deltoide anterior foi medida em corte axial (mm) conforme técnica padronizada. A qualidade muscular foi classificada por degeneração gordurosa semiquantitativa (sem, <50%, ≥50%). O desfecho primário foi o escore ASES aos 3, 6, 12 e 24 meses, analisado por modelos lineares de efeitos mistos com intercepto aleatório. Complicações até 24 meses e lesão do manguito rotador na RM de 6 meses foram analisadas por regressão logística e testes exatos. Resultados: No subconjunto com RM (n=25), não houve associação significativa entre espessura do deltoide e ASES ao longo do seguimento (β=1,93 por mm; IC95% −2,21 a 6,07; p=0,360). O ASES aumentou progressivamente ao longo do tempo. Degeneração gordurosa e lesão do manguito mostraram tendência a maior chance de complicações sem significância estatística. Conclusões: Em pacientes idosos submetidos a ORIF, a morfologia do deltoide aos 6 meses não previu recuperação funcional até 24 meses e não se associou de forma consistente a complicações. ***Nível de Evidência II; Tipo de Estudo: Estudo prognóstico (análise secundária; coorte observacional).***

Descritores: *Fraturas do Ombro; Fixação Interna de Fraturas; Músculo Deltoide; Imageamento por Ressonância Magnética; Manguito Rotador; Resultado do Tratamento.*

Citation: Zanesco L, Mena L, Dias AFF, Zulietti GV, Silva FBA, Gracitelli MEC, Malavolta EA. Anterior deltoid thickness and muscle quality do not predict functional outcomes after orif for proximal humeral fractures. Acta Ortop Bras. [online]. 2026;34(Spe.2): Page 1 of 6. Available from URL: http://www.scielo.br/aob.

All authors declare no potential conflict of interest related to this article.

The study was conducted at Instituto de Ortopedia e Traumatologia do Hospital das Clinicas da Faculdade de Medicina da Universidade de Sao Paulo (IOT-HCFMUSP), Sao Paulo, SP, Brazil.
Correspondence: Eduardo Angeli Malavolta. 333, Rua Dr. Ovidio Pires de Campos, 3º andar, Cerqueira Cesar, Sao Paulo, SP, Brazil. 05403-010. eduardomalavolta@gmail.com

Article received on 02/19/2026 approved on 05/13/2026.
Handling Editor: Américo Zoppi Filho

INTRODUCTION

Proximal humeral fractures commonly affect older adults and represent a significant cause of pain, disability, and healthcare resource utilization[1]. Open reduction and internal fixation (ORIF) is frequently employed, especially in biologically active patients and those with reconstructable fracture patterns[2]. Although surgical techniques and implant designs have advanced, functional outcomes after ORIF remain variable, and accurate prediction of postoperative recovery remains difficult[3].

Muscle morphology has emerged as an important determinant of shoulder function following surgical intervention, particularly in reverse shoulder arthroplasty. In this context, the deltoid muscle plays a central biomechanical role by compensating for rotator cuff deficiency and acting as the primary motor of shoulder elevation. Studies have demonstrated associations between deltoid size or muscle quality and postoperative functional outcomes after reverse shoulder arthroplasty[4]. More recently, Lie et al[5]. proposed a reproducible MRI-based method for measuring deltoid thickness and reported that greater deltoid thickness was associated with improved functional recovery following reverse shoulder arthroplasty. These findings have generated interest in the potential role of deltoid morphology as a prognostic marker in shoulder surgery. However, it is crucial to recognize that the biomechanical advantages of deltoid-driven compensation in arthroplasty do not necessarily apply to fracture fixation procedures such as ORIF. While arthroplasty relies on the deltoid for primary function due to rotator cuff deficiencies[6], ORIF emphasizes fracture healing and rotator cuff integrity, potentially diminishing the impact of deltoid morphology. The prognostic relevance of anterior deltoid thickness and muscle quality in patients undergoing ORIF for proximal humeral fractures remains unclear. Unlike reverse shoulder arthroplasty, ORIF relies on fracture healing, tuberosity restoration, and maintained or recoverable rotator cuff function, potentially diminishing the significance of deltoid morphology[7]. To our knowledge, no longitudinal studies have examined the association between deltoid muscle characteristics and functional recovery after ORIF.

This study aimed to evaluate the association between anterior deltoid thickness and muscle quality, as measured by MRI, and postoperative functional outcomes and complication rates following ORIF for proximal humeral fractures. The hypothesis was that greater deltoid thickness and higher muscle quality would be associated with improved functional recovery.

METHODS

Study design and setting

This study is an exploratory secondary analysis of data derived from a previously conducted institutional randomized clinical trial performed at a single tertiary referral centre[8].The present analysis was undertaken to explore the potential prognostic value of anterior deltoid muscle thickness and quality for postoperative functional outcomes and complication rates among patients treated surgically with open reduction and internal fixation (ORIF). No analyses related to deltoid morphology were prespecified in the original trial protocol, and no sample size calculation was performed for the present study. The study was conducted in accordance with institutional ethical standards, and all participants in the original randomized trial provided written informed consent.

Participants

Patients enrolled in the original randomized clinical trial who underwent ORIF for acute proximal humeral fractures were eligible. For the purposes of this exploratory analysis, inclusion additionally required the availability of 6 months' postoperative shoulder magnetic resonance imaging (MRI) to assess deltoid morphology. Patients without available postoperative MRI were excluded from analyses involving deltoid thickness or fatty degeneration but were retained in descriptive summaries and longitudinal outcome analyses when applicable. Fractures were classified according to the Neer classification system.

Surgical Procedure

All surgical procedures were performed by a single experienced shoulder surgeon with over 15 years of training. Patients were positioned in the beach-chair position under general anaesthesia, typically combined with an interscalene brachial plexus block, in accordance with institutional protocols. A standard deltopectoral approach was used in all cases, with neither the anterolateral nor transdeltoid approach employed. Blunt dissection was performed through the deltopectoral interval, preserving the deltoid origin and insertion, and ensuring meticulous handling of the soft tissues. Fracture fragments were identified and reduced under direct visualization and fluoroscopic guidance. Sutures were placed through the rotator cuff as required for tuberosity control, followed by fixation with a proximal humerus locking plate in accordance with established principles of plate osteosynthesis. Plate position, screw length, and humeral head alignment were confirmed intraoperatively using fluoroscopy. The rotator cuff was secured to the plate according to standard practice. When indicated, concomitant procedures such as long head of the biceps tenodesis at the pectoralis major level were performed at the surgeon's discretion and documented.

Variables

The primary exposures were anterior deltoid muscle thickness and deltoid fatty degeneration, both assessed on the 6-month postoperative shoulder MRI. Variables collected from the parent randomized trial and summarized for the present cohort (Table 1) included demographic and clinical characteristics (age, sex, smoking status, and comorbidities including diabetes mellitus, hypertension, and depression) and fracture-related parameters (Neer classification [types 2–4] and number of fracture fragments [2-, 3-, or 4-part]). Additional postoperative variables summarized in Table 1 included the presence of a rotator cuff tear (yes/no) and any postoperative complication (yes/no), as defined below.

Assessment of anterior deltoid thickness and muscle quality

Anterior deltoid thickness was assessed on postoperative shoulder MRI using the standardized and reproducible technique described(5). Measurements were obtained on axial MRI sequences at a consistent anatomical level corresponding to the midportion of the anterior deltoid muscle belly, where the muscle was clearly visualized and separated from adjacent structures. Deltoid thickness was defined as the maximum perpendicular distance between the superficial and deep margins of the anterior deltoid, measured orthogonally to the muscle fibers. All measurements were recorded in millimeters and analyzed as a continuous variable.

Deltoid muscle quality was evaluated through visual assessment of fatty infiltration on axial MRI images. Fatty degeneration was graded semiquantitatively using a system modeled after the MRI-based Fuchs classification of fatty infiltration(9), adapted for the deltoid muscle. Based on the estimated proportion of fatty infiltration within the muscle belly, deltoid degeneration was classified as no fatty degeneration, less than 50% fatty degeneration, or 50% or greater fatty degeneration.

Rotator cuff tear

Rotator cuff integrity was assessed on the 6-month postoperative shoulder MRI. A rotator cuff tear was defined as the presence of at least one full-thickness tear involving any rotator cuff tendon (supraspinatus, infraspinatus, subscapularis, or teres minor). Tears were coded as a binary variable for analysis.

Outcomes

The primary outcome was shoulder function measured with the adapted American Shoulder and Elbow Surgeons (ASES) score[10], collected at 3, 6, 12, and 24 months postoperatively (0–100 scale; higher scores indicate better function).

Postoperative complications were recorded prospectively during follow-up. A complication was defined as any adverse event attributable to the index fracture fixation and postoperative course, including infection or wound complications, implant- or fixation-related failure (e.g., loss of reduction, screw perforation, plate failure), malunion or nonunion, humeral head avascular necrosis, and neurovascular complications. Reoperation related to the index procedure (including implant removal or revision surgery) was considered a complication. For analysis, complications were treated as a binary outcome indicating occurrence at any time through 24 months.

Statistical analysis

Baseline characteristics were described using means with standard deviations (or medians with interquartile ranges when appropriate) for continuous variables and counts with percentages for categorical variables.

To examine whether anterior deltoid morphology was associated with postoperative recovery, we fitted linear mixed-effects models[11] with ASES score(10) as the repeated outcome measured at 3, 6, 12, and 24 months after surgery. Follow-up time was handled as a categorical variable to avoid assuming a linear recovery pattern. We specified two mixed-model frameworks. One used anterior deltoid thickness (mm) as the exposure, with fixed effects for time and a time-by-thickness interaction to assess variation across follow-up. The other used deltoid fatty degeneration (no degeneration, <50%, ≥50%) as the exposure, with fixed effects for time and a time-by-degeneration interaction. Each model included a participant-level random intercept to account for within-individual correlation. Alternative random-effects structures, including random slopes, were explored. Models were estimated using restricted maximum likelihood. Effects are reported as β coefficients with 95% confidence intervals and two-sided p-values.

Associations with any postoperative complication were evaluated using logistic regression, reporting odds ratios with 95% confidence intervals. Univariable models examined complications in relation to deltoid fatty degeneration category and rotator cuff tear (yes/no) identified on the 6-month MRI. Because the MRI subset was small and sparse cells were anticipated, relationships between categorical MRI variables were evaluated using exact methods; specifically, Fisher's exact test was used when appropriate rather than relying on asymptotic chi-square assumptions.

No formal sample-size calculation was performed for this secondary analysis; analyses were limited to participants available from the parent randomized trial. Logistic regression models for complications were specified parsimoniously a priori to reduce overfitting given the limited number of events, and exact tests were used for categorical comparisons when appropriate. Analyses followed a complete-case approach without imputation. All tests were two-sided, with p-values reported descriptively. Analyses were performed in Stata 19 (StataCorp, College Station, TX, USA).

RESULTS

A total of 43 patients were screened for inclusion in this secondary analysis. Of these, 31 were selected, and 25 underwent postoperative MRI allowing assessment of anterior deltoid muscle quality; these 25 patients comprised the analytic cohort for deltoid-related variables. Six selected patients did not undergo MRI and were therefore excluded from analyses involving deltoid measurements. Baseline characteristics stratified by anterior deltoid fatty degeneration (no degeneration, n = 6; <50% degeneration, n = 10; ≥50% degeneration, n = 9) are shown in Table 1. In this cohort (N = 25), mean age was 68.4 ± 5.3 years and most patients were female (23/25, 92%). There were no significant differences across degeneration groups in age, sex, smoking status, diabetes, hypertension, depression, Neer classification, or number of fracture fragments (all $p > 0.05$). In contrast, anterior deltoid thickness differed markedly across groups, decreasing with increasing fatty degeneration (9.0 ± 1.2 mm in the no-degeneration group vs 6.0 ± 0.8 mm in the ≥50% group; $p < 0.001$). The distribution of clinical comorbidities, including smoking status, diabetes mellitus, hypertension, and depression, was also comparable between groups. Differences were observed in fracture-related characteristics: patients with higher degrees of deltoid fatty degeneration had a greater proportion of Neer type 4 fractures and a higher frequency of fractures

Table 1. Baseline characteristics according to anterior deltoid fatty degeneration.

Characteristic	Overall (N = 25)	No degeneration (n = 6)	<50% degeneration (n = 10)	≥50% degeneration (n = 9)	p-value*
Age, years	68.4 5.3	65.0 3.6	68.8 6.0	69.9 6.4	0.325
Female Sex, n (%)	23 (92.0)	5 (83.3)	9 (90.0)	9 (100)	0.700
Smoking, n (%)	3 (12.0)	1 (16.7)	1 (10.0)	1 (11.1)	1.000
Diabetes mellitus, n (%)	8 (32.0)	2 (33.3)	2 (20.0)	4 (44.4)	0.494
Hypertension, n (%)	14 (56.0)	4 (66.7)	4 (40.0)	6 (66.7)	0.523
Depression, n (%)	1 (4.0)	0 (0.0)	0 (0.0)	1 (11.1)	0.600
Neer classification**, n (%)					0.408
Type 2	7 (28.0)	2 (33.3)	3 (30.0)	2 (22.2)	
Type 3	6 (24.0)	3 (50.0)	2 (20.0)	1 (11.1)	
Type 4	12 (48.0)	1 (16.7)	5 (50.0)	6 (66.7)	
Number of fracture fragments***, n (%)					0.292
2 fragments	5 (20.0)	2 (33.3)	1 (10.0)	2 (22.2)	
3 fragments	7 (28.0)	3 (50.0)	3 (30.0)	1 (11.1)	
4 fragments	13 (52.0)	1 (16.7)	6 (60.0)	6 (66.7)	
Anterior deltoid thickness, mm	7.6 1.7	9.0 1.2	8.2 1.2	6.0 0.8	<0.001

Values are reported as mean ± standard deviation for continuous variables and as n (column percentage) for categorical variables. Deltoid fatty degeneration was graded on the 6-month postoperative MRI and categorized as no fatty degeneration, <50% fatty degeneration, or ≥50% fatty degeneration. *P-values reflect comparisons across deltoid degeneration categories: continuous variables were tested with Kruskal–Wallis, and categorical variables with Fisher's exact test. **(12), ***(13)

involving four fragments, whereas patients without degeneration more commonly presented with less complex fracture patterns.

Table 2 summarizes postoperative events in the MRI subset (n=25) stratified by deltoid fatty degeneration. Overall, any complication occurred in 11 patients (44%). Event rates were numerically higher with increasing fatty degeneration—for example, any complication rose from 33.3% in patients without degeneration to 55.6% in those with ≥50% degeneration, and rotator cuff tear increased from 16.7% to 44.4% across the same categories. Osteonecrosis was observed in 12.0% overall and occurred only in patients with some degree of fatty degeneration. However, no between-group differences reached statistical significance (all Fisher's exact p-values > 0.60).

Effect of deltoid thickness on ASES scores

The association between anterior deltoid thickness and longitudinal ASES scores was evaluated using linear mixed-effects models, with follow-up time treated as a categorical variable and patient-specific random intercepts to account for repeated measurements. All available ASES observations across follow-up were included in the analysis.

In the overall cohort, anterior deltoid thickness was not significantly associated with ASES scores over time (β = 1.93 per mm; 95% CI −2.21 to 6.07; p = 0.360; Table 3). In contrast, follow-up time demonstrated a strong association with functional improvement. Compared with the 3-month reference, mean ASES scores increased by 11.4 points at 6 months, 16.1 points at 12 months, and 20.8 points at 24 months, with all time contrasts reaching statistical significance (p < 0.01; Table 3). Predicted ASES trajectories stratified by deltoid fatty degeneration similarly demonstrated progressive improvement over time across all groups, with relatively stable differences between degeneration categories (Figure 1).

Postoperative Complication

In univariable logistic regression restricted to the MRI subset (n=25), neither deltoid fatty degeneration nor rotator cuff tear demonstrated a statistically significant association with postoperative complications (Table 4). Compared with no fatty degeneration, the odds of complications were higher in patients with <50% degeneration (OR 1.33) and ≥50% degeneration (OR 2.50), but estimates were imprecise with wide confidence intervals. Rotator cuff tear was also associated with higher odds of complications (OR 3.06), although this did not reach statistical significance. As shown in Table 4, the direction of effect estimates was consistently toward increased odds of complications with greater deltoid degeneration and in the presence of a rotator cuff tear, but the small MRI sample limited precision. Deltoid fatty degeneration and rotator cuff tear showed only a weak, nonsignificant positive association (Spearman's ρ = 0.23; p = 0.27)

DISCUSSION

In this exploratory secondary analysis of older patients undergoing open reduction and internal fixation (ORIF) for displaced proximal humeral fractures, anterior deltoid thickness and deltoid fatty degeneration measured on the 6-month postoperative MRI were

Table 3. Linear mixed-effects model for ASES scores over time.

Variable	β coefficient	95% CI	p-value
Anterior deltoid thickness (per mm)	1.93	−2.21 to 6.07	0.360
Time (ref: 3 months)			
6 months	11.44	4.08 to 18.81	0.002
12 months	16.09	8.72 to 23.45	<0.001
24 months	20.84	13.48 to 28.21	<0.001
Intercept	43.14	10.68 to 75.61	0.009
Random-effects variance			
Component	**Variance (95% CI)**		
Patient-level random intercept	251.15 (130.58–483.08)		
Residual	176.40 (128.08–242.94)		

Values represent fixed-effect estimates from a linear mixed-effects model with patient-specific random intercepts. Follow-up time was modelled as a categorical variable with 3 months as the reference category. β coefficients represent mean differences in the ASES score. CI indicates confidence interval.

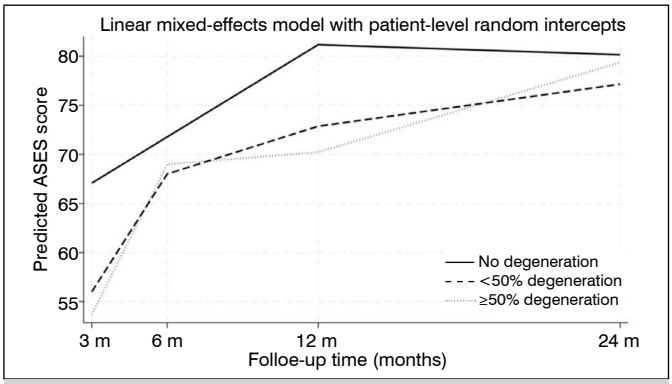

Figure 1. Predicted ASES trajectories over time according to deltoid fatty degeneration category are illustrated in Figure A. Across all categories, ASES scores increased progressively with follow-up, while differences between degeneration groups remained relatively stable over time.

Table 4. Univariable logistic regression for any postoperative complication (MRI subset, n=25).

Predictor	OR	95% CI	p
Deltoid fatty degeneration (ref: No degeneration)			
└ <50% vs none	1.33	0.16–11.07	0.790
└ ≥50% vs none	2.50	0.29–21.40	0.403
Rotator cuff tear (Yes vs No)	3.06	0.53–17.46	0.209

Reports univariable logistic regression models with any postoperative complication (yes/no) as the dependent variable, restricted to the MRI subset (n=25). Effect estimates are presented as odds ratios (ORs) with 95% confidence intervals (CIs).

Table 2. Postoperative events stratified by deltoid fatty degeneration.

Outcomes	Total (n=25)	No degeneration(n=6)	<50% degeneration(n=10)	≥50% degeneration (n=9)	p-value*
Infection	1 (4.0)	0 (0.0)	0 (0.0)	1 (11.1)	0.600
Malunion	2 (8.0)	0 (0.0)	1 (10.0)	1 (11.1)	1.000
Osteonecrosis (any)	3 (12.0)	0 (0.0)	2 (20.0)	1 (11.1)	0.765
Any complication	11 (44.0)	2 (33.3)	4 (40.0)	5 (55.6)	0.679
Rotator cuff tear	8 (32.0)	1 (16.7)	3 (30.0)	4 (44.4)	0.657

Values are presented as *n (column percentage)*. Deltoid fatty degeneration categories were defined on the 6-month postoperative MRI as no fatty degeneration, <50% fatty degeneration, or ≥50% fatty degeneration. Rotator cuff tear was defined as the presence of at least one full-thickness tear of any rotator cuff tendon on the same MRI. *P-values are from Fisher's exact test comparing proportions across deltoid degeneration categories.

<< SUMÁRIO

not significantly associated with longitudinal functional recovery through 24 months. Although ASES scores improved substantially over time, deltoid morphology did not demonstrate a consistent independent relationship with recovery trajectories. These findings suggest that deltoid morphology—at least as captured on mid-term postoperative MRI—has limited incremental value for explaining recovery after ORIF.

Notably, the cohort was predominantly female (23/25, 92%), which provides a more focused, sex-homogeneous sample. This likely reduced between-patient variability related to sex-specific differences in muscle composition and recovery, thereby strengthening the internal consistency of the findings—although it may limit generalizability to male patients.

These results differ from the arthroplasty literature, particularly reverse shoulder arthroplasty (RSA), where deltoid morphology has a clearer mechanistic role[5]. In RSA, the deltoid becomes the primary driver of elevation and stability, and MRI-based studies have reported associations between greater anterior deltoid thickness and improved postoperative outcomes. In contrast, ORIF is intended to restore native anatomy and relies more heavily on fracture healing, alignment, restoration of tuberosity position, rotator cuff function, and rehabilitation progression[14,15]. In addition, functional outcomes after ORIF appear more tightly linked to fracture pattern, the quality of reduction and fixation, and mechanical complications[1].

Rotator cuff integrity is also clinically relevant in this setting. Concomitant rotator cuff pathology is common after proximal humeral fractures and may contribute to persistent pain, weakness, and limited recovery despite fracture union. MRI-based cohorts have suggested that tears present at injury and those identified during follow-up can be associated with worse functional outcomes in some populations[16]. However, the clinical impact remains debated: other studies have found that postoperative outcomes can still be satisfactory and are not consistently influenced by the presence of rotator cuff tears[17]. In the present study, rotator cuff tears identified on the 6-month MRI showed a directional trend toward higher complication odds. Still, estimates were imprecise and not statistically significant.

Surgical approach is an important interpretive consideration when evaluating studies linking deltoid morphology to outcomes. Deltoid-splitting/anterolateral exposures have theoretical advantages for fragment visualization[18]. Still, they involve direct manipulation near the axillary nerve and the deltoid muscle and have historically raised concern about iatrogenic denervation or deltoid dysfunction[19]. A retrospective study suggests that anterolateral approaches can be safe in selected settings, with low rates of clinically evident axillary nerve deficit, although malunion and subacromial impingement remain important reported complications[20]. By design, all fixations in the present study were performed through a deltopectoral approach[8], reducing the likelihood that postoperative deltoid atrophy or fatty degeneration reflected approach-related denervation and strengthening the inference that deltoid morphology—at least as assessed at 6 months—was not a major driver of recovery after ORIF.

Several additional methodological considerations should be acknowledged. Assessing deltoid morphology at 6 months after surgery restricts its value as a strictly "prognostic" factor. Thickness and fatty degeneration at this time point may reflect postoperative disuse, pain inhibition, immobilization, complications, or adherence to rehabilitation rather than baseline muscle biology. Second, the MRI subset was small, leading to wide confidence intervals and limited power to detect modest effects, particularly for complication analyses. Third, we used a semiquantitative grading system for deltoid fatty degeneration, modeled after established MRI-based fatty infiltration frameworks that have demonstrated clinical relevance and reproducibility in the shoulder musculature[9]; however, nondifferential misclassification remains possible[21]. Finally, because of the limited number of participants and events, covariate adjustment was intentionally parsimonious, and residual confounding cannot be excluded.

Clinically, these findings suggest that routine mid-term MRI assessment of anterior deltoid thickness or fatty degeneration is unlikely to improve prognostication after ORIF of proximal humeral fractures meaningfully. Greater emphasis should remain on fracture characteristics, reduction and fixation quality, tuberosity healing, rotator cuff integrity, and structured rehabilitation. More broadly, the results reinforce the clinical relevance of muscle morphology, which is procedure-specific, appearing substantially greater in arthroplasty-based reconstructions than in fracture fixation. Future studies incorporating preoperative or early postoperative muscle assessments, quantitative imaging approaches, and larger cohorts are warranted to clarify whether deltoid characteristics have any early prognostic utility after fracture fixation.

CONCLUSION

In patients treated with open reduction and internal fixation for proximal humeral fractures, preoperative anterior deltoid thickness and muscle quality on MRI did not correlate with functional outcomes or complications. While function improved over time, deltoid morphology had no independent prognostic value, unlike in reverse shoulder arthroplasty. These results suggest that fracture- and biology-related factors have a greater impact on recovery. Larger studies using quantitative MRI may help further clarify the role of muscle in fracture healing.

CONTRIBUTIONS OF THE AUTHORS

Each author made a personal and significant contribution to the development of this article. ZL: Formal analysis; Writing – original draft. ML: Formal analysis; Writing – original draft. DAFF: Writing – review & editing. ZGV: Writing – review & editing. SFBA: Writing – review & editing. GMEC: Writing – review & editing. MEA: Methodology; Writing – review & editing.

DATA AVAILABILITY DECLARATION

The data will be made available upon request by the reviewers.

REFERENCES

1. Antonios T, Bakti N, Nzeako O, Mohanlal P, Singh B. Outcomes following fixation for proximal humeral fractures. J Clin Orthop Trauma. 2019;10(3):468-73. doi: 10.1016/j.jcot.2019.01.029.
2. Bage TG, Naeem MH, Titchener A. Proximal humeral fractures, current evidence including ProFHER. Surgery (Oxf). 2025;43(2):80-4. doi: 10.1016/j.mpsur.2024.12.007.
3. Codman EA. The shoulder: rupture of the supraspinatus tendon and other lesions in or about the subacromial bursa. Boston: Thomas Todd Co.; 1934. p. 29.
4. de Boer FA, Pasma JH, Huijgen WHF, Huijsmans PE, Flikweert PE. Long-term relation between deltoid muscle volume and clinical outcomes in a reverse shoulder arthroplasty. Semin Arthroplasty JSES. 2022;32(4):664-70. doi: 10.1053/j.sart.2022.07.010.

5. Fjalestad T, Hole MØ, Blücher J, Hovden IAH, Stiris MG, Strømsøe K. Rotator cuff tears in proximal humeral fractures: an MRI cohort study in 76 patients. Arch Orthop Trauma Surg. 2010;130(5):575-81. doi: 10.1007/s00402-009-0953-2.
6. Fuchs B, Weishaupt D, Zanetti M, Hodler J, Gerber C. Fatty degeneration of the muscles of the rotator cuff: assessment by computed tomography versus magnetic resonance imaging. J Shoulder Elbow Surg. 1999;8(6):599-605. doi: 10.1016/S1058-2746(99)90097-6.
7. Gracitelli MEC, Andrade-Silva FB, Zanesco L, Assunção JH, Kojima KE, Silva JS, et al. Proximal humeral fractures in patients over 60 years old: a randomized study of nonoperative versus operative treatment with locking plate. J Shoulder Elbow Surg. 2025;34(9):2165-77. doi: 10.1016/j.jse.2024.12.036.
8. Gracitelli MEC, Lobo FL, Ferreira GMA, Palma MV, Malavolta EA, Benegas E, et al. Outcomes evaluation of locking plate osteosynthesis in displaced fractures of the proximal humerus. Rev Bras Ortop. 2013;48(6):491-9. doi: 10.1016/j.rboe.2013.12.014.
9. Gracitelli MEC, Malavolta EA, Assunção JH, Matsumura BA, Kojima KE, Ferreira Neto AA. Ultrasound evaluation of the rotator cuff after osteosynthesis of proximal humeral fractures with locking intramedullary nail. Rev Bras Ortop. 2017;52(5):601-7. doi: 10.1016/j.rboe.2016.10.016.
10. Iking J, Fischhuber K, Stolberg-Stolberg J, Raschke MJ, Katthagen JC, Köppe J. Quality of life and pain after proximal humeral fractures in the elderly: a systematic review. Medicina (Kaunas). 2023;59(10):1728. doi: 10.3390/medicina59101728.
11. Jurek AM, Greenland S, Maldonado G, Church TR. Proper interpretation of non-differential misclassification effects: expectations vs observations. Int J Epidemiol. 2005;34(3):680-7. doi: 10.1093/ije/dyi060.
12. Knaut LA, Moser ADL, Melo SA, Richards RR. Tradução e adaptação cultural à língua portuguesa do American Shoulder and Elbow Surgeons Standardized Shoulder Assessment Form (ASES) para avaliação da função do ombro. Rev Bras Reumatol. 2010;50(2):176-89. doi: 10.1590/S0482-50042010000200007.
13. Lie HM, Lee WQ, Lie DTT. Greater deltoid coverage on preoperative MRI correlates with improved early functional outcomes after reverse shoulder arthroplasty. J ISAKOS. 2025;13:100912. doi: 10.1016/j.jisako.2025.100912.
14. Montesinos-López OA, Montesinos-López A, Crossa J. Linear mixed models. In: Multivariate statistical machine learning methods for genomic prediction. Cham: Springer; 2022. p. 141-70. doi: 10.1007/978-3-030-89010-0_5.
15. Mouraria GG, Zoppi A, Kikuta FK, Moratelli L, Silveira PP, Etchebehere M. Proximal humeral fractures treated with osteosynthesis using the anterolateral approach. Acta Ortop Bras. 2019;27(3):173-7. doi: 10.1590/1413-785220192703218226.
16. Oldrini LM, Sangiorgio A, Feltri P, Marbach F, Filardo G, Candrian C. Proximal humerus fractures: deltopectoral open reduction and internal fixation vs deltosplit minimally invasive plate osteosynthesis: which surgical approach provides superior results?. EFORT Open Rev. 2023;8(8):662-71. doi: 10.1530/eor-22-0110.
17. Özbey Büyükkuşcu M, Kulduk A, Mısır A, Çetinkaya E, Çamurcu İY, Gürsu ŞS. Effect of surgical approaches on deltoid innervation and clinical outcomes in the treatment of proximal humeral fractures. Jt Dis Relat Surg. 2020;31(3):516-22. doi: 10.5606/ehc.2020.74218.
18. Petros RSB, Ribeiro FR, Tenor Junior AC, Brasil Filho R, Filardi Junior CS, Dal Molin DC. Proximal humerus fracture with locking plate: functional and radiographic results. Acta Ortop Bras. 2019;27(3):164-8. doi: 10.1590/1413-785220192703142049.
19. Roche CP. Reverse shoulder arthroplasty biomechanics. J Funct Morphol Kinesiol. 2022;7(1):13. doi: 10.3390/jfmk7010013.
20. Sidor ML, Zuckerman JD, Lyon T, Koval K, Cuomo F, Schoenberg N. The Neer classification system for proximal humeral fractures. An assessment of interobserver reliability and intraobserver reproducibility. J Bone Joint Surg Am. 1993;75(12):1745-50. doi: 10.2106/00004623-199312000-00002.
21. Solberg BD, Moon CN, Franco DP, Paiement GD. Surgical treatment of three and four-part proximal humeral fractures. J Bone Joint Surg Am. 2009;91(7):1689-97. doi: 10.2106/JBJS.H.00133.

DOI: http://dx.doi.org/10.1590/1413-785220263402e300986

FUNCTIONAL ASSESSMENT AFTER ARTHROSCOPIC SHOULDER RELEASE IN ADHESIVE CAPSULITIS

AVALIAÇÃO FUNCIONAL APÓS LIBERAÇÃO ARTROSCÓPICA DO OMBRO EM CAPSULITE ADESIVA

Daniela Pereira Bortolin[1], *Isis Mendes Silva*[1], *Ricardo Boina de Barbe*[1], *Rodrigo Balieiro Leal*[1], *Diego Wagmacker Nascimento*[1], *Jair Simmer Filho*[1]

1. Hospital Estadual Jayme Santos Neves, Departamento de Ortopedia e Traumatologia, Serra, ES, Brazil.

ABSTRACT

Introduction: Adhesive capsulitis is a musculoskeletal condition characterized by shoulder pain and progressive restriction of motion. Although most cases respond to conservative management, some remain refractory and require surgical intervention. Objective: To evaluate the functional outcomes of arthroscopic capsular release in patients with refractory adhesive capsulitis. Methods: This retrospective observational study analyzed medical records of 10 patients who underwent shoulder arthroscopy between 2005 and 2025. Clinical and demographic variables, pre- and postoperative range of motion, and Shoulder Pain and Disability Index (SPADI) scores were collected. Results: The mean age was 62.3 ± 9.5 years, with a predominance of females (90%). According to Zuckerman's classification, four cases were primary (idiopathic), while six were secondary. An improvement was observed in anterior elevation (119.2° to 141.7°) and external rotation (28.8° to 59.2°). Postoperatively, all patients presented SPADI scores ≤ 20, consistent with minimal pain/disability, reflecting satisfactory functional recovery. Conclusion: Arthroscopic capsular release proved to be effective and safe in improving function in patients with refractory adhesive capsulitis, even in the presence of comorbidities and associated lesions. ***Level of Evidence IV; Retrospective observational study.***

Keywords: Adhesive Capsulitis; Frozen Shoulder; Arthroscopy; Capsular Release.

RESUMO

Introdução: A capsulite adesiva é uma condição musculoesquelética caracterizada por dor e limitação progressiva da amplitude de movimento do ombro. Embora a maioria dos casos responda ao tratamento conservador, parte evolui de forma refratária, demandando intervenção cirúrgica. Objetivo: Avaliar os resultados funcionais da liberação capsular artroscópica em pacientes com capsulite adesiva refratária ao tratamento conservador. Métodos: Estudo observacional retrospectivo, com análise de prontuários de 10 pacientes submetidos à artroscopia do ombro entre 2005 e 2025. Foram coletadas variáveis clínicas e demográficas, amplitude de movimento pré e pós-operatória e escores do Shoulder Pain and Disability Index (SPADI). Resultados: A média de idade foi 62,3 ± 9,5 anos, com predomínio do sexo feminino (90%). Pela classificação de Zuckerman, quatro casos foram classificados como primários e seis como secundários. Observou-se melhora da elevação anterior (119,2º para 141,7º) e da rotação lateral (28,8º para 59,2º). No pós-operatório, todos os pacientes apresentaram escores SPADI ≤ 20, indicando dor e incapacidade mínimas e recuperação funcional satisfatória. Conclusão: A liberação capsular artroscópica mostrou-se eficaz e segura para restaurar função em pacientes com capsulite adesiva refratária, mesmo na presença de comorbidades e lesões associadas. ***Nível de Evidência IV; Estudo observacional retrospectivo.***

Descritores: *Capsulite Adesiva; Ombro Congelado; Artroscopia; Liberação Capsular.*

Citation: Bortolin DP, Silva IM, Barbe RB, Leal RB, Nascimento DW, Simmer Filho J. Functional assessment after arthroscopic shoulder release in adhesive capsulitis. Acta Ortop Bras. [online]. 2026;34(Spe.2): Page 1 of 5. Available from URL: http://www.scielo.br/aob.

INTRODUCTION

Adhesive capsulitis, also known as "frozen shoulder," is a musculoskeletal condition characterized by inflammation and progressive fibrosis of the glenohumeral joint capsule, resulting in pain, stiffness, and restricted range of motion. From a pathophysiological perspective, the disease begins with synovitis, followed by capsular fibrosis and contracture. Histologically, fibroblast proliferation and increased capsular collagen are observed, leading to thickening and adherence of the capsule, particularly in the anteroinferior and axillary regions[1]. Clinically, adhesive capsulitis progresses through three phases: painful (or inflammatory), stiff (or freezing), and resolution, and may last for more than two years. Even after clinical improvement, up to 40% of patients may continue to present some degree of functional limitation.[2-4]

Although most patients show favourable outcomes with conservative treatment, a significant proportion persist with pain and marked

All authors declare no potential conflict of interest related to this article.

The study was conducted at Departamento de Ortopedia e Traumatologia, Hospital Estadual Jayme Santos Neves Serra, Espirito Santo, Brazil.
Correspondence: Daniela Pereira Bortolin. s/n, Avenida Paulo Pereira Gomes, Morada de Laranjeiras, Serra, ES, Brazil. 29166828. danibortolim@hotmail.com

Article received on 05/21/2026 approved on 09/25/2025.
Handling Editor: Jorge Henrique Assunção

restriction of joint mobility, especially during the stiff phase. In such cases, persistent functional disability compromises quality of life and requires more invasive therapeutic alternatives.[5]

Adhesive capsulitis affects between 2% and 5% of the general population, being more common in women between 40 and 60 years of age and, in most cases, involving the nondominant limb.[6] Systemic conditions such as diabetes mellitus and hypothyroidism increase the risk of developing the disease and are associated with greater severity, poorer prognosis, and higher recurrence rates after treatment.[7-9]

Conservative management includes physical therapy, analgesics, intra-articular corticosteroid injections, hydrodilatation, and suprascapular nerve blocks.[6] However, when such measures fail, surgical intervention becomes necessary. Arthroscopic capsular release, often associated with manipulation under anesthesia, is considered an effective therapeutic option in these cases. Studies have demonstrated that this procedure provides significant pain relief, marked improvement in range of motion, and sustained functional recovery in the long term.[10-12]

Despite the widespread use of arthroscopy in the management of adhesive capsulitis, gaps remain regarding the functional impact of this intervention across different populations. The adoption of validated scores, such as the Shoulder Pain and Disability Index (SPADI), allows for an objective and reproducible assessment of the procedure's effects on pain and functional disability. Therefore, investigating the outcomes of arthroscopic capsular release in our setting is relevant to expand clinical evidence and support decision-making in patient's refractory to conservative therapies.

The aim of this study is to retrospectively evaluate the efficacy of arthroscopic capsular release in patients with adhesive capsulitis unresponsive to conservative treatment, through the comparison of pre- and postoperative ranges of motion and functional analysis using the SPADI score.

Our hypothesis is that 360º arthroscopic capsular release provides significant improvements in range of motion and pain reduction, resulting in enhanced postoperative functional scores.

METHODS

This is a retrospective, observational, and descriptive study based on the review of medical records of patients diagnosed with idiopathic adhesive capsulitis who underwent arthroscopic surgery between 2005 and 2025. The study was approved by the Research Ethics Committee of Universidade Vila Velha (UVV/ES), under protocol CAAE: 82335924.8.0000.5064, in accordance with national ethical guidelines.

A total of 645 medical records of patients diagnosed with adhesive capsulitis were reviewed. Of these, 23 patients had undergone arthroscopic capsular release of the shoulder due to refractoriness to clinical treatment after at least six months, either because of persistent pain during this period or lack of improvement in the range of motion of the affected shoulder over the previous 90 days. However, only 10 patients met the inclusion criteria and were deemed eligible for the study (Figure 1).

The inclusion criteria comprised patients with a clinical and imaging diagnosis consistent with adhesive capsulitis, classified as primary or secondary according to Zuckerman, refractory to conservative treatment for at least six months, who underwent arthroscopic capsular release and had documented postoperative follow-up. In addition, the availability of complete data on range of motion and SPADI scores in the postoperative period was mandatory. Exclusion criteria included incomplete medical records or a history of previous surgery on the affected shoulder.

The classification proposed by Zuckerman divides adhesive capsulitis into two major groups: primary (or idiopathic) and secondary.[13] The primary form is characterized by the absence of an apparent cause or association with other diseases and is attributed to an inflammatory and fibrotic process of the joint capsule, whose etiology remains poorly understood. The secondary form, in turn, results from an identifiable cause or is associated with other clinical conditions. Within this group, three subtypes are distinguished: (i) intrinsic, when related to shoulder disorders such as rotator cuff tendinopathies, long head of the biceps tenosynovitis, shoulder fractures, bursitis, or acromioclavicular osteoarthritis; (ii) extrinsic, when associated with conditions distant from the shoulder, including wrist and hand fractures, central or peripheral nervous system diseases (such as stroke, epilepsy, or nerve injuries of the upper limb), cervical spine disorders with or without radiculopathy, as well as cardiac (myocardial ischemia) and pulmonary diseases (chronic lung disease or apical tumors); and (iii) systemic, when associated with metabolic or endocrine disorders, such as diabetes mellitus and thyroid dysfunction. This classification is valuable both for clinical characterization and for guiding therapeutic decision-making.[13]

Clinical and demographic variables were collected, including sex and age; limb dominance and affected side; comorbidities (diabetes mellitus, thyroid disorders); presence of associated lesions

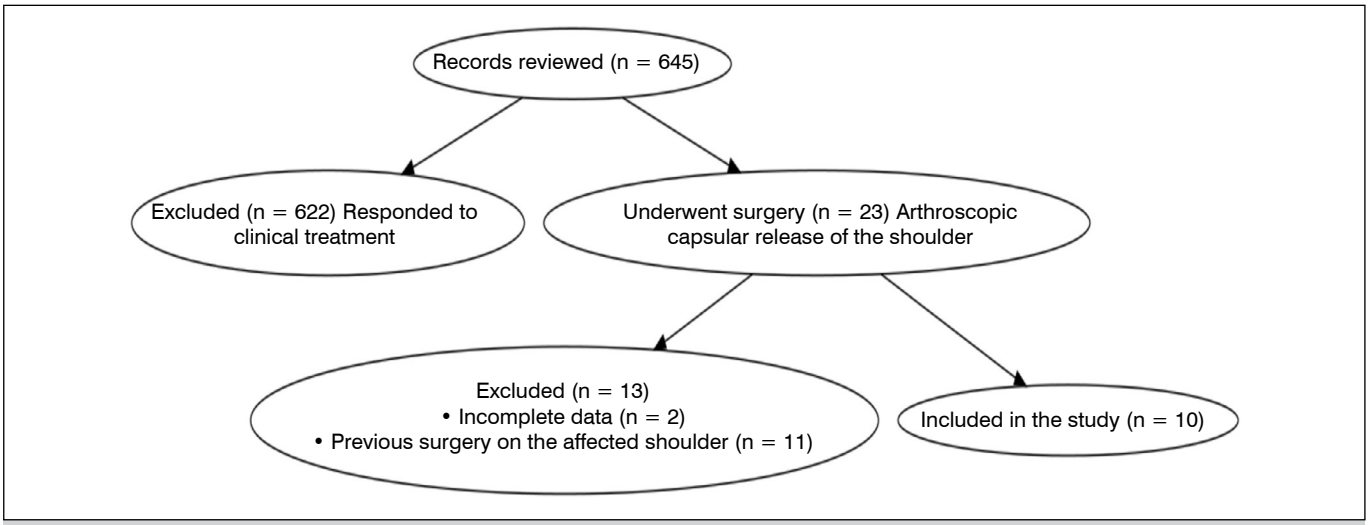

Legend: CONSORT-style flowchart. Source: Present study, 2025.

Figure 1. Flowchart of patient selection with adhesive capsulitis included in the study.

(tendinopathies and partial tears); duration of symptoms; and type of conservative treatment performed.

For functional assessment, pre- and postoperative range of motion was analyzed, including anterior elevation and lateral rotation in degrees, as well as medial rotation using anatomical landmarks. In addition, the SPADI score was applied postoperatively as a subjective instrument to measure pain and functional limitation. The SPADI is a validated scale consisting of 13 items, divided into two domains: pain (5 items) and functional disability (8 items), each scored from 0 to 10 (0 = no pain/difficulty; 10 = maximum).[14] The Pain and Disability scores were calculated as the mean of the items answered in each domain and converted to a 0–100 scale. For descriptive clinical interpretation, the following categorization was adopted: 0–20 = minimal; 21–40 = mild to moderate; 41–60 = moderate to severe; >60 = severe.

All arthroscopic procedures were performed in public and private facilities by the same surgeon, under general anesthesia combined with suprascapular nerve block, with the patient placed in the lateral decubitus position. With the arthroscope introduced through the posterior portal and the radiofrequency probe through the anterior portal, the anterior rotator interval was opened, followed by skeletonization of the posterior surface and coracoid process, and release of the coracohumeral ligament at the base of the coracoid. Using a basket forceps inserted through the anterior portal, superior, anterior, and anteroinferior capsulotomies were performed, allowing visualization of the subscapular muscle fibers (Figure 2).

Next, the visualization was inverted by placing the arthroscope through the anterior portal, and the posterosuperior, posterior, and posteroinferior capsulotomies were performed with the basket forceps introduced through the posterior portal. To complete the procedure, visualization was again inverted, with the arthroscope repositioned in the posterior portal, and the capsulotomy of the axillary recess was performed using the basket forceps through the anterior portal. At the end, a wide view of the joint space could be observed, in sharp contrast to the beginning of the procedure, when the space was markedly restricted, hindering arthroscope maneuverability (Figure 3).

An important technical tip for accessing the anteroinferior and posteroinferior capsule and the axillary recess is to place a thick cushion in the axilla and apply slight adduction of the arm, which facilitates visualization of the axillary recess by displacing the humeral head away from the glenoid (Figure 4).

After arthroscopy, complementary joint manipulation was performed. All patients used a simple sling for comfort during the first two postoperative days. Thereafter, they were instructed to discontinue immobilization early and encouraged to begin active movements of the operated shoulder.

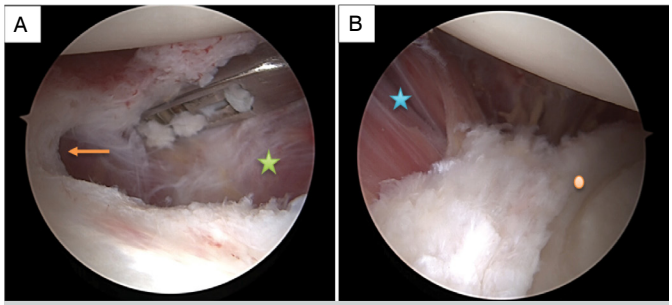

Legend: A. Visualization of the anterior capsulotomy (orange arrow) from the posterior portal, with identification of the subscapular tendon muscle belly (green star). B. Visualization of the posterior capsulotomy through the anterior portal, showing muscle fibers of the infraspinatus tendon (blue star) and the posterior glenoid labrum (orange circle). Source: Present study, 2025.

Figure 2. Arthroscopy of the left shoulder showing anterior (A) and posterior (B) capsulotomies.

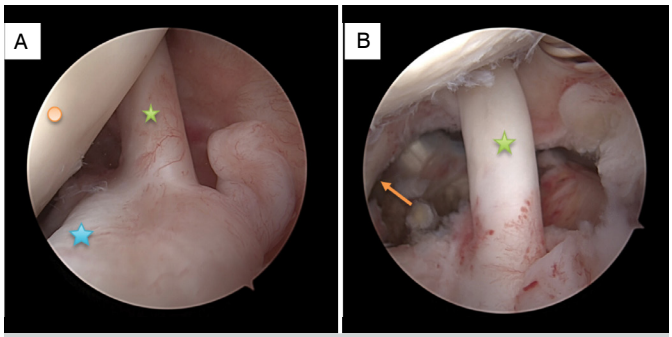

Legend: A. Initial aspect of the procedure, showing hyperemia of the structures in a restricted joint space, with identification of the long head of the biceps tendon (green star), the humeral head (orange circle), and the superior glenoid labrum (blue star). B. Final aspect after circumferential 360° arthroscopic capsulotomy, demonstrating significant widening of the joint space, allowing visualization of a larger intra-articular portion of the long head of the biceps tendon (green star) and the subscapular tendon (orange arrow), which was not visible in the initial image due to the limited arthroscopic field. Source: Present study, 2025.

Figure 3. Arthroscopic view of the left shoulder from the posterior portal.

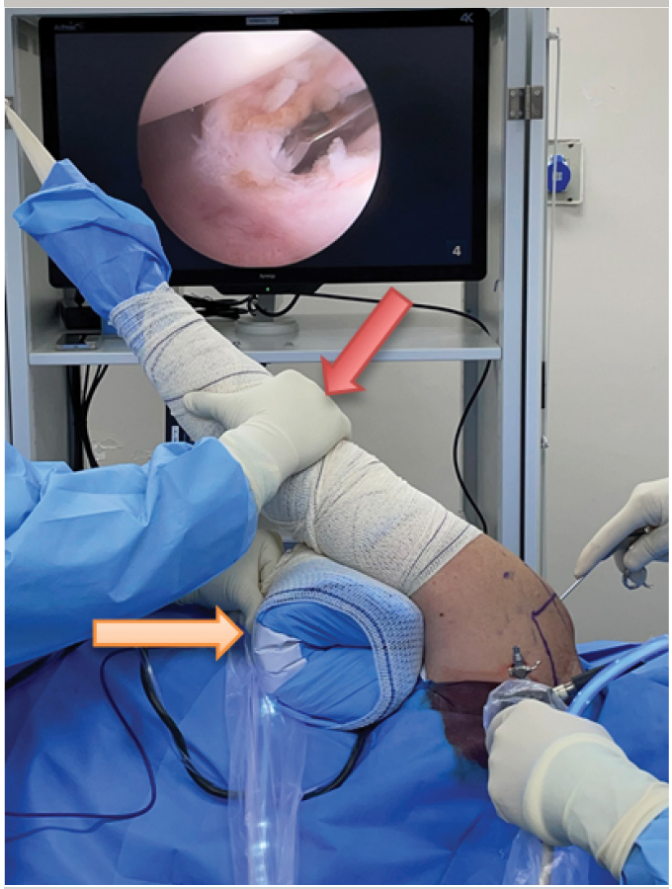

Legend: The arthroscope is positioned in the posterior portal, while the capsulotomy is performed using a basket forceps introduced through the anterior portal. A broad cushion is placed under the patient's axilla (orange arrow) by the assistant, combined with slight adduction of the arm (red arrow), in order to enlarge the joint space adjacent to the axillary recess. Source: Present study, 2025.

Figure 4. Arthroscopic capsulotomy of the left shoulder.

Data were analyzed descriptively and comparatively. For continuous variables, means and standard deviations were calculated; for categorical variables, absolute frequencies were reported. The analysis focused on the progression of range of motion and functional scores, in order to identify the impact of arthroscopic release on patient recovery.

RESULTS

The sample consisted of 10 patients, 9 female and 1 male, with a mean age of 62.3 ± 9.5 years (range, 46–75 years). The left shoulder was the most frequently affected (8 cases), followed by the right shoulder (2 cases) (Table 1).

Regarding comorbidities, systemic diseases were present in a significant proportion of the sample, including hypertension, diabetes mellitus, thyroid disorders, dyslipidemia, and osteopenia. Only two patients presented associated lesions: one with a fracture of the proximal third of the humerus and another with calcific tendinitis (Table 1). All patients initially received multimodal analgesic therapy and physical therapy. In addition, seven patients underwent suprascapular nerve blocks in the outpatient setting every two weeks for at least six months.

According to Zuckerman's classification, four cases were characterized as primary (idiopathic), while the remaining cases were classified as secondary, distributed among the systemic (n = 4) and intrinsic (n = 2) subtypes.[13] It is noteworthy that both cases classified as the intrinsic secondary subtype also presented comorbidities associated with adhesive capsulitis: hypothyroidism and diabetes mellitus.

After the surgical procedure, a significant improvement in range of motion was observed compared with the preoperative period. Postoperative data were collected at a minimum of eight weeks after surgery. Table 2 shows the results, with anterior elevation increasing from 119.2° ± 23.5° to 141.7° ± 11.1°, and external rotation increasing from 28.8° ± 23.9° to 59.2° ± 16.2°.

Postoperative functional assessment using the SPADI revealed favorable outcomes in most patients. Eight patients presented a score of 0, indicating absence of pain and limitation, while two others obtained scores below 20, consistent with minimal pain and disability. No patient presented high scores, reinforcing the trend of functional recovery observed after the procedure. Individual results are shown in Table 3.

One patient developed axillary nerve neurapraxia, which resolved completely within six months, with full recovery of strength, deltoid trophism, and cutaneous sensation in the region. No patient reported glenohumeral instability or required additional anesthetic blocks in the postoperative period.

Table 2. Comparison of pre- and postoperative range of motion in patients with adhesive capsulitis.

Motion (degrees)	Preoperative (mean ± SD)	Postoperative (mean ± SD)
Forward elevation	119.2° ± 23.5°	141.7° ± 11.1°
External rotation	28.8° ± 23.9°	59.2° ± 16.2°

Legend: Means and standard deviations of forward elevation and external rotation in patients with adhesive capsulitis undergoing arthroscopic capsular release (n = 10). SD: standard deviation. Source: Present study, 2025.

Table 3. Shoulder Pain and Disability Index (SPADI) scores postoperatively.

Patient	Sex	Functional Disability (0-100)	Pain (0-100)	SPADI (0-100)	Classification
1	F	0	0	0	Minimal
2	F	0	0	0	Minimal
3	F	0	0	0	Minimal
4	F	0	0	0	Minimal
5	M	0	0	0	Minimal
6	F	18.75	0	9.38	Minimal
7	F	0	0	0	Minimal
8	F	0	0	0	Minimal
9	F	17.50	8.00	12.75	Minimal
10	F	0	0	0	Minimal

Legend: Distribution of Functional Disability and Pain scores (0–100) among patients evaluated postoperatively. F: female; M: male. Classification: 0–20 = minimal; 21–40 = mild to moderate; 41–60 = moderate to severe; >60 = severe. Source: Present study, 2025.

DISCUSSION

The findings of this observational and retrospective study demonstrate that arthroscopic capsular release in patients with adhesive capsulitis refractory to conservative treatment resulted in significant improvement in range of motion and favorable functional outcomes according to the SPADI score, corroborating current evidence on the effectiveness of the arthroscopic approach.[1]

The functional improvement observed was consistent across the group, regardless of etiology, suggesting that arthroscopy may be effective in both primary and secondary cases. Although one patient experienced a transient axillary nerve neurapraxia, it resolved

Table 1. Clinical and demographic characteristics of patients included in the study (n = 10).

Patient	Sex	Age (years)	Affected side	Comorbidities	Associated lesion	Symptom duration (months)	Zuckerman classification
1	F	46	L	None	None	10	Primary
2	F	73	L	Hypothyroidism	Fracture of the proximal third of the humerus managed conservatively	6	Intrinsic secondary
3	F	66	R	DM type 2, hypothyroidism, dyslipidemia.	Bilateral calcific tendinitis	24	Intrinsic secondary
4	F	54	L	HTN	None	24	Primary
5	F	58	R	None	None	12	Primary
6	M	69	L	HTN, DM	None	18	Sistemic secondary
7	F	70	L	hypothyroidism, dyslipidemia, osteopenia.	None	6	Sistemic secondary
8	F	62	L	DM	None	6	Sistemic secondary
9	F	50	L	Hashimoto's thyroiditis	None	6	Sistemic secondary
10	F	75	L	None	None	6	Primary

Legend: Distribution of patients according to age, sex, affected side, comorbidities, associated lesions, symptom duration until surgery, and classification according to Zuckerman. R: right; L: left; HTN: systemic arterial hypertension; DM: diabetes mellitus. Source: Present study, 2025.

spontaneously within six months without interfering with pain relief or functional recovery. We attribute this complication to axillary nerve stretching during joint manipulation performed at the end of the procedure, since arthroscopic capsulotomy is carried out under direct visualization and without nerve manipulation.

Anterior elevation increased on average from 119.2° to 141.7°, while external rotation improved from 28.8° to 59.2°. Functional assessment using the SPADI showed that most patients progressed with minimal pain and disability: eight had a score of 0 and two presented values below 20. The absence of unsatisfactory outcomes reinforces the effectiveness of 360° arthroscopic capsular release in functional recovery within a short period after surgery, suggesting not only rapid improvement in range of motion and function but also in patient satisfaction.[15,16] These results are consistent with previous literature, which reports sustained improvement in the range of motion after arthroscopic release, particularly of the anteroinferior capsule, with a direct impact on external rotation, which is usually the most restricted movement in these patients.[10-12,17]

A strength of this study is that, despite the small sample size and short follow-up period, it demonstrated rapid and consistent functional improvement, highlighting the positive impact of surgery in cases of adhesive capsulitis resistant to conservative treatment. Another noteworthy aspect is the standardization of the technique, performed by a single surgeon, which provides consistency to the results and reduces biases related to technical variability.

CONCLUSION

The 360° arthroscopic capsular release proved effective in promoting significant improvement in range of motion and favorable functional outcomes in the short and mid-term in patients with idiopathic, primary, or secondary adhesive capsulitis who did not improve with conservative treatment. Despite limitations such as the small sample size and the absence of a control group, the findings indicate that arthroscopy represents a safe and effective therapeutic alternative for refractory cases.

CONTRIBUTIONS OF THE AUTHORS

Each author made a personal and significant contribution to the development of this article. SFJ: performed all surgeries; critical review of the manuscript; intellectual concept of the study. BDP: data analysis; manuscript drafting. SIM: data analysis. BRB: data analysis. LRB: critical review of the manuscript. NDW: critical review of the manuscript. All authors declare that they meet the minimum authorship criteria (conception/design; acquisition, analysis, or interpretation of data; drafting; critical review; final approval) and approve the final version of the manuscript for publication.

DATA AVAILABILITY DECLARATION

The contents underlying the research are contained in the manuscript.

REFERENCES

1. Patel R, Urits I, Wolf J, Murthy A, Cornett EM, Jones MR, et al. A comprehensive update of adhesive capsulitis and minimally invasive treatment options. Psychopharmacol Bull. 2020;50(4 Suppl 1):91-107. doi: 10.64719/pb.4384.
2. Neviaser JS. Adhesive capsulitis of the shoulder: a study of the pathological findings in periarthritis of the shoulder. J Bone Joint Surg Am. 1945;27(2):211-22.
3. Reeves B. The natural history of the frozen shoulder syndrome. Scand J Rheumatol. 1975;4(4):193-6. doi: 10.3109/03009747509165255.
4. Miyazaki AN, Santos PD, Silva LA, Sella GV, Carrenho L, Checchia SL. Avaliação dos resultados do tratamento artroscópico da capsulite adesiva do ombro. Rev Bras Ortop. 2017;52(1):61-8. doi: 10.1016/j.rbo.2016.04.001.
5. Cho CH, Bae KC, Kim DH. Treatment strategy for frozen shoulder. Clin Orthop Surg. 2019;11(3):249-57. doi: 10.4055/cios.2019.11.3.249.
6. Cohen M, Amaral MV, Brandão BL, Pereira MR, Monteiro M, Motta Filho GDR. Assessment of the results from arthroscopic surgical treatment of adhesive capsulitis. Rev Bras Ortop. 2013;48(3):272-7. doi: 10.1016/j.rbo.2012.08.004.
7. Tighe CB, Oakley WS Jr. The prevalence of a diabetic condition and adhesive capsulitis of the shoulder. South Med J. 2008;101(6):591-5. doi: 10.1097/SMJ.0b013e3181705d39.
8. Schiefer M, Teixeira PFS, Fontenelle C, Carminatti T, Santos DA, Righi LD, et al. Prevalence of hypothyroidism in patients with frozen shoulder. J Shoulder Elbow Surg. 2017;26(1):49-55. doi: 10.1016/j.jse.2016.04.026.
9. Chuang SH, Chen YP, Huang SW, Kuo YJ. Association between adhesive capsulitis and thyroid disease: a meta-analysis. J Shoulder Elbow Surg. 2023;32(6):1314-22. doi: 10.1016/j.jse.2023.01.033.
10. Le HV, Lee SJ, Nazarian A, Rodriguez EK. Adhesive capsulitis of the shoulder: review of pathophysiology and current clinical treatments. Shoulder Elbow. 2017;9(2):75-84. doi: 10.1177/1758573216676786.
11. Le Lievre HMJ, Murrell GAC. Long-term outcomes after arthroscopic capsular release for idiopathic adhesive capsulitis. J Bone Joint Surg Am. 2012;94(13):1208-16. doi: 10.2106/JBJS.J.00952.
12. Dattani R, Ramasamy V, Parker R, Patel VR. Improvement in quality of life after arthroscopic capsular release for contracture of the shoulder. Bone Joint J. 2013;95-B(7):942-6. doi: 10.1302/0301-620X.95B7.31197.
13. Zuckerman JD, Rokito A. Frozen shoulder: a consensus definition. J Shoulder Elbow Surg. 2011;20(2):322-5. doi: 10.1016/j.jse.2010.07.008.
14. Venturin D, Giannotta G, Pellicciari L, Rossi A, Pennella D, Goffredo M, et al. Reliability and validity of the Shoulder Pain and Disability Index in a sample of patients with frozen shoulder. BMC Musculoskelet Disord. 2023;24(1):212. doi: 10.1186/s12891-023-06268-2.
15. Boutefnouchet T, Jordan R, Bhabra G, Modi C, Saithna A. Comparison of outcomes following arthroscopic capsular release for idiopathic, diabetic and secondary shoulder adhesive capsulitis: a systematic review. Orthop Traumatol Surg Res. 2019;105(5):839-46. doi: 10.1016/j.otsr.2019.02.014.
16. Challoumas D, Biddle M, McLean M, Millar NL. Comparison of treatments for Frozen Shoulder: A Systematic Review and Meta-analysis. JAMA Netw Open. 2020;3(12):e2029581.doi:10.1001/jamanetworkopen.2020.29581.
17. Forsythe B, Lavoie-Gagne O, Patel BH, Lu Y, Ritz E, Chahla J, et al. Efficacy of arthroscopic surgery in the management of adhesive capsulitis: a systematic review and network meta-analysis of randomized controlled trials. Arthroscopy. 2021;37(7):2281-97. doi: 10.1016/j.arthro.2020.09.041.

DOI: http://dx.doi.org/10.1590/1413-785220263402e297312

FUNCTIONAL OUTCOME OF WEBER OSTEOTOMY IN CHRONIC ANTERIOR GLENOHUMERAL DISLOCATION IN YOUNG PATIENTS

RESULTADO FUNCIONAL DA OSTEOTOMIA DE WEBER NA LUXAÇÃO GLENOUMERAL ANTERIOR CRÔNICA EM JOVENS

Felipe Bosco Mendes da Silva[1], *Stela da Silva Chiquetto*[1], *Marcio Alves Cruz*[1], *Fernando Kenji Kikuta*[1], *Sergio de Paula Coelho*[1], *Guilherme Grisi Mouraria*[1]

1. Universidade de Campinas (Unicamp), Departamento de Ortopedia e Traumatologia, Divisao de Cirurgia do Ombro e Cotovelo, Campinas, SP, Brazil.

ABSTRACT

Objective: This study aimed to evaluate the functional outcomes of humeral head derotational osteotomy according to the Weber technique as a therapeutic alternative for the treatment of chronic anterior shoulder dislocation in young patients. Methods: This prospective case series included patients younger than 50 years who underwent clinical and radiographic evaluation. Outcomes were assessed using plain radiographs, computed tomography (CT), the Visual Analog Scale (VAS) for pain, the 36-Item Short Form Health Survey (SF-36), and range of motion measurements. The mean age of the participants was 47.67 years. Results: The procedure resulted in a significant reduction in pain, with a mean decrease of 5.7 points on the VAS, as well as improvements of 30° in extension and 28° in external rotation ($p < 0.05$). The SF-36 demonstrated an average improvement of 27 points in overall quality of life and functional status, and 54 points in the pain domain. No cases of recurrent dislocation were observed. Conclusion: Weber humeral head derotational osteotomy provides satisfactory functional recovery, significant pain relief, and may be considered a viable treatment option for chronic anterior glenohumeral dislocation in young patients. ***Level of Evidence IV; Case Series.***

Keywords: Shoulder Dislocation; Shoulder Injuries; Osteotomy.

RESUMO

Objetivo: Este estudo teve como objetivo avaliar os resultados funcionais da osteotomia de desrotação da cabeça umeral segundo a técnica de Weber, como alternativa terapêutica para a luxação anterior crônica do ombro em pacientes jovens. Métodos: Trata-se de um estudo prospectivo de uma série de casos, incluindo pacientes com menos de 50 anos, avaliados por radiografias, tomografia, Escala Visual Analógica (EVA) para dor, escala SF-36 e avaliação da amplitude de movimento. A média de idade dos participantes foi de 47,67 anos. Resultados: Os resultados mostraram melhora significativa da dor (redução média de 5,7 pontos na escala EVA), além de ganho de 30° na extensão e 28° na rotação lateral ($p<0,05$). O escore do SF-36 indicou melhora média de 27 pontos na qualidade de vida e funcionalidade, e 54 pontos no domínio da dor. Nenhum caso apresentou recorrência. Conclusão: A osteotomia de Weber promove boa recuperação funcional, alívio da dor e pode ser considerada uma opção viável para o tratamento da luxação glenoumeral anterior crônica em pacientes jovens. ***Nível de Evidência IV; Série de Casos.***

Descritores: *Luxação do Ombro; Lesões do Ombro; Osteotomia.*

Citation: Silva FBM, Chiquetto SS, Cruz MA, Kikuta FK, Coelho SP, Mouraria GG. Functional outcome of weber osteotomy in chronic anterior glenohumeral dislocation in young patients. Acta Ortop Bras. [online]. 2026;34(Spe.2): Page 1 of 5. Available from URL: http://www.scielo.br/aob.

INTRODUCTION

Chronic anterior shoulder dislocation is a rare condition defined as a glenohumeral dislocation that has not been reduced since the third week of the traumatic event[1]. Chronic anterior dislocation is less prevalent than posterior dislocation, which is related to the fact that it is more symptomatic (more loss of movement and pain) in its acute phase when compared to posterior dislocation[2]. In this context, patients with cognitive alterations (secondary to multiple trauma, neurological diseases, and alcoholism) may make initial diagnosis difficult and facilitate the progression to chronic dislocation[3,4].

Prolonged glenohumeral joint incongruence can lead to degenerative changes such as severe bony deformity in the humeral head (large Hill-Sachs lesion) and/or the glenoid associated with capsuloligamentous injury[1,5]. Associatedly, there is a shortening of the posterior capsule and a lengthening of the anterior one. In addition to the anatomical complexities inherent to the pathology, dislocation when not reduced presents continuous joint deterioration and functional loss. Therefore, therapeutic management is challenging and requires precise strategies to restore joint functionality and stability[6,7].

Treatment for chronic anterior shoulder dislocation is controversial. Conservative treatment may be performed when the patient is not in a clinical condition for surgical treatment. Other comorbidities such as epilepsy and uncontrolled alcoholism may prevent surgical treatment[8,9].

All authors declare no potential conflict of interest related to this article.

The study was conducted at Universidade de Campinas, Faculdade de Ciencias Medicas.
Correspondence: Felipe Bosco Mendes da Silva. 126, Rua Tessalia Vieira de Camargo, Barao Geraldo, Campinas, SP, Brazil. 13083-970. felipeboscoms@gmail.com

Article received on 05/29/2025 approved on 09/03/2025.
Handling Editor: Américo Zoppi Filho

The decision on the type of surgical treatment is influenced by several factors such as age, time of dislocation, and size of the bone defect in the glenoid and humerus[10,11]. Elderly patients with chronic dislocation and large bone defects can be treated with arthroplasty. Currently, reverse arthroplasty is the implant of choice[12,13].

Treatment in young patients is challenging because many techniques are ineffective, especially in cases of large bone defects in the humeral region. Arthroplasty in this cohort of patients is limited due to the risk of early revisions and postoperative instability[12]. Shortening of the posterior capsule, failure of the anterior capsule, and internal rotators caused by chronic dislocation increase the risk of surgical failure in classic techniques such as open reduction, labral repair, and Latarjet surgery, and have a high rate of dislocations or subluxations after the procedure[14]. Treatment with bone graft in the posterolateral portion of the head can prevent recurrence. However, the need for extensive detachment of the supraspinatus and, in some cases, the infraspinatus to access the defect can determine postoperative functional impairment even when reinsertion is correctly performed[1,15].

The first cases of proximal humeral osteotomies date back to the end of the 19th century. Advances in internal fixation methods, particularly in plate and screw systems, have significantly increased postoperative bone stability about the results of osteotomies[16]. In 1984, Weber performed an osteotomy to retrovert the humeral head about the diaphysis for Hill-Sachs lesions that presented entrapment in the glenoid when the patient performed a lateral rotation of the shoulder. The original objective of the technique was to treat patients with traumatic glenohumeral instability. With the advent of labral repair (Bankart) and bone blocks (Bristow, Latarjet), it was progressively abandoned[17,18].

There is no consensus in the literature regarding the ideal procedure for the treatment of chronic anterior glenohumeral dislocation in young patients with large Hill-Sachs lesions. Thus, the technique developed by Weber becomes an option in the treatment of this challenging disease by retroverting the humeral head and avoiding the engagement of the Hill-Sachs defect in the glenoid.

The objective was to evaluate the functional and radiological results of a series of cases of young patients diagnosed with chronic anterior glenohumeral dislocation who underwent Weber humeral osteotomy.

MATERIALS AND METHODS

A prospective study was performed on a case series of patients with chronic anterior glenohumeral dislocation who underwent Weber osteotomy.

The inclusion criteria were patients aged between 18 and 50 years with a diagnosis of chronic dislocation for at least 3 months, who were compensated for any associated diseases (epilepsy, alcoholism). Patients with associated fractures, the presence of osteonecrosis of the humeral head, and patients with less than one year of postoperative follow-up were excluded.

All patients underwent pre- and postoperative radiological evaluation with true anteroposterior, lateral, and axillary radiographs. Computed tomography was performed only preoperatively. The Visual Analogue Pain Scale (VAS) was assessed to measure patients' pain complaints in the pre- and postoperative periods. Functional analysis was conducted using the SF-36 (Short Form Health Survey) and by recording the range of motion using a standard goniometer[19].

The procedure was performed with the patient in the beach chair position. A 15 cm deltopectoral access port was created. The subscapularis tendon was detached and repaired. The interposed scar tissue in the joint was then removed and the humeral head was reduced. The humeral head was fixed to the glenoid with a provisional 3 mm Kirschner. A 2.5 mm Kirschner wire was inserted into the humeral head from anterior to posterior and a second 2.5 mm Kirschner wire was inserted into the humeral shaft forming an approximate 30º medial inclination angle about the anterior. A proximal humeral locking plate (Hexagon R) with 4 holes and fixed in its proximal portion with 2 locked screws. An osteotomy is performed at the surgical neck and a 30-degree lateral rotation of the humeral diaphysis about the head using the 2 Kirschner wires as a reference (the wires remain parallel after the humeral rotation). The plate is fixed in its distal portion and then completed in its proximal portion (Figure 1). The entire procedure is guided by intraoperative radioscopy. The subscapularis tendon is inserted, followed by complete closure of the wound and immobilization with a sling. The immobilization is maintained until the fourth week when it is removed and the shoulder movement is regained.

During the postoperative follow-up, radiographic control and clinical evaluation were performed as previously described at two weeks, one, three, six, and twelve months postoperatively. The fracture

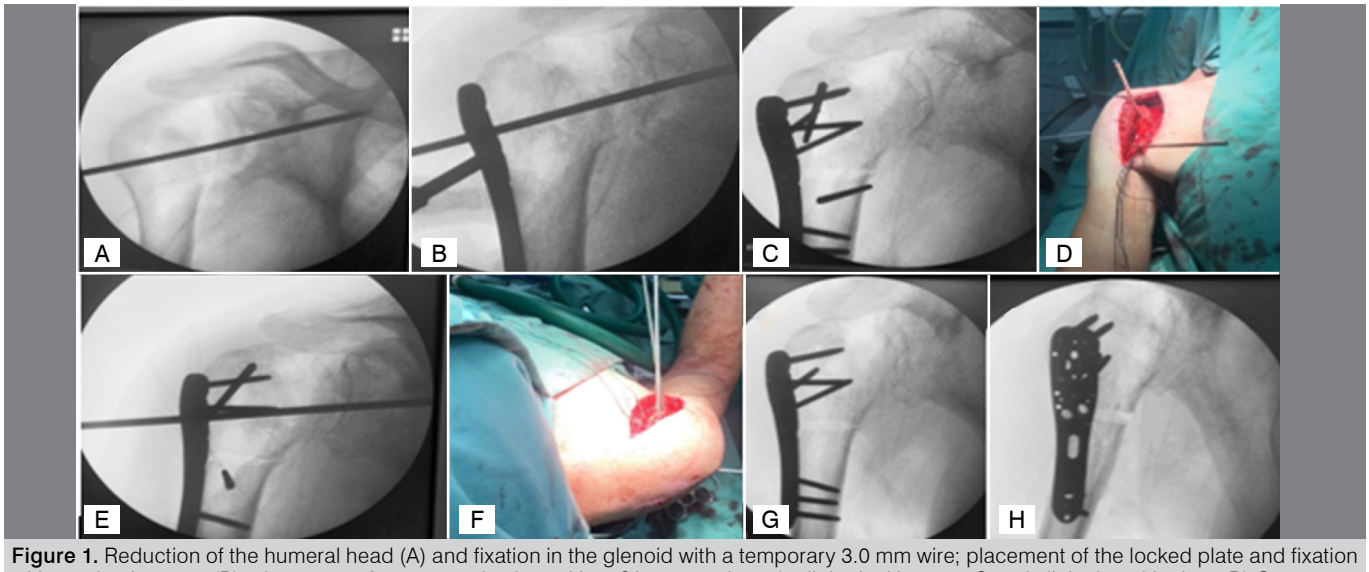

Figure 1. Reduction of the humeral head (A) and fixation in the glenoid with a temporary 3.0 mm wire; placement of the locked plate and fixation with proximal screws (B); placement of temporary k-wires with 30º between them (radiological image - C and clinical positioning - D) Osteotomy and external rotation of the arm of 300 (radiological image E clinical image F where parallelism between the k-wires is observed; fixation of the locked plate completed and removal of k-wires (radiograph in anteroposterior position G and lateral view H).

was deemed consolidated when the osteotomy sign was no longer visible in three radiographic views (Figure 2).
Non-categorical variables were tested using the Kolmogorov-Smirnov test to define sample normality, and the paired t-test was used to compare non-categorical variables in the pre-and postoperative periods. A significance level of $P < 0.05$ was considered. SPSS statistics software version 29 was used.
The project was approved by the research ethics committee under number CAAE:84493524.0.0000.5404.

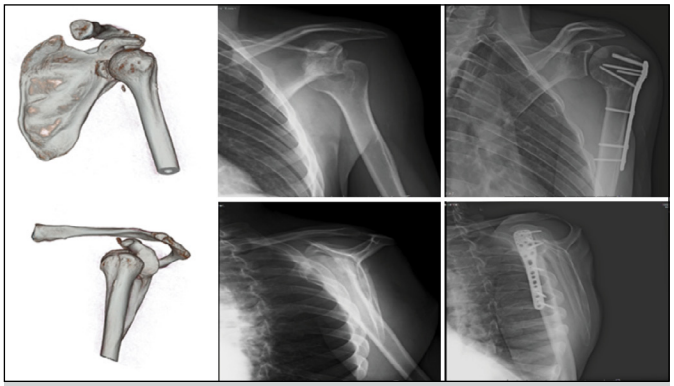

Figure 2. Tomography with 3D reconstruction and pre- and post-operative radiographs.

RESULTS

Three patients were included, all male, with a mean age of 47.67 + 8.73 years. The mean dislocation time was 3.6 + 0.57 months. There was osteotomy consolidation in all cases and none developed infection or postoperative neurological deficit.
The gain in the range of motion after the procedure occurred in all planes except abduction and adduction. Medial rotation was measured functionally. Two patients evolved postoperatively with rotation at the level of L5 (Figure 3) and one with rotation at the level of the greater trochanter (without improvement about the postoperative period). Flexion and elevation of the scapular plane were the movements with the greatest postoperative gain. (Table 1).
A significant improvement in postoperative pain was observed. There was an average decrease of 5.7 + 3.05 points in the VAS score (Table 2).

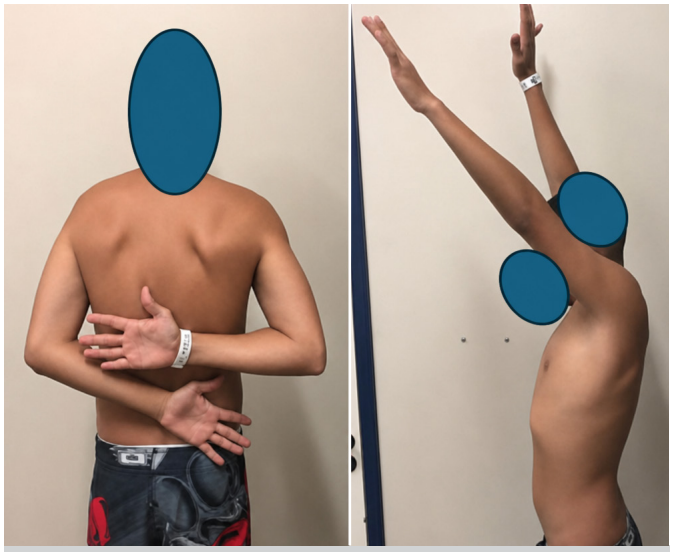

Figure 3. Postoperative evolution (internal rotation at L5 level) and 150º of flexion.

The SF-36 quality of life assessment score showed an improvement in all domains except vitality and mental health. The main improvement observed in the SF-36 was related to pain control with a mean increase of 53.66 + 37.28 points. The assessment of general health by the postoperative SF -36 was significant with an increase of 27.66 + 5.13 points. In the functional capacity domain, there was a mean increase of 26.67 + 16.07 points (Table 2).

Table 1. Pre- and postoperative range of motion.

Range of motion	preoperative (degrees)	Postoperative (degrees)	IC (degrees)	p-value*
Flexion	26.67 + 15.27	101.67 + 47.52	23.58 - 173.58	0.04
Lateral rotation	20.00 + 10.00	48.33 + 2.88	4.41 - 9.36	0.01
Extension	6.67 + 2.88	36.67 + 5.77	17.57 - 42.42	0.05
Abduction	23.33 + 15.27	51.67 + 33.29	21.86 - 78.53	0.06
Adduction	3.82 + 4.2	5.91 + 2.6	2.19-6.37	0.10

* Paired t-test.

Table 2. Visual analogue pain scale and SF-36 score pre- and postoperatively.

Score	preoperative (stitches)	postoperative (stitches)	IC (points)	p-value*
VAS	8.33 + 0.57	2.67 + 3.05	14.39 + 3.05	0.05
Sf-36 (general health)	30,00 + 10,00	57.67 + 9.81	14.9 - 40.4	0.05
Sf-36 (functional capacity)	18.33 + 17.55	45.00 + 26.45	13.20 - 66.59	0.05
Sf-36 (pain)	16.67 + 5.77	70.33 + 34.06	38.96 – 98.46	0.05
Sf-36 (vitality)	15.00 + 5.00	45.33 + 10.50	3, 48 - 64.15	0.06
Sf-36 (mental health)	18.33 + 2.88	28.67 + 11.84	11.93 - 32.59	0.09

* Paired t-test; SF-36 =Short Form Health Survey; VAS =Visual Analogue Pain Scale.

DISCUSSION

Chronic anterior glenohumeral dislocation is a rare disease[1]. The case series presented here was constructed after 5 years. Thus, the incidence of surgical treatment was less than 1 case per year. No patient developed postoperative subluxation or dislocation. The lower prevalence of recurrence found in osteotomy compared with traditional techniques may be associated with the fact that osteotomy not only avoids the engagement of the Hill-Sachs lesion in the glenoid but also tensions the anterior capsule and lengthens the posterior capsule. This re-tensioning improves the balance of forces acting on the humeral head, which is altered in chronic anterior dislocation.
Reverse arthroplasty indicated for chronic anterior shoulder dislocation has shown promising results, with significant improvement in pain complaints and range of motion. However, the studies evaluated only patients over 50 years of age. In addition, patients undergoing arthroplasty developed a higher complication rate (instability and need for revision) when compared to those undergoing arthroplasty due to rotator cuff arthropathy[20,21].
Although Latarjet surgery evolves with good functional recovery in patients with shoulder instability, it does not present the same way in cases of chronic anterior dislocation. The Latarjet technique has demonstrated a high rate of subluxations, surgical revisions, and early osteoarthritis, especially when subscapularis tenotomy is necessary during the surgical approach, which is often essential due to soft tissue contracture and the need to remove interposition tissues in chronic anterior dislocation[14,22,23].

Open reduction associated with soft tissue re-tensioning and bone grafting in the Hill-Sachs defect or open reduction associated with Bankart repair has a high complication rate, especially in young patients[8,24].

Clinical analysis based on the visual analog scale (VAS) demonstrated an improvement in pain after the surgical procedure. Previous studies, such as those by Rai et al. and Li and Jiang, also showed improvements in pain parameters, especially in the early postoperative period. However, in these studies, patients who presented subluxation returned to preoperative pain levels, a common phenomenon in techniques such as Latarjet in the treatment of chronic anterior dislocation. This suggests that, unlike what is observed in Weber osteotomy, the improvement in pain in traditional approaches may be transient and dependent on joint stability[14,25].

Functional and quality of life analysis of patients undergoing osteotomy revealed significant improvements in some postoperative parameters. Flexion and elevation in the scapular plane were the movements that evolved with the greatest gains. In the study by Rai et al, which used the Latarjet technique, a significant improvement in abduction was observed, increasing from 37.7° to 108.2°; however, the other movements were not evaluated, limiting the comparison between the techniques. In addition to functional gains, the quality of life of patients was positively impacted, as demonstrated by the increase in the score of the general health domain of the SF-36, which increased from 30.00 ± 10.00 to 57.67 ± 9.81 ($p < 0.005$). The study by Li and Jiang also demonstrated statistically significant improvements in lateral rotation and functionality, although using scores other than the SF-36, such as ASES, UCLA, and Constant. However, the positive evolution in these studies was observed only in patients without episodes of new dislocation or subluxation. Since new dislocation is a complication frequently associated with the Latarjet technique, it is possible that the functional and range of motion gains reported in these studies would be smaller with a longer postoperative follow-up[14].

The main limitation of the study was the small number of cases evaluated. However, considering that the disease has a low prevalence and that classical techniques for the treatment of chronic anterior shoulder dislocation have significant recurrence rates, the proposal of Weber osteotomy for the treatment of this disease is of great value.

Weber osteotomy appears as a promising technique in the treatment of chronic anterior glenohumeral dislocation and constitutes an alternative for chronic anterior shoulder dislocation. Prospective multicenter studies are needed to confirm the efficacy of this procedure, strengthening its applicability in clinical practice.

CONCLUSION

Weber´s retroversion osteotomy of the humeral head evolved with good functional recovery, and improvement of pain associated with an absence of recurrence of chronic anterior glenohumeral dislocation and can be considered an option for the treatment of this complex condition.

ACKNOWLEDGMENT

A special acknowledgment is extended to the entire team of the Shoulder and Elbow Division at the University of Campinas (UNICAMP) for their support in making this scientific work possible.

CONTRIBUTIONS OF THE AUTHORS

Each author made a personal and significant contribution to this article. SFBM, CSS, CMA: Investigation, Data curation; KFK, CSP: Investigation (surgical procedures); MGG: Conceptualization, Writing – review & editing.

DATA AVAILABILITY DECLARATION

The data underlying the research text are contained within the manuscript.

REFERENCES

1. Checchia SL, Doneux P, Miyazaki AN, Bauer G, Akkari M, Miguel AJ, et al. Luxação anterior inveterada de ombro: resultados obtidos no tratamento cirúrgico. Rev Bras Ortop. 1996;31(8):663-9.
2. Goth AP, Klug A, Gosheger G, Hiort ML, Akgün D, Schneider KN. Traumatic anterior shoulder dislocation: epidemiology, diagnosis, and treatment. Dtsch Arztebl Int. 2025;122(4):89-95. doi: 10.3238/arztebl.m2024.0254.
3. Cohen M, Fonseca R, Galvão Amaral MV, Monteiro MT, Motta Filho GR. Treatment of chronic locked posterior dislocation of the shoulder with the modified McLaughlin procedure. J Shoulder Elbow Surg. 2022;31(1):100-6. doi: 10.1016/j.jse.2021.05.026.
4. Haritinian EG, Stoica IC, Popescu R, Gheorghievici GL, Nové-Josserand L. Treatment and outcomes of chronic locked posterior shoulder dislocations: a retrospective case series. BMC Musculoskelet Disord. 2023;24(1):82. doi: 10.1186/s12891-023-06200-8.
5. Hawkins RJ. Unrecognized dislocations of the shoulder. Instr Course Lect. 1985;34:258-63.
6. Yanmis I, Komurcu M, Oguz E, Basbozkurt M, Gur E. The role of arthroscopy in chronic anterior shoulder dislocation: technique and early results. Arthroscopy. 2003;19(10):1129-32. doi: 10.1016/j.arthro.2003.10.021.
7. Sahajpal DT, Zuckerman JD. Chronic glenohumeral dislocation. J Am Acad Orthop Surg. 2008;16(7):385-98. doi: 10.5435/00124635-200807000-00004.
8. Franklin CC, Weiss JM. The natural history of pediatric and adolescent shoulder dislocation. J Pediatr Orthop. 2019;39(6 Suppl 1):S50-2. doi: 10.1097/BPO.0000000000001374.
9. Nunes J, Sarmento A, Valente C, Andrade R, Espregueira-Mendes J. Luxação do ombro: avaliação e tratamento. Rev Med Desportiva. 2021;12(3):31-3. doi: 10.23911/Clinica_Dragao_2021_mai.
10. Makaram NS, Becher H, Oag E, Heinz NR, McCann CJ, Mackenzie SP, et al. Predicting recurrence of instability after a primary traumatic anterior shoulder dislocation. Bone Joint J. 2024;106-B(10):1111-7. doi: 10.1302/0301-620X.106B10.BJJ-2023-1454.R1.
11. Wasserstein DN, Sheth U, Colbenson K, Henry PDG, Chahal J, Dwyer T, et al. The true recurrence rate and factors predicting recurrent instability after nonsurgical management of traumatic primary anterior shoulder dislocation: a systematic review. Arthroscopy. 2016;32(12):2616-25. doi: 10.1016/j.arthro.2016.05.039.
12. Paxton ES, Dodson CC, Lazarus MD. Shoulder instability in older patients. Orthop Clin North Am. 2014;45(3):377-85. doi: 10.1016/j.ocl.2014.04.002.
13. Arner JW, Peebles LA, Bradley JP, Provencher MT. Anterior shoulder instability management: indications, techniques, and outcomes. Arthroscopy. 2020;36(11):2791-3. doi: 10.1016/j.arthro.2020.09.024.
14. Li Y, Jiang C. The effectiveness of the Latarjet procedure in patients with chronic locked anterior shoulder dislocation: a retrospective study. J Bone Joint Surg Am. 2016;98(10):813-23. doi: 10.2106/JBJS.15.00832.
15. Goga IE. Chronic shoulder dislocations. J Shoulder Elbow Surg. 2003;12(5):446-50. doi: 10.1016/S1058-2746(03)00088-0.
16. Weber BG, Simpson LA, Hardegger F. Rotational humeral osteotomy for recurrent anterior shoulder dislocation of the shoulder associated with a large Hill-Sachs lesion. J Bone Joint Surg Am. 1984;66:1443–1450.
17. Rockwood CA, Matsen FA, Wirth MA, Lippitt SB, Fehringer EV, Sperling JW, editors. Rockwood and Matsen's the shoulder. 5th ed. Philadelphia (PA): Elsevier; 2017.
18. Ikemoto RY, Murachovsky J, Nascimento LGP, Bueno RS, Almeida LHO, Strose E, et al. Resultados da cirurgia de Latarjet no tratamento da instabilidade anterior traumática do ombro associada à erosão óssea da cavidade glenoidal – seguimento mínimo de um ano. Rev Bras Ortop. 2011;46(5):553-60. doi: 10.1590/S0102-36162011000500012.
19. Wu Q, Chen Y, Zhou Y, Zhang X, Huang Y, Liu R. Reliability, validity, and sensitivity

of short-form 36 health survey (SF-36) in patients with sick sinus syndrome. Medicine (Baltimore). 2023;102(24):e33979. doi: 10.1097/MD.0000000000033979.
20. Maia RB, Barros RM, Silva LFC, Santos MVS. Artroplastia Reversa do Ombro: Indicações Emergentes e Resultados. Rev Cient Hosp Santa Izabel. 2019;3(3):78-85.
21. Storti TM, Ribeiro TS, Faria RSS, Simionatto JE, Simionatto C, Paniago AF. Reverse shoulder arthroplasty: evaluation of the clinical and functional outcomes per etiology. Rev Bras Ortop (Sao Paulo). 2022;57(5):868-75. doi: 10.1055/s-0041-1731674.
22. Sahu D, Rathod V, Phadnis A, Shyam A. Results and complications of head-preserving techniques in chronic neglected shoulder dislocation: a systematic review. J Shoulder Elbow Surg. 2021;30(3):685-94. doi: 10.1016/j.jse.2020.10.010.
23. Chaudhary D, Joshi D, Jain V, Mohindra M, Mehta N. A six months old neglected anterior shoulder dislocation managed by closed reduction and Latarjet procedure. Chin J Traumatol. 2016;19(5):295-7. doi: 10.1016/j.cjtee.2016.06.005.
24. Sacolick DA, Williams RR, Wu SJ, Kraeutler MJ, McCulloch PC. Surgical treatment of anterior glenohumeral instability: a historical review. J Shoulder Elbow Surg. 2024;33(12):2766-79. doi: 10.1016/j.jse.2024.07.029.
25. Rai AK, Bandebuche AR, Bansal D, Gupta D, Naidu A. Chronic unreduced anterior shoulder dislocation managed by Latarjet procedure: a prospective study. Cureus. 2022;14(1):e21769. doi: 10.7759/cureus.21769. X

DOI: http://dx.doi.org/10.1590/1413-785220263402e297893

BIOMECHANICAL STUDY OF PULLOUT RESISTANCE OF CORTICAL SCREWS IN SWINE LUMBAR VERTEBRAE

ESTUDO BIOMECÂNICO DA RESISTÊNCIA AO ARRANCAMENTO DE PARAFUSOS CORTICAIS EM VÉRTEBRAS LOMBARES SUÍNAS

Rogério Lúcio Chaves de Resende[1], *Jefferson Soares Leal*[1], *Jefferson J. Vilela*[2], *Renato de Mello Guimarães*[1], *Ângelo Ribeiro Vaz de Faria*[1], *Marco Antônio Percope de Andrade*[1]

1. Universidade Federal de Minas Gerais (UFMG), Faculdade de Medicina, Belo Horizonte, MG, Brazil.
2. Centro de Desenvolvimento da Tecnologia Nuclear (CDTN), Comissao Nacional de Energia Nuclear (CNEN), Belo Horizonte, MG, Brazil.

ABSTRACT

Introduction: This study aimed to evaluate the mechanical resistance to pullout of the lumbar cortical bone trajectory (CBT) screw with and without transfixation of the second cortical in a biomechanical assay in swine vertebrae. Methods: A pullout test was performed in 16 swine vertebrae (L5 and L6) fixed with 32 CBT screws using the same protocol. Of these, 16 were inserted in a monocortical manner according to the original technique and 16 through a modified technique which included the transfixation of the second cortical bone. Results: The average maximum load value for pulling out the inserted screws with the modified technique including the transfixation of the second cortical bone was 140.50 Kgf (± 56.56), while in the original technique it was 95.69 Kgf (± 42.19) (p = 0.004). Conclusion: The biomechanical tests applied to the studied sample showed that the pullout resistance of the CBT screws inserted with the bicortical technique was, on average, 46% higher than the screws inserted according to the original monocortical technique. **Level of Evidence II; Experimental study.**

Keywords: Spinal arthrodesis; Lumbar cortical screw; Cortical bone trajectory; Pullout resistence; Biomechanical testing.

RESUMO

Objetivo: Este estudo teve como objetivo avaliar a resistência mecânica ao arrancamento de parafusos com trajetória cortical (CBT) na coluna lombar, com e sem transfixação da segunda cortical, por meio de ensaio biomecânico em vértebras suínas. Métodos: Foram realizados testes de arrancamento em 16 vértebras lombares suínas (L5 e L6), nas quais foram inseridos 32 parafusos CBT utilizando o mesmo protocolo. Desses, 16 foram inseridos de forma monocortical, conforme a técnica original, e 16 com uma técnica modificada que incluía a transfixação da segunda cortical. Resultados: O valor médio da carga máxima para arrancamento dos parafusos inseridos com a técnica modificada, incluindo a transfixação da segunda cortical, foi de 140,50 Kgf (± 56,56), enquanto que na técnica original foi de 95,69 Kgf (± 42,19) (p = 0,004). Conclusão: Os testes biomecânicos aplicados à amostra estudada mostraram que a resistência ao arrancamento dos parafusos CBT inseridos com a técnica bicortical foi, em média, 46% superior à dos parafusos inseridos segundo a técnica monocortical original. ***Nível de Evidência II; Estudo experimental.***

Descritores: *Artrodese espinhal; Parafuso cortical lombar; Trajetória cortical; Resistência ao arrancamento; Teste biomecânico.*

Citation: Resende RLC, Leal JS, Vilela JJ, Guimarães RM, Faria ARV, Andrade MAP. Biomechanical study of pullout resistance of cortical screws in swine lumbar vertebrae. Acta Ortop Bras. [online]. 2026;34(Spe.2): Page 1 of 4. Available from URL: http://www.scielo.br/aob.

INTRODUCTION

Spinal surgery is increasingly common worldwide, with a considerable growth in the last two decades, especially in the elderly population.[1,2] Among the various fixation techniques to promote thoraco-lumbar arthrodesis, the most commonly used today is the pedicular fixation,[3] in which the screw is inserted into the cancellous bone inside the vertebral pedicle. This technique is considered the gold standard nowadays. Spine fixation with pedicle screws shows superior biomechanical performance compared to the old methods, but still with fixation failures, especially in osteoporotic bones.[4-6]

Searching for a new spine fixation system, in 2009, Santoni et al[7] described a screw technique for the lumbar spine, the so called cortical bone trajectory (CBT) screw, with mechanical advantages, especially when applied to osteoporotic bones[7-9]

The particular characteristic of this screw which supports its own name - cortical bone trajectory - is the pericortical bone positioning in almost its entire path.

The CBT screw can reach up to four points of contact with the cortical bone, namely: the screw entry point in the *pars interarticularis*, the inferomedial wall of the pedicle, the anterolateral wall of the pedicle

All authors declare no potential conflict of interest related to this article.

The study was conducted at Universidade Federal de Minas Gerais (UFMG), Belo Horizonte, MG, Brazil.
Correspondence: Rogerio Lucio Chaves de Resende. 190, Av. Prof. Alfredo Balena, Santa Efigenia, Belo Horizonte, MG, Brazil. 30130-100. rogerioluciоc@yahoo.com.br

Article received on 06/16/2025 approved on 09/24/2025.
Handling Editor: Eduardo Angeli Malavolta

<< SUMÁRIO

and the lateral cortical of the vertebral body, where the screw ends its path by touching it, but not transfixing it.[10] Among these, *pars interarticularis* is the anatomically highest bone density point that the screw has contact with.[10]
This study uses a modification of the Santoni et al[7] technique, which consists of the transfixation of the second cortical bone, which would lead it to be considered as a bicortical screw technique. The hypothesis of the study is that this modification of the original technique has better mechanical performance in pullout tests, when compared to screws inserted without cortical transfixation.
This study aimed to compare the mechanical strength of CBT screws when used in a bicortical way compared to those used in a unicortical way, as described by Santoni et al.[7]

MATERIAL AND METHODS

To carry out the study, the two most distal lumbar vertebrae (L5 and L6) of pigs slaughtered for human consumption were used. These samples were obtained from animals weighing approximately 100 kilograms (Kg), with an average age of 150 days, all male and from the Landrace breed. The total of 10 L5 and 10 L6 vertebrae from 10 recently slaughtered pigs were dissected and kept in a refrigerator at an average temperature of -20º Celsius until the tests were carried out. For the execution of the biomechanical tests, the anatomical pieces were placed at the room temperature until they were completely thawed, in order to have their mechanical properties recovered.
To carry out the tests, the vertebral bodies were adapted and supported on a firm base through a metallic device similar to a hollow cube, which had its lateral walls with a groove to fit the screws. An *Instron 5882* universal testing machine with a load cell with a maximum capacity of 100 KiloNewtons was used, coupled with the *Bluehill2 software* that allowed the registration of the force required to pull the screws out of the vertebrae.
All screws used in the tests were a 4.5 mm-diameter and 45 mm-length titanium alloy polyaxial pedicle screws (Spherx II Nuvasive - Manufacturer: Nuvasive, INC - USA).
The preparation of CBT screws paths, through the pedicles of the pigs lumbar vertebral bodies (L5 and L6), was made according to the technique described by Santoni et al.[7,11,12] followed by the fixation with the screws, which were performed by a single surgeon, freehand, identical to the technique of the surgical procedures.
The screw entry point was at the junction of a vertical line that passes through the medial face of the lower facet of the adjacent cranial vertebra and a horizontal line, perpendicular to it, which passes approximately 1 millimeter below and parallel to the lower edge of the transverse process.[7,11,12] (Figure 1)
The initial perforation of the entry point was made with the initial awl, followed by the Lenke probe until it touched the vertebral body's cortical wall, to complete the CBT screw path. The path is 8-10 degrees from medial to lateral in the axial plane and 25-30 degrees from caudal to cephalic in the sagittal plane.[7,11,12] The same procedure was made through the contralateral pedicle. (Figure 2)

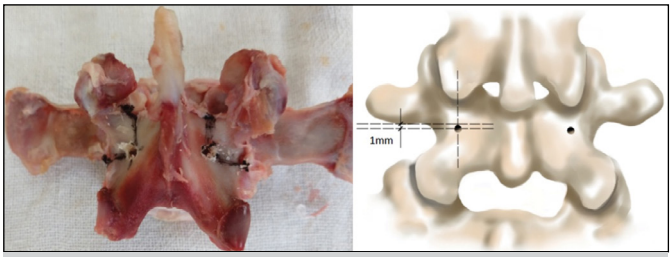

Figure 1. Entry point of the cortical screw as described by Santoni et al.[7] and used in this study.

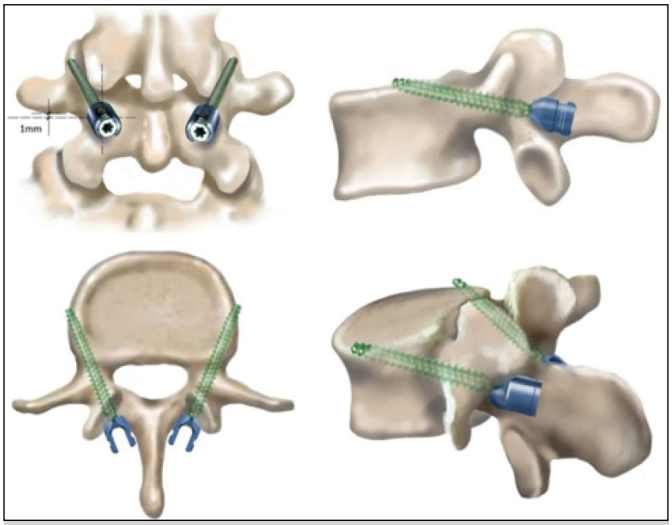

Figure 2. Demonstration of the bicortical bone trajectory screws in the coronal, sagittal, axial and oblique planes.

Once the paths were created bilaterally, following the technique described by Santoni et al.[7,11,12] and with the cannula having already touched the cortical wall, a simple randomization was carried out, for each independent vertebra, to define on which side the screw would transfix the second cortical bone - using the technique described by the authors.
The pedicles were then fixed in sequence, one side at a time, one side with transfixation of the cortical bone and the other without transfixation and subjected to mechanical tests. Therefore, for each vertebra, there was a conventional Santoni et al.[7] fixation and a bicortical fixation proposed by the present authors. (Figure 3 and 4)
The tests were all carried out at the room temperature and with a test speed of 5 mm/min. The force required to pull out the screw inserted in the two types of CBT paths was measured in kilogram-force (Kgf) and was recorded during the application of the mechanical tests. The definition of the force required to pull out the screw was the maximum load required to start displacing the screw.
The D'Agostino-Pearson and Shapiro-Wilk tests were used for exploratory analysis to determine the normality of the data. Given the parametric nature of the data, the evaluation of possible statistical differences was performed using the paired "*t*" test between the two techniques for CBT screws. In all analyzes performed,

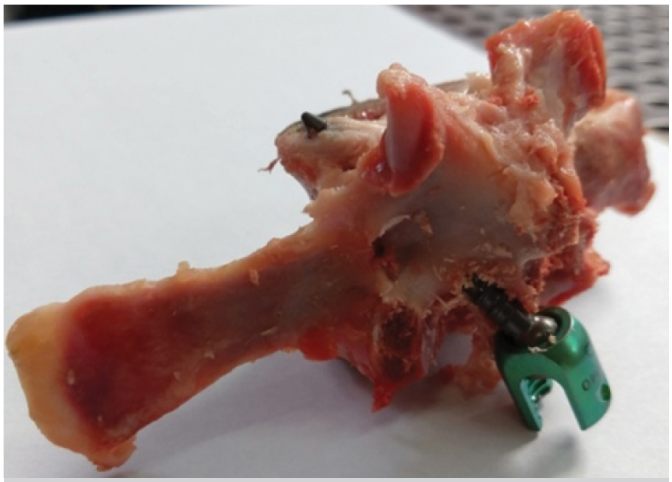

Figure 3. Demonstration of the CBT screw with cortical vertebral transfixation.

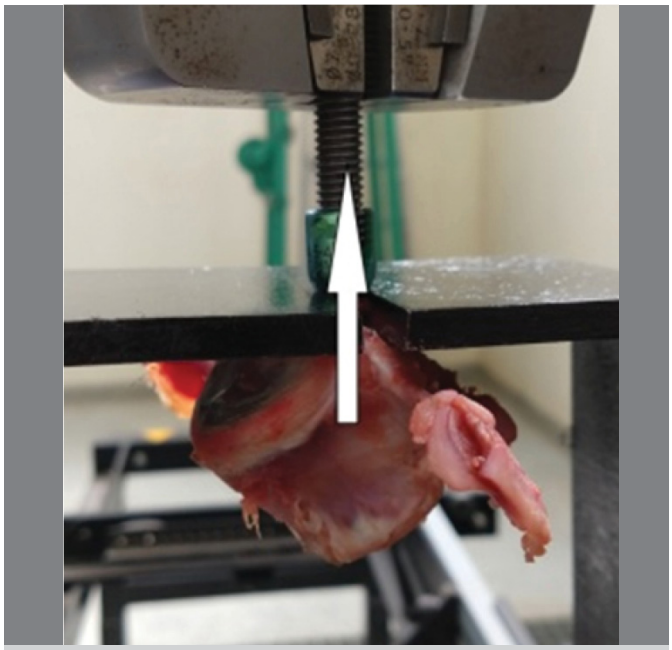

Figure 4. Demonstration of the pull out force in the same direction as the screw.

the differences obtained were statistically significant when the *p* value was less than 0.05 ($p<0.05$). All analyzes were performed using the *GraphpadPrism*® program, version 5.0 for Windows. The mean and standard deviation data for the maximum load variable required for removing the screws were obtained.

RESULTS

Tests were performed on 20 lumbar vertebrae testing a total of 40 screws. Twenty screws were inserted in a CBT path with transfixation of the second cortical bone and 20 without transfixation. The loss rate was 20%, considering that 4 vertebrae were discarded out of a total of 20, due to broken pedicles during the passage of the screws or during the tests; 16 vertebrae with 32 pedicles for screw insertion made up the final sample of this study.

Based on the pullout force (maximum load), the sample used in the present study obtained a statistical power of 81.99% [95% CI = 66.10 to 23.51; [] = 0.05]. The standard deviation of the difference between screws with and without transfixation was ± 39.97 and the average difference between them was 44.81.

The mean value for pulling out the screws inserted with the transfixation of the second cortical bone was 140.50 Kgf (± 56.56), while in the technique without transfixation it was 95.69 Kgf (± 42.19) ($p = 0.0004$). In the technique with transfixation of the second cortical bone, the force required to pull out the screw was, on average, 46% higher. (Table 1) (Graphic 1)

DISCUSSION

The idea of using bicortical screws in the lumbar spine has been tempting for years, especially for the population with osteoporotic bones. Several authors[13-16] described the traditional pedicle insertion technique in a bicortical manner and demonstrated mechanical advantages when compared with the monocortical pedicle screws, but the unfavorable vascular anatomy[15-16] increases the risk of vascular injuries with the technique of bicortical pedicle screws and therefore it is not routinely used.

Unlike pedicle screws, the CBT screws used with transfixation of the second cortical bone, as reported in this study, would be prominent

Table 1. Maximum load values (Kgf) with and without transfixation of the second cortical bone.

Vertebrae studied	Type of vertebrae	Without cortical transfixation (Kgf)	With transfixation of the second cortical bone (Kgf)	p value
V1	L5	68.59	73.65	0.0004 T
V2	L6	30.25	66.60	
V3	L5	27.66	42.22	
V5	L5	103.30	238.06	
V6	L6	96.11	154.30	
V7	L5	124.85	125.40	
V9	L5	99.34	120.38	
V10	L6	140.94	251.54	
V11	L5	63.10	135.94	
V12	L6	64.30	103.09	
V14	L6	46.48	120.10	
V15	L5	114.05	166.47	
V16	L6	128.58	174.09	
V18	L6	162.91	183.72	
V19	L5	105.00	154.90	
V20	L6	155.62	137.52	
MEAN		95.69	140.50	
SD		42.19	56.56	

Database = 32 tests were performed (total of 16 vertebrae in general - 2 independent tests on each vertebra). 16 screws with transfixation and 16 without cortical transfixation were used. SD = standard deviation.T = paired t-test.

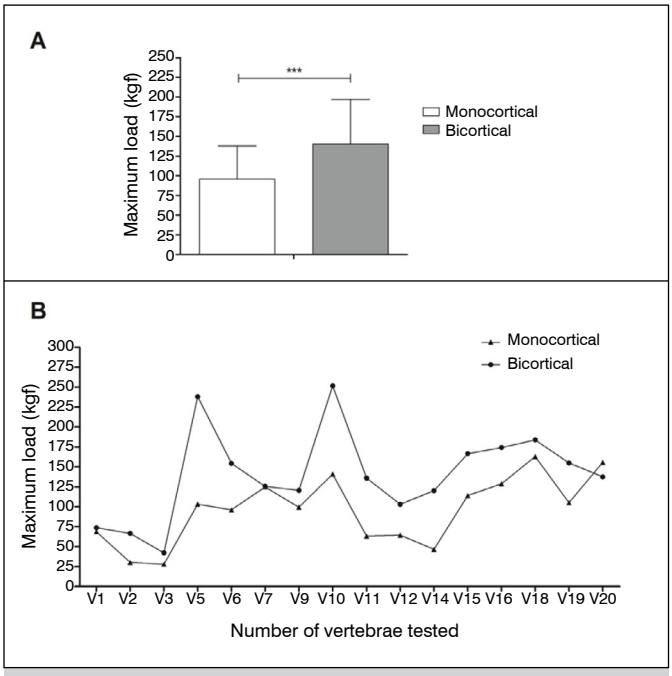

The bars represent the average of each technique and the lines, the standard deviation. A) *** = represents a statistically significant difference between the techniques, according to the paired t test ($p < 0.05$); B) maximum individual load obtained in each tested vertebra.

Figure 5. Average value of the maximum load presented by CBT screws without transfixing the cortical bone (monocortical) and with transfixation of the second cortical bone (bicortical).

in the lateral vertebral body cortex, in its cranial third and in its two posterior thirds[7,10] in a region considered safe, regarding the risks to the great vessels or to the lumbar arteries.[15,16]

In order to study the vascular safety, Guimarães at al.[17] studied, through a retrospective analysis of 50 abdominal angiotomography scans, the anatomical relationship of the probable region corresponding to

the exit point of the CBT screw, used in a bicortical manner, on the anterolateral face of the vertebra with the vascular structures adjacent to the spine. The measurements obtained between the prevertebral vessels and the possible exit points of the screw did not demonstrate contact in any of the vertebrae studied. This initial result suggests safety in the use of the cortical screw transfixing the second cortical bone, but further studies are necessary for a better understanding. Knowing the position of the vessels is essential to reduce intra- and postoperative complications related to spinal instrumentation.

Matsukawa et al.[18] described the CBT screw with transfixation of the second cortical bone in the first sacral vertebrae (S1) in 19 patients. This technical variation was considered safe by the authors. The authors demonstrated an average of 141% higher insertion torque than the traditional monocortical technique.

The belief in the literature is that the inclusion of the second bone cortex increases the mechanical resistance of the implants.[13-16,18] The pullout of the screws is the main failure mechanism of the fixation systems of the spine and, therefore, this mechanical property, pullout resistance, was chosen for this study.[4-6] However, the superiority of the transfixation of the second cortical bone, demonstrated in this study, cannot be yet confirmed for other situations of biomechanical.

Spirig et al.[19] described the biomechanical performance of pericortical-CBT versus bicortical-CBT screws (pCBT versus bCBT) in a randomized cadaveric study submitted to physiological cyclic loading tests, including shear and tension loads, as well as bending moments. They demonstrated a slight decrease in translational and angular displacements of the bCBT screws when compared to pCBT, however, the results were non-significant ($p>0.05$) and therefore the authors do not recommend the placement of CBT screws bicortically.

In this study, an average 46% ($p = 0.0004$) increase in pullout resistance was demonstrated when the second cortical bone was transfixed instead of just touching it.

CONCLUSIONS

The technique of the CBT screw inserted in a bicortical manner showed, in the lumbar column of swine, a pullout resistance 46% higher, on average when compared with the CBT screw described by Santoni et al. Further studies are needed to better understand the biomechanical characteristics and safety of this alternative technique of fixation of the lumbar spine.

CONTRIBUTIONS OF THE AUTHORS

Each author made a personal and significant contribution to the development of this article. RLCR: study conception, performance of biomechanical testing, data analysis, and manuscript drafting. JSL: study conception, scientific supervision, and critical review of the intellectual content. JJV: performance of the tests, statistical analysis, and contribution to manuscript drafting and simulations. RMG: sample preparation, participation in the tests, and support in manuscript drafting. ARVF: sample preparation, participation in the tests, and support in manuscript drafting. MAPA: scientific supervision, interpretation of the results, and critical review of the manuscript. All authors approved the final version of the manuscript.

DATA AVAILABILITY DECLARATION

The content underlying the research is included in the manuscript.

REFERENCES

1. Grotle M, Småstuen MC, Fjeld O, Grøvle L, Hegeland J, Storheim K, et al. Lumbar spine surgery across 15 years: trends, complications and reoperations in a longitudinal observational study from Norway. BMJ Open. 2019;9(8):e028743. doi: 10.1136/bmjopen-2018-028743.
2. Rajaee SS, Bae HW, Kanin LE, Delamarter RB. Spinal fusion in the United States: analysis of trends from 1998 to 2008. Spine (PhilaPa 1976). 2012;37(1):67-76. doi: 10.1097/BRS.0b013e31820cccfb.
3. Roy-Camille R, Saillant G, Berteaux D, Salgado V. Osteosynthesis of thoraco--lumbar spine fractures with metal plates screwed through the vertebral pedicles. Reconstr Surg Traumatol. 1976;15:2-16.
4. Davne SH, Myers DL. Complications of lumbar spinal fusion with transpedicular instrumentation. Spine (PhilaPa 1976). 1992;17(6 Suppl):S184-9. doi: 10.1097/00007632-199206001-00021.
5. Galbusera F, Volkheimer D, Reitmaier S, Berger- Roscher N, Kienle A, Wilke HJ. Pedicle screw loosening: a clinically relevant complication?. Eur Spine J. 2015;24(5):1005-16. doi: 10.1007/s00586-015-3768-6.
6. Weiser L, Huber G, Sellenschloh K, Viezens L, Püschel K, Morlock MM, et al.Insufficient stability of pedicle screws in osteoporotic vertebrae: biomechanical correlation of bone mineral density and pedicle screw fixation strength. Eur Spine J. 2017;26(11):2891-7. doi: 10.1007/s00586-017-5091-x.
7. Santoni BG, Hynes RA, McGilvray KC, Rodriguez-Canessa G, Lyons AS, Henson MA, et al. Cortical bone trajectory for lumbar pedicle screws. Spine J. 2009;9(5):366-73. doi: 10.1016/j.spinee.2008.07.008.
8. Sansur CA, Caffes NM, Ibrahimi DM, Pratt NL, Lewis EM, Murgatroyd AA, et al. Biomechanical fixation properties of cortical versus transpedicular screws in the osteoporotic lumbar spine: an in vitro human cadaveric model. J Neurosurg Spine. 2016;25(4):467-76. doi: 10.3171/2016.2.SPINE151046.
9. Mai HT, Mitchell SM, Hashmi SZ, Jenkins TJ, Patel AA, Hsu WK. Differences in bone mineral density of fixation points between lumbar cortical and traditional pedicle screws. Spine J. 2016;16(7):835-41. doi: 10.1016/j.spinee.2015.11.034.
10. Matsukawa K, Yoshiyuki Y. Lumbar pedicle screw fixation with cortical bone trajectory: A review from anatomical and biomechanical standpoints. Spine Surg Relat Res. 2017;1(4):164-73. doi: 10.22603/ssrr.1.2017-0006.
11. Matsukawa K, Yato Y, Nemoto O, Imabayashi H, Asazuma T, Nemoto K. Morphometric measurement of cortical bone trajectory for lumbar pedicle screw insertion using computed tomography. J Spinal Disord Tech. 2013;26(6):E248-53. doi: 10.1097/BSD.0b013e318288ac39.
12. Matsukawa K, Taguchi E, Yato Y, Imabayashi H, Hosogane N, Asazuma T, et al. Evaluation of the Fixation Strength of Pedicle Screws Using Cortical Bone Trajectory: What Is the Ideal Trajectory for Optimal Fixation?. Spine (Phila Pa 1976). 2015;40(15):E873-8. doi: 10.1097/BRS.0000000000000983.
13. Karakasli A, Acar N, Uzun B. Straight-Forward versus Bicortical Fixation Penetrating Endplate in Lumbosacral Fixation-A Biomechanical Study. J Korean Neurosurg Soc. 2018;61(2):180-5. doi: 10.3340/jkns.2017.0404.004.
14. Karami KJ, Buckenmeyer LE, Kiapour AM, Kelkar PS, Goel VK, Demetropoulos CK, et al. Biomechanical evaluation of the pedicle screw insertion depth effect on screw stability under cyclic loading and subsequent pullout. Spinal Disord Tech. 2015;28(3):E133-9. doi: 10.1097/BSD.0000000000000178.
15. Liu L, Wang H, Wang Q, Cheng S, Li Y, Jin W, et al. The methods for inserting lumbar bicortical pedicle screws from the anatomical perspective of the prevertebral great vessels. BMC Musculoskelet Dis. 2019;20:380. doi: 10.1186/s12891-019-2756-0.
16. Liu L, Wang H, Wang Q, Wang J, Liang Y, Li Y, et al. A study of the sagittal angle of lumbar bicortical pedicle screws from the anatomic perspective of the lumbar artery. World Neurosurg. 2019;125:e435-41. doi: 10.1016/j.wneu.2019.01.100.
17. Guimaraes RM, Resende RLC, Leal JS, França LC, Almeida GR. Relationship between vertebral vessels and cortical path screw in cortical transfixation. Coluna/Columna. 2022;21(1):e250506. doi: 10.1590/S1808-185120222101250506.
18. Matsukawa K, Yato Y, Kato T, Imabayashi H, Asazuma T, Nemoto K. Cortical bone trajectory for lumbosacral fixation: penetrating S-1 endplate screw technique: technical note. J Neurosurg Spine. 2014;21(2):203-9. doi: 10.3171/2014.3.SPINE13665.
19. Spirig JM, Winkler E, Cornaz F, Fasser MR, Betz M, Snedeker JG, Widmer J,Farshad M. Biomechanical performance of bicortical versus pericortical bone trajectory (CBT) pedicle screws. Eur Spine J. 2021;30(8):2292-300. doi: 10.1007/s00586-021-06878-1.